Simpelt atlas over nogle mikrofossiler med relevans til Limfjordens moleområder

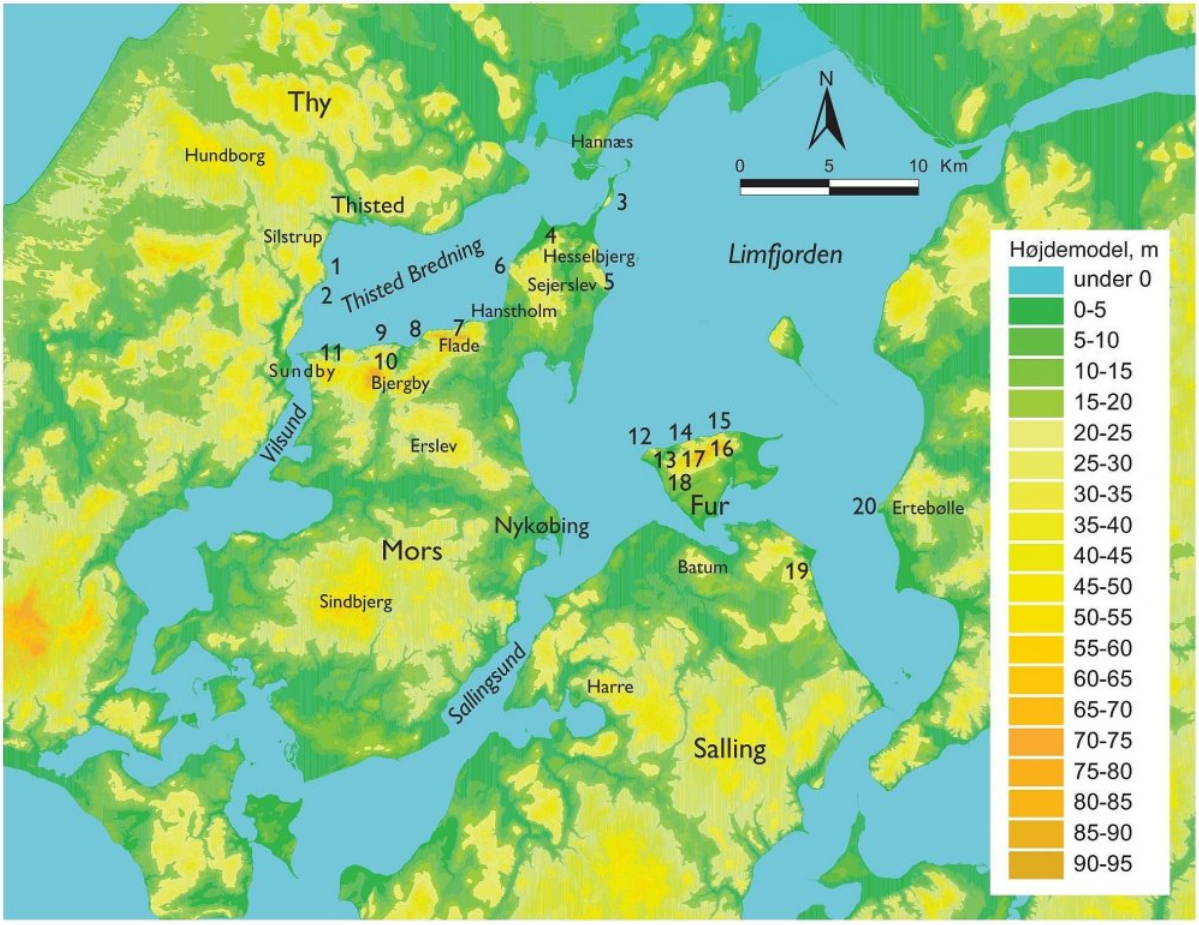

Fig. 1. Lokalitetskort over molerområdet. Moler kan ses i kystklinter og råstofgrave, som er vist med numre svarende til tabellen i Fig.8. Endvidere kender man forekomster af moler fra Hannæs og nord herfor, samt fra Hundborg. Højdemodellen er baseret på KMS kortdatabase TOP10DK.

Lokalitet		Referencer	Bemærk
Silstrup 'Firkanten'	1	Bøggild 1918, Gry 1940, Pedersen & Surlyk 1983.	Østvendt kystklint i Thy. Overskydningskontakt til Sydklint Led, Brejning Fm (Oligocæn).
Silstrup 'Sydklint'	2	Bøggild 1918, Gry 1979, Pedersen & Surlyk 1983, Heilmann-Clausen 1982, 1994b, 1997, Von Salis 1993, Rasmussen *et al*. 2010.	Østvendt kystklint i Thy. Lokalitet med de øverste askelag. Aflejringskontakt til Sydklint Led, Brejning Fm.
Feggeklit	3	Bøggild 1918, Gry 1940, 1979, Pedersen & Surlyk 1983, Espersen 1994, Pedersen 1996, Hundahl 1997, Houmark-Nielsen 1999, 2003, Rasmussen *et al*. 2010.	Østvendt kystklint på nordspidsen af Mors. Typelokalitet for 'glaciotectonites'. Tæppefolder. En ø i *Donax/Littorina* havet.
Skarrehage molergrave Museumsgraven Lynghøjgraven	4	Gry 1940, 1979, Pedersen & Surlyk 1983, Pedersen 1982, 1989, 2000a, 2005, Pedersen & Petersen 1986.	Molergrave på det nordvestlige Mors. Der har været gravet moler i næsten 100 år. Molergravene efterbehandles under hensyntagen til Molermuseets ønsker om formidling.
Ejerslev molergrav, Ejerslev kystklint Harhøj	5	Bøggild 1918, Gry 1940, 1979, Pedersen & Surlyk 1983, Pedersen 1993, 1996, 1998, 2000a, 2008a, Houmark-Nielsen *et al*. 2006.	Molergrav på det nordøstlige Mors. Der har været gravet moler i næsten 100 år. Molergravene efterbehandles under hensyntagen til rekreative værdier. Harhøj er en efterbehandlet molergrav tæt ved Ejerslev.
Skærbæk Klint	6	Bøggild 1918, Gry 1940, 1979, Pedersen & Surlyk 1983, Korsager 2002, Houmark-Nielsen 2003, Rasmussen *et al*. 2010.	Vestvendt kystklint på Nordmors. Klinten indeholder også sort, miocænt ler (Vejle Fjord Fm), samt kvartære lag tilbage til Saale og Elster.
Salgjerhøj	7	Bøggild 1918, Håkansson & Sjørring 1982.	Højeste punkt på Mors. Ved kystklinten nord for findes foldede lag, som også står frem i havbunden.
Hanklit	8	Bøggild 1918, Gry 1940, Klint & Pedersen 1995, Houmark-Nielsen 1999, 2003, Pedersen 2011.	Vestvendt kystklint på Nordmors. Tværsnit gennem Salgjerhøj randmorænekompleks. Største glacialtektoniske forsætning.
Svalklit, Stærhøj	9	Pedersen & Petersen 1985, Pedersen & Platen 2007, Pedersen 2008c.	Nordvendt kystklint.
Gullerup molergrav	10	Gry 1940, Pedersen & Platen 2007, Pedersen 2008c.	Nedlagt molergrav på Nordmors, nu tilvokset.

Lokalitet		Referencer	Bemærk
Sundby, Klitgård og Klovbakker molergrave	11	Bøggild 1918, Gry 1940, Bonde 1986, 1987,1997b, Heilmann-Clausen *et al.* 1985, Pedersen & Petersen 1985, Pedersen & Platen 2007, Pedersen 2008c, Bonde *et al.* 2008, 2010.	Nedlagte, delvis efterbehandlede molergrave på Nordmors med Oligocænt ler direkte oven på moleret. Randmorænestrøg. Strandblotning med Paleocæn/Eocæn grænsen.
Fur Knudeklint	12	Bøggild 1918, Gry 1940, 1965, Nielsen 1959, Pedersen & Surlyk 1983, Heilmann-Clausen 1982, Heilmann-Clausen *et al.* 1985, Bonde 2008, Larsen *et al.* 2003.	Nordvestvendt kystklint på Fur. Omfatter 'Knudefolderne' (Gry 1940). Typelokalitet for Fur Formationen, Knudeklint Led og Knudshoved Led. Aflejringskontakt Røsnæs Ler/ Branden Ler.
Knuden, molergrave	13	Gry 1940, Pedersen & Jakobsen 1993.	Nedlagte molergrave på det nordvestlige hjørne af Fur. Efterbehandlet til rekreative formål.
Fur Stolleklint	14	Bøggild 1918, Gry 1940, 1965, 1979, Pedersen & Surlyk 1983, Heilmann-Clausen *et al.* 1985, Heilmann-Clausen 1995, Bonde 1997b, Willumsen 1998, 2004, Larsen *et al.* 2003.	Nordvendt kystklint på Fur. Typelokalitet for Stolleklint Ler, som er aflejret under PETM, med egen fiske- og insektfauna. Holme-hus Formationen, Østerrende Ler og Paleocæn/ Eocæn grænsen.
Fur Østklint	15	Bøggild 1918, Gry 1940, Andersen & Sjørring 1992, Larsen *et al.* 2003.	Nordvendt kystklint på Fur.
Færker molergrav Morten Thiese grav	16	Gry 1940, Andersen & Sjørring 1992.	Tilgroede molergrave på østlige Fur. Normalforkastninger, sandkiler.
Molergrave, centrale Fur, Bakkekronen	17	Gry 1979, Pedersen & Surlyk 1983, Pedersen & Petersen 1988, Pedersen 2000b, 2002.	Aktive molergrave, som besøges af gæster på Fur Museum. Sandkiler. 'Bispehuen', eksempel på normal-forkastning. Efterbehandles løbende med hensyn til rekreative formål.
Hestegården molergrav Anshede	18	Pedersen 2000a, b.	Grænsen mellem Stolleklint Ler og Fur Formation, tilskredet.
Junget kystklint og molergrav	19	Pedersen & Surlyk 1983, Jakobsen *et al.* 1994.	Tilgroet molergrav på nordøstlige Salling.
Ertebølle klint	20	Bøggild 1918, Gry 1940, Pedersen & Surlyk 1983, Petersen 1986, 1990.	Vestvendt kystklint i Himmerland. Typelokalitet for køkkenmøddinger fra Ertebøllekulturen.

Dinoflagellater

Dinoflagellater er marine, planktoniske alger. Mange arter danner hvilesporer (cyster), hvis væg består af et resistent organisk materiale (dinosporin), som kan bevares fossilt (Fig. 49). Da dinoflagellatcysterne optræder i stort antal og mange arter i de fleste shelfsedimenter, er de velegnede til biostratigrafisk datering og korrelation. Dinoflagellater af slægten Apectodinium havde globalt en stor opblomstring (en acme zone) i tidligste Eocæn. Apectodinium acmet er veldokumenteret fra mange profiler (Fig. 49 billede 3–4).
Denne dinoflagellat-slægt blev favoriseret af det varme vand og de næringsstoffer, som blev tilført med flodvand. I acme-zonen udgør Apectodinium omkring 50 % af den totale mængde af dinoflagellatcyster.Basis af acme-zonen er sammenfaldende med basis af kulstofisotop-anomalien (CIE) ved starten af varmeperioden PETM . Acme-zonen er registreret fra basis af Ølst Formationen til den nederste del af Fur Formationen (lidt over askelag –33), hvorefter indholdet af Apectodinium aftager gradvist til nær nul lidt under askelag −19b.
Over askelag −19b er der en markant forandring i dinoflagellatselskabet, og over +130 findes en acme-forekomst af Deflandrea oebisfeldensis (Fig. 49 billede 6–7). Dinoflagellatcysterne i Fur Formationen er undersøgt i en lang række publikationer, og er anvendt til korrelation og datering af de sent paleocæne og tidligt eocæne aflejringer i Danmark og Nordsøen.

Planter

Der er fundet en del plantefossiler i Fur Formationen (Fig. 50). Blade af planten Macclintockia kanei blev tidligt anvendt til at bestemme formationens alder som Eocæn (Fig. 50A). Floraen med Macclintockia, Cercidophyllum (hjertetræ) og visse andre planter i Nordvesteuropa og Grønland er blevet kaldt den 'Arkto-Tertiære Flora'.
Macclintockia kan være bevaret således, at aftræk af overfladens cellelag kan foretages, hvilket giver op lysninger om bladenes klimatilpasning.
Størstedelen af plantefossilerne er kviste, grene og stammer, som formodentlig er drevet med floderne til havs (Fig. 50B). Blade er sjældne, hvilket kan forklares ved, at de lettere nedbrydes under transporten, men de findes hyppigt i Skarrehagelaget. En 8 m lang træstamme er bestemt til at være nært beslægtet med rødtræ (Sequoia), som bl.a. kendes som kæmpetræer i Californien. Kviste og pollen fra rødtræ (Sequoia) er også fundet i Fur Formationen (Fig. 50C). Fossilt ved er for nylig beskrevet fra et træ, som var beslægtet med Juglandicarya, og som formodentlig var en gammel form af den moderne valnød. Andre fossiler menes at repræsentere fyr og abetræ/stuegran (Araucaria), bl.a. grene med blade (nåle) og en gren med en klump rav. Der er også kogler fra nåletræer. Der er fundet egeblade med insektangreb (Fig. 50D) og blade af tempeltræ (Ginkgo).
Endvidere er der fundet mange lange, bambuslignende blade (Fig. 50E), blade af vandbregnen Salvinia, samt en del frø og frugter. De hyppigste er små kuglerunde frugter fra palmer. Andre frø og frugter stammer fra platan, japansk hjertetræ kaldet Jenkinsella, løn og vin. Planterne tyder på, at landet har haft en bevoksning af nåletræsskove (rødtræ, abetræ, fyr, gran, sumpcypres og taks) vekslende med en mere åben, steppeagtig bevoksning. Blandt løvtræer kendes ask, poppel og valnød og de ovenfor nævnte arter, især er sådanne blade almindelige i Skarrehagelaget. Der er også fundet bregner og padderokker. Insekterne antyder, at der må have været mange blomsterplanter, men selv om disse er stærkt underrepræsenteret blandt fossilerne, kendes en spinkel lille blomst som fossil (Fig. 50F).

Sporer og pollen

Sporer og pollen fra landplanter er blevet undersøgt i 74 prøver fra tre lokaliteter (Fur Stolleklint, Silstrup 'Firkanten' og Silstrup Sydklint) samt i 6 prøver fra den øverste del af Stolleklint Ler. Der er i alt identificeret 42 arter af sporer og 108 arter af pollen (Fig. 51).
På basis af spore- og pollenselskaberne kan Fur Formationen inddeles i fire biozoner, som er korreleret direkte med ændringer i dinoflagellatcyst-selskabet. Dette viser, at der samtidigt skete ændringer i landplanterne og i de marine alger.

De sporer og pollen, som kendes fra Fur Formationen, kan korreleres med de biozoner, som er opstillet i Europa og Nordsøen, hvilket viser, at sporer og pollen er et godt værktøj for korrelationer over lange afstande. Ved at undersøge hvornår bestemte pollen, som f.eks. Thomsonipollis magnificus, optræder første gang i henholdvis USA og Danmark, kan man også kortlægge hvordan forskellige planter er blevet spredt.

Sumpcypres og valnød

Fur Formationen er domineret af pollen fra sumpcypresser og valnød (Taxodiaceae og Juglandaceae). Pollen fra de to botaniske familier er benævnt Caryapollenites spp. (amerikansk valnød) og Inaperturopollenites spp.(Fig. 51 billede 1–3).
De flest arter i slægten sumpcypres findes idag i subtropiske til tempererede områder,som f.eks. området omkring den Mexikanske Golf.
Valnødfamilien (Juglandaceae) vokser idag i tempererede regioner som Europa, Asien og Nord- og Sydamerika og omfatter større og mindre løvfældende træer, som kendes på de duftende blade, de store,spiselige nødder og de kegleformede hanrakler.

Palmer og tropiske pollen

I Fur Formationen er der også fundet palmepollen (Arecipites spp.) og pollen fra tropiske slægter som Symplocos samt slægten Anacolosa, som idag findes i Asien og på Madagaskar (Willumsen 1997, 2004).
Palæotropiske elementer som Labrapollis globosus og Interpollis pollen optræder kun i den øverste, ældste del af Stolleklint Ler. Der mangler palynologiske data fra størstedelen af Stolleklint Leret, da undersøgelsens nederste prøve er taget ca. 3m under askelag –34.

Hvad siger floraen om klimaet?

Rust (1999a) karakteriserede vegetationen som paratropisk. Dette dækker vegetationsformer, som opstår i lavlandet uden for troperne eller i midten af tropiske bjergområder (eksempelvis Hong Kong og Taiwan). I Sen Paleocæn og Tidlig Eocæn havde denne type af vegetation sin største udbredelse på den nordlige halvkugle og nåede til 60 - 65° N. Selv om der er identificeret mange forskellige arter af eocæne sporer og pollen, mangler der at blive lavet en samlet klimatisk tolkning baseret på både makro- og mikrofloraen fra Fur Formationen. Forløbige undersøgelser viser, at den årlige middeltemperatur i Tidlig Eocæn varierede mellem 15° og 21° og den årlige nedbør i Tidlig Eocæn er anslået til at have været 1200–1400 mm.

Fra: Moleområdets geologi - sedimenter, fossiler, askelag og glacialtektonik, Geologisk Tidsskrift dec.2011: Gunver Krarup Pedersen, Stig Schack Pedersen, Niels Bonde, Claus Heilmann-Clausen, Lotte Melchior Larsen, Bent Lindow, Henrik Madsen, Asger Ken Pedersen, Jes Rust, Bo Pagh Schultz, Michael Storey, Pi Suhr Willumsen

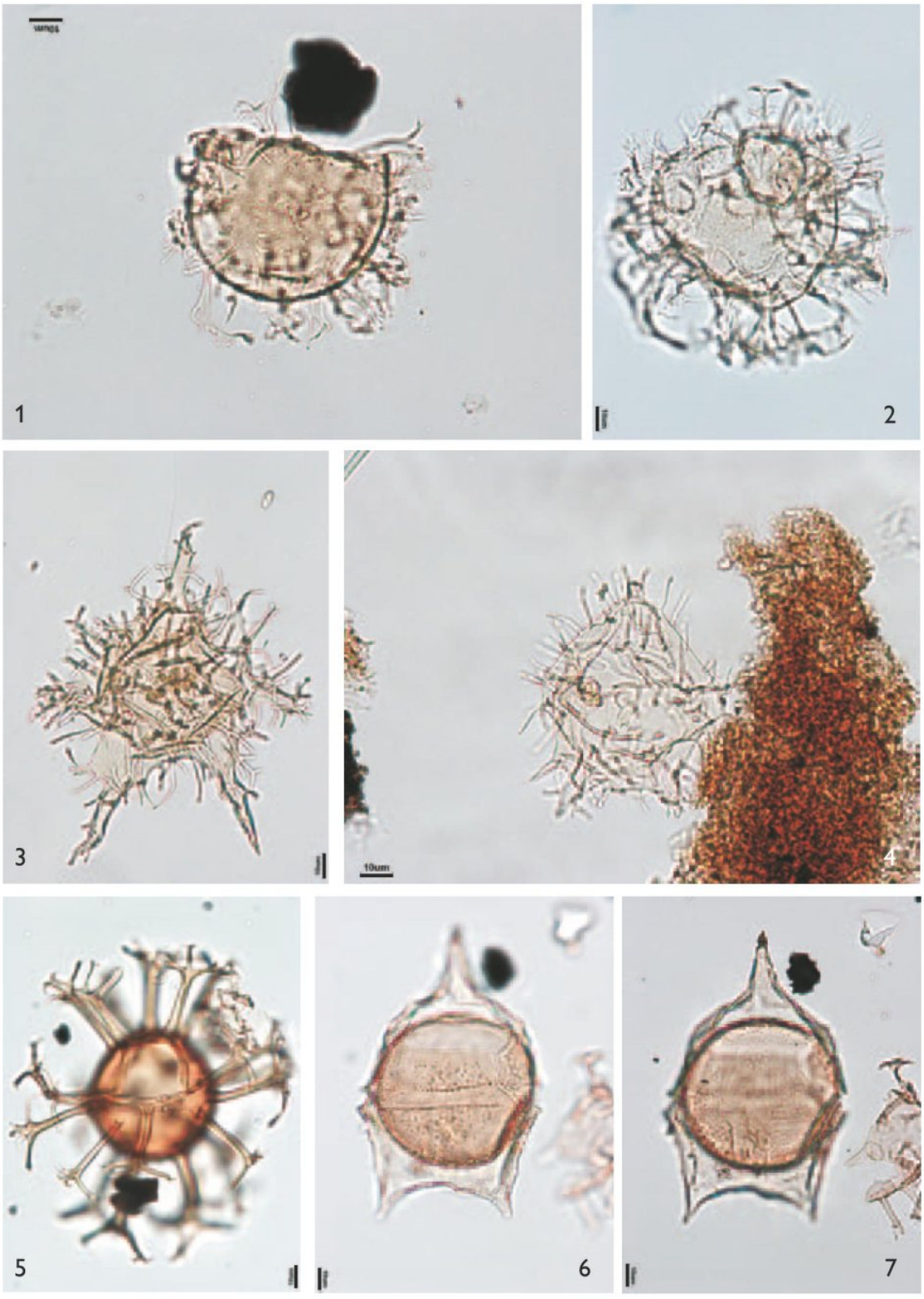

Fig. 49. Organisk-væggede dinoflagellatcyster fotograferet i normalt lysmikroskop, skala = 10mm. For alle arter er der givet følgende oplysninger: a) Artsnavn, b) Lokalitet (St= Stolleklint, Sy= Silstrup Sydklint) og prøvenummer. Prøverne stratigrafiske indplacering findes i Willumsen (1997; 2004: Fig. 3). **1**, *Glaphyrocysta ordinata*, St25; **2**, *Glaphyrocysta* cf. *divaricata* , St51; **3**, *Apectodinium* cf. *parvum* , St12; **4**, *Apectodinium quinquelatum* , St12; **5**, *Achomosphaera alcicornu* , Sy10; **6** og **7**, *Deflandrea oebisfeldensis* , Sy10. Foto Pi Suhr Willumsen.

Fig. 50. Plante makrofossiler. **A**, 18 cm langt blad af *Macclintockia,* findested ukendt; **B**, Velbevaret forkislet træ med knaster, længden på stammerne er 100 cm og 135 cm fra negativ serie i Ejerslev og Silstrup; **C**, 15 cm lang kvist af rødtræ (Sequoia), findested ukendt; **D**, Egeblad med spor af insektangreb, længde 8 cm, ved -13 , Skarrehage; **E,** Langt smalt blad bevaret i moler fra Ejerslev, længde, 14 cm, omkring +25 - +30, stratigrafisk niveau ikke kendt; **F**, Blomst, findested ukendt. A, **C**, **F**, Foto Bo Pagh Schultz, **B**, **D**, **E**, Foto Henrik Madsen.

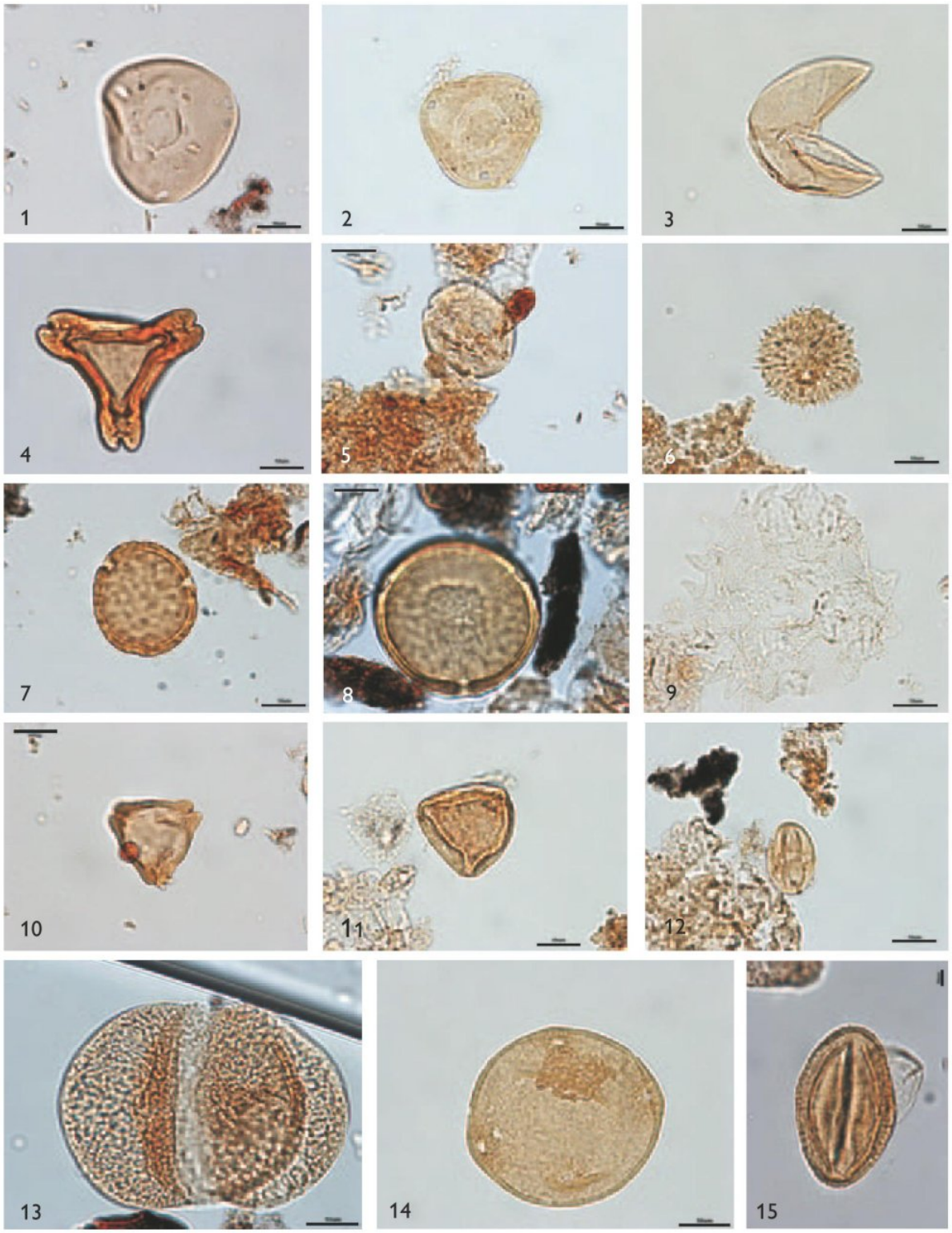

Fig. 51. Sporer og pollen fotograferet i normalt lysmikroskop, skala på alle billeder er 10mm. For alle arter er der givet følgende oplysninger: a) Artsnavn, b) Lokalitet (St=Stolleklint) og prøvenummer. For taxonomiske referencer og prøvernes stratigrafiske indplacering: se Willumsen (1997, 2004). **1**, *Caryapollenites triangulus*, St02; **2**, *Caryapollenites triangulus*, St06; **3**, *Inaperaturopollenites hiatus*, St20; **4**, *Basopollis atumenscens*, St28; **5**, *Labrapollis globosus*, St02; **6**, *Compositiopollenites medius*, St03; **7**, *Subtriporopollenites subporatus*, St02; **8**, *Subtriporopollenites constans* subsp. *medius*, St20; **9**, *Pediastrum* sp., St03; **10**, *Plicapollis pseudoexcelsus*, St02; **11**, *Interpollis microsupplingensis*, St03; **12**, *Triporopollenites cingulum*, St03; **13**, *Pityosporites microalatus*, St20; **14**, *Polyporopollenites* spp., St20; **15**, *Tricolporopolleniets europaeus*, St28. Foto Pi Suhr Willumsen.

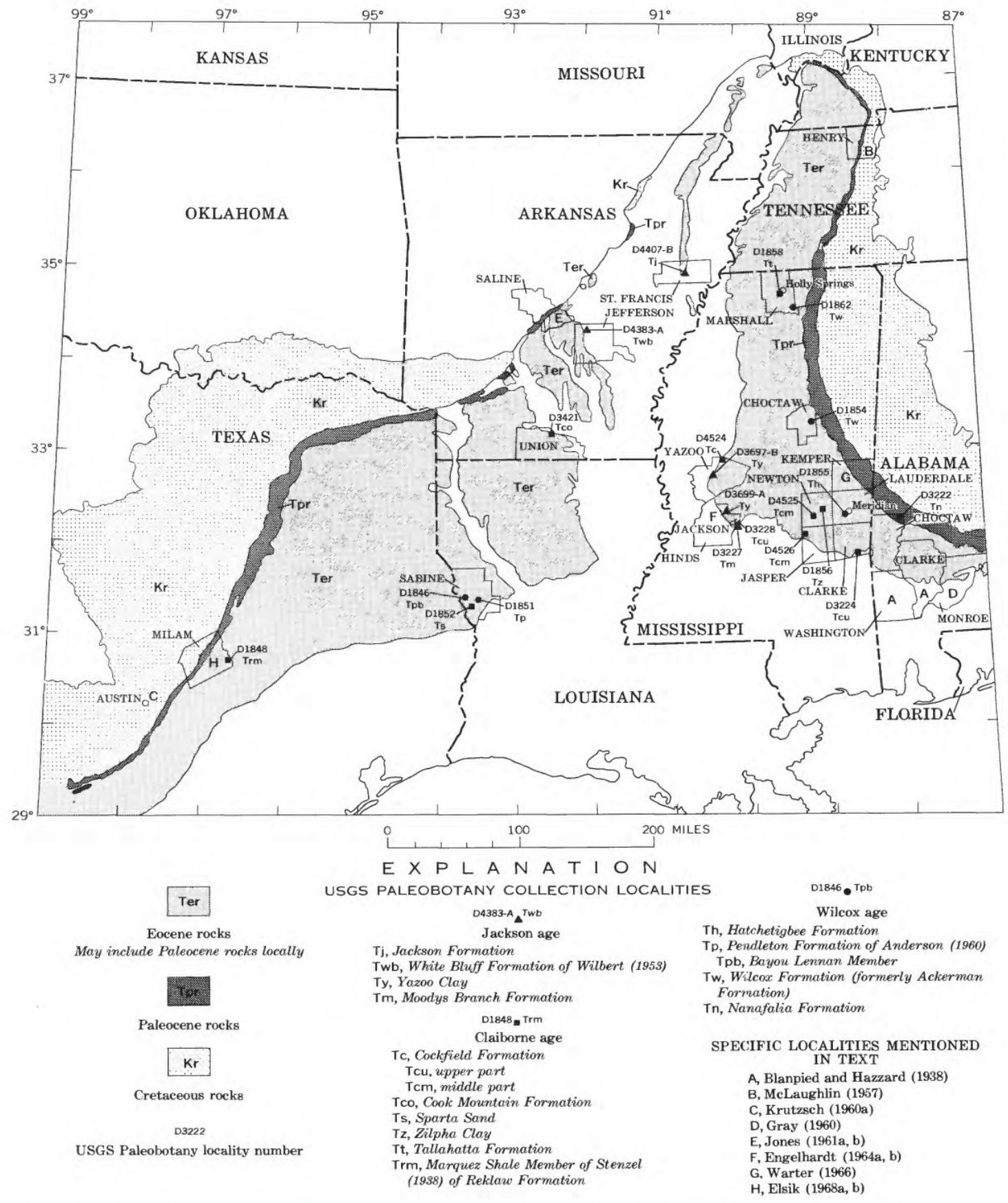

EXPLANATION

USGS PALEOBOTANY COLLECTION LOCALITIES

Ter — Eocene rocks
May include Paleocene rocks locally

Tpr — Paleocene rocks

Kr — Cretaceous rocks

D3222 — USGS Paleobotany locality number

D4383-A ▲ Twb

Jackson age

Tj, *Jackson Formation*
Twb, *White Bluff Formation of Wilbert (1953)*
Ty, *Yazoo Clay*
Tm, *Moodys Branch Formation*

D1848 ■ Trm

Claiborne age

Tc, *Cockfield Formation*
Tcu, *upper part*
Tcm, *middle part*
Tco, *Cook Mountain Formation*
Ts, *Sparta Sand*
Tz, *Zilpha Clay*
Tt, *Tallahatta Formation*
Trm, *Marquez Shale Member of Stenzel (1938) of Reklaw Formation*

D1846 ● Tpb

Wilcox age

Th, *Hatchetigbee Formation*
Tp, *Pendleton Formation of Anderson (1960)*
Tpb, *Bayou Lennan Member*
Tw, *Wilcox Formation (formerly Ackerman Formation)*
Tn, *Nanafalia Formation*

SPECIFIC LOCALITIES MENTIONED IN TEXT

A, Blanpied and Hazzard (1938)
B, McLaughlin (1957)
C, Krutzsch (1960a)
D, Gray (1960)
E, Jones (1961a, b)
F, Engelhardt (1964a, b)
G, Warter (1966)
H, Elsik (1968a, b)

FIGURE 1.—Generalized geologic map of Mississippi embayment showing fossil localities. Modified from geologic map of the United States, 1932.

490-095 O - 73 - 2

PLATE 1

[Magnification × 1,000]

FIGURES 1, 2. *Maceopolipollenites tenuipolus* (p. B9).
1. D3222, slide 3, coordinates 103.2×15.0, diameter 17μ, Nanafalia Formation.
2. D3222, slide 1, coordinates 108.4×20.5, diameter 19μ, Nanafalia Formation.

3, 4. *Kyandopollenites anneratus* (p. B9).
3. D1846, slide 1, coordinates 102.4×11.8, diameter 55μ, Pendleton Formation of Andersen (1960), low focus.
4. Same specimen, high focus.

5. *Myocolpopollenites reticulatus* (p. B12).
D1846, slide 9, coordinates 80.7×20.7, 53×44μ, Pendleton Formation of Andersen (1960).

6, 7. *Nudopollis* spp. of the *N. thiergarti* type (p. B12).
6. D3222, slide 2, coordinates 108.2×6.4, diameter 29μ, Nanafalia Formation.
7. D3222, slide 1, coordinates 107.4×15.2, diameter 27μ, Nanafalia Formation.

8, 9. *Thomsonipollis* spp. (p. B12).
8. D1855, slide 5, coordinates 107.1×18.9, diameter 29μ, Hatchetigbee Formation.
9. D1854, slide 3, coordinates 93.2×18.0, 30×33μ, Wilcox Formation (formerly Ackerman Formation).

10–12. *Spinaepollis spinosus* (p. B12).
10. D3222, slide 1, coordinates 81.6×19.0, diameter 29μ, Nanafalia Formation. Apertures obscure in this species.
11. D1848, slide 1, coordinates 107.7×2.9, diameter 27μ, Reklaw Formation.
12. D1846, slide 4, coordinates 86.1×12.8, diameter 27μ, Pendleton Formation of Andersen (1960). Note rosette arrangement of basal part of spines.

13–17. *Tricolporopollenites* n. sp. A (psilate, large pores) (p. B12).
13. D1854, slide 3, coordinates 107.7×11.3, 37×29μ, Wilcox Formation (formerly Ackerman Formation).
14. D1854, slide 3, coordinates 107.7×14.7, 39×29μ, Wilcox Formation (formerly Ackerman Formation).
15. D1854, slide 3, coordinates 87.0×13.5, 35×32μ, Wilcox Formation (formerly Ackerman Formation).
16. D1854, slide 3, coordinates 106.9×11.8, 32×29μ, Wilcox Formation (formerly Ackerman Formation). This specimen and figure 17 represent dicolporate variations of the same species shown in figures 13–15.
17. D1854, slide 2, coordinates 109.8×19.9, 30×27μ, Wilcox Formation (formerly Ackerman Formation).

18–20. *Triatriopollenites quietus* (p. B12).
18. D3222, slide 1, coordinates 78.8×17.3, diameter 19μ, Nanafalia Formation.
19. D3222, slide 1, coordinates 88.7×15.9, diameter 19μ, Nanafalia Formation.
20. D1862, slide 5, coordinates 114.6×18.5, diameter 20μ, Wilcox Formation (formerly Ackerman Formation).

21–26. *Tricolporopollenites* spp. of the *T. baculoferus* type (p. B12).
21. D1862, slide 6, coordinates 86.9×4.5, diameter 40μ, Wilcox Formation (formerly Ackerman Formation). view of specimen with long colpi.
22. D1846, slide 5, coordinates 87.2×10.8, 47×40μ, Pendleton Formation of Andersen (1960). Note well-developed pores and colpi here and in figure 23.
23. D1862, slide 6, coordinates 81.6×21.6, 39×31μ, Wilcox Formation (formerly Ackerman Formation).
24. D1855, slide 6, coordinates 98.9×4.9, 34×30μ, Hatchetigbee Formation. Colporate condition poorly developed or absent in this specimen and in figure 25.
25. D3222, slide 1, coordinates 79.6×18.5, 37×32μ, Nanafalia Formation.
26. D1862, slide 1, coordinates 105.8×12.5, diameter 35μ, Wilcox Formation (formerly Ackerman Formation). Not the short colpi in this specimen in contrast to the long colpi displayed on figure 21.

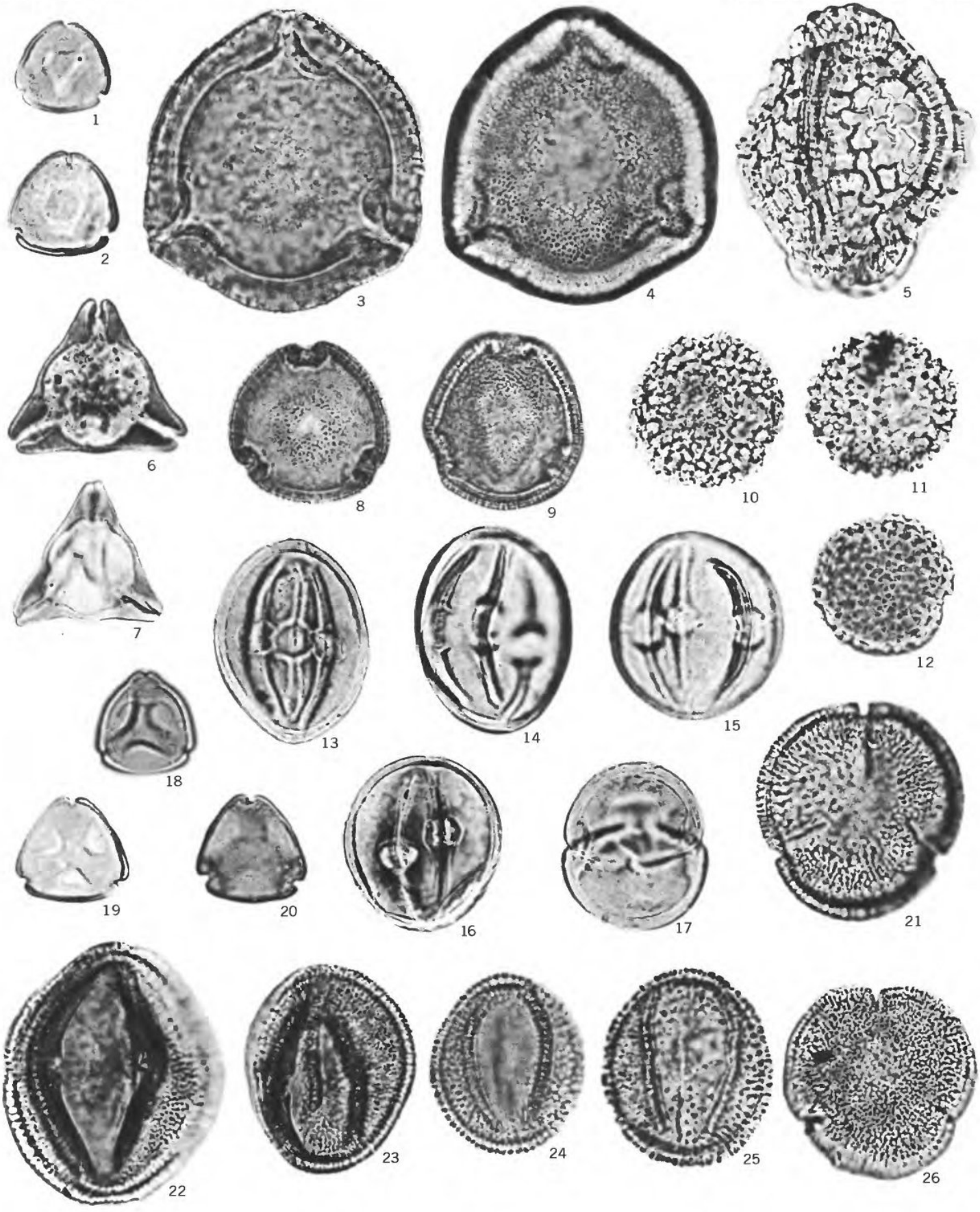

POLLEN FROM WILCOX GROUP

PLATE 2

[Magnification × 1,000]

FIGURES 1, 2. *Triporopollenites* spp. of the *T. robustus* type (p. B13).
1. D3222, slide 1, coordinates 76.5×5.9, diameter 29μ, Nanafalia Formation. High focus.
2. Same specimen, low focus.

3, 4. *Triporopollenites* n. sp. A (thin walled) (p. B13).
3. D3222, slide 1, coordinates 98.5×14.0, diameter 34μ, Nanafalia Formation. Almost circular form.
4. D1846, slide 5, coordinates 93.0×6.3, diameter 40μ, Pendleton Formation of Andersen (1960). Deltoid form with larger pores.

5, 6. *Trivestibulopollenites* spp. of the *T. betuloides* type (p. B13).
5. D1862, slide 6, coordinates 107.3×7.4, diameter 27μ, Wilcox Formation (formerly Ackerman Formation).
6. D1862, slide 6, coordinates 82.1×12.7, 29×24μ, Wilcox Formation (formerly Ackerman Formation). Oblique equatorial view.

7, 8. *Triatriopollenites* spp. of the *T. aroboratus* type (p. B13).
7. D3222, slide 3, coordinates 107.8×11.0, diameter 45μ, Nanafalia Formation. Note granulate endexine in area of atria.
8. D3222, slide 2, coordinates 108.3×17.0, diameter 38μ, Nanafalia Formation.

9–12. *Tricolpites* n. sp. A (microreticulate) (p. B13).
9. D3222, slide 2, coordinates 109.6×20.5, diameter 19μ, Nanafalia Formation.
10. D1855, slide 6, coordinates 82.0×20.7, diameter 23μ, Hatchetigbee Formation.
11. D3699–A, slide 3, coordinates 101.9×8.9, diameter 36μ, Yazoo Clay.
12. D3699–A, slide 4, coordinates 92.1×14.2, diameter 38μ, Yazoo Clay.

13–15. *Aesculiidites circumstriatus* (p. B13).
13. D1854, slide 4, coordinates 107.9×4.2, 22×18μ, Wilcox Formation (formerly Ackerman Formation). Colporate condition clearly displayed.
14. D1851, slide 2, coordinates 99.7×11.7, 23×19μ, Pendleton Formation of Andersen (1960).
15. D1851, slide 1, coordinates 100.1×10.0, 25×18μ, Pendleton Formation of Andersen (1960). Pores obscure in this specimen and in figure 14.

16, 17. *Calamuspollenites pertusus* (p. B14).
16. D1854, slide 3, coordinates 98.5×12.4, 35×23μ, Wilcox Formation (formerly Ackerman Formation).
17. D1854, slide 3, coordinates 95.9×18.3, 31×24μ, Wilcox Formation (formerly Ackerman Formation).

18–20. *Nudopollis* spp. of the *N. terminalis* type (p. B14).
18. D1862, slide 3, coordinates 100.0×3.1, diameter 35μ, Wilcox Formation (formerly Ackerman Formation).
19. D1848, slide 2, coordinates 92.8×8.8, diameter 24μ, Reklaw Formation.
20. D3222, slide 1, coordinates 79.2×20.9, diameter 30μ, Nanafalia Formation.

21, 22. *Pistillipollenites mcgregorii* (p. B14).
21. D1854, slide 4, coordinates 101.7×15.4, diameter 22μ, Wilcox Formation (formerly Ackerman Formation).
22. D1854, slide 4, coordinates 79.7×10.5, diameter 26μ, Wilcox Formation (formerly Ackerman Formation).

23, 24. *Symplocospollenites* spp. (three aperturate) (p. B14).
23. D1848, slide 1, coordinates 110.8×10.4, diameter 22μ, Reklaw Formation.
24. D1862, slide 7, coordinates 113.0×21.5, diameter 29μ, Wilcox Formation (formerly Ackerman Formation).

25, 26. *Carya* sp. 22μ–28μ (p. B14).
25. D1848, slide 2, coordinates 101.5×15.9, diameter 28μ, Reklaw Formation.
26. D3222, slide 1, coordinates 99.0×15.0, diameter 28μ, Nanafalia Formation.

27–29. *Dicolpopollis* cf. *D. kalewensis* (p. B14).
27. D1855, slide 6, coordinates 94.1×13.5, 28×21μ, Hatchetigbee Formation.
28. D1855, slide 6, coordinates 98.0×3.5, 27×22μ, Hatchetigbee Formation.
29. D1855, slide 6, coordinates 80.0×15.1, 28×20μ, Hatchetigbee Formation.

30–34. *Platycarya* spp. (p. B14).
30. D1855, slide 5, coordinates 91.4×21.2, diameter 19μ, Hatchetigbee Formation.
31. D1855, slide 6, coordinates 82.0×20.7, diameter 20μ, Hatchetigbee Formation.
32. D1848, slide 2, coordinates 109.5×12.9, diameter 29μ, Reklaw Formation. This and the succeeding two specimens can be assigned to the form genus *Plicatopollis*.
33. D1848, slide 2, coordinates 107.3×13.9, diameter 27μ, Reklaw Formation.
34. D1848, slide 1, coordinates 113.3×6.4, diameter 28μ, Reklaw Formation.

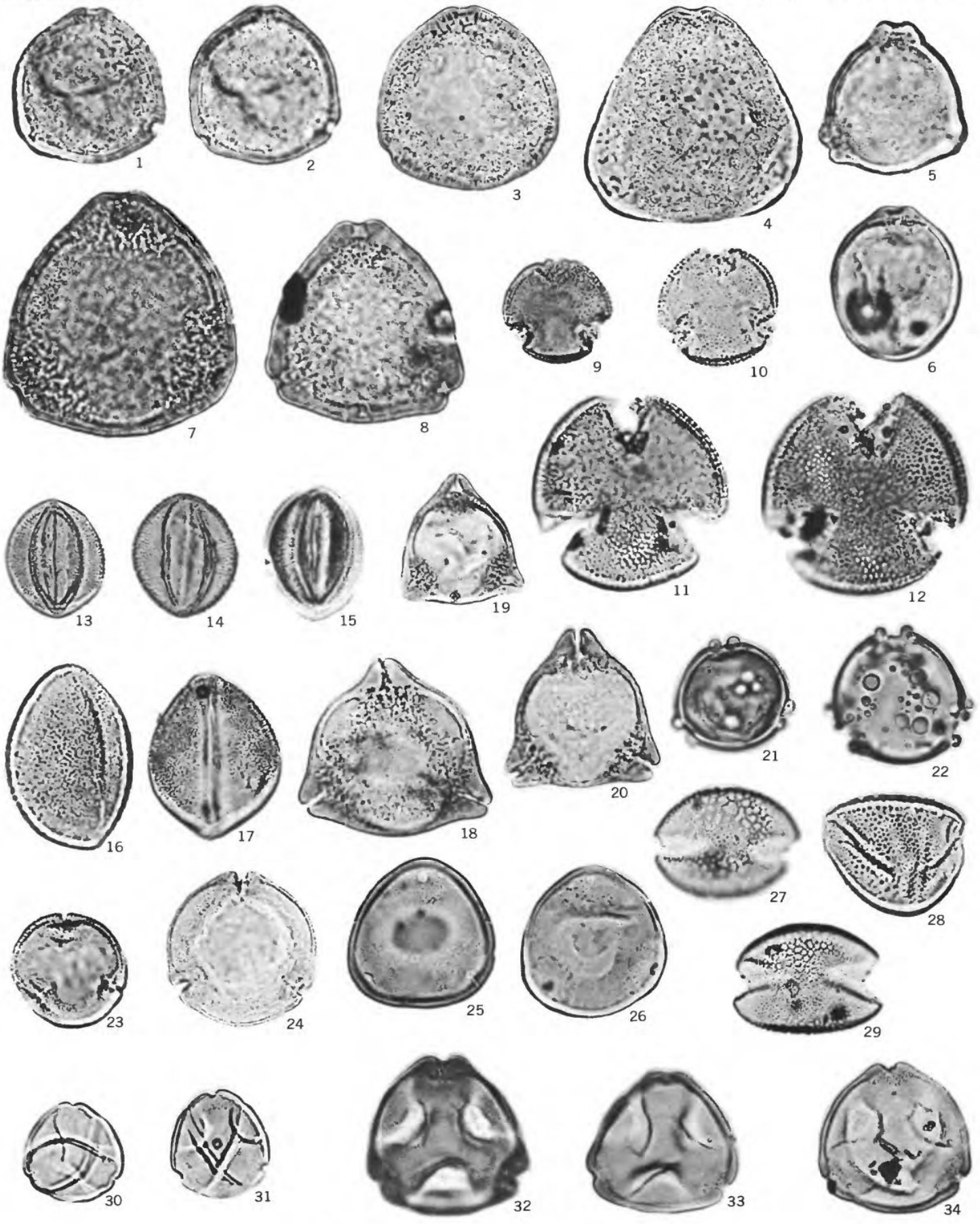

POLLEN FROM WILCOX AND CLAIBORNE GROUPS

PLATE 3

[Magnification × 1,000]

FIGURES 1–4. *Proxapertites* spp. (p. B15).

1. D1848, slide 2, coordinates 82.4×18.6, 46×38μ, Reklaw Formation. This specimen as well as that represented by figure 4 are isolated halves. The complete fossil is represented by figures 2 and 3.
2. D1848, slide 2, coordinates 109.2×15.7, 48×40μ, Reklaw Formation.
3. D1848, slide 3, coordinates 109.3×17.7, 45×38μ, Reklaw Formation.
4. D1848, slide 2, coordinates 84.0×16.6, 48×39μ, Reklaw Formation.

5, 6. *Porocolpopollenites* spp. (psilate-microreticulate). (p. B15).

5. D1852, slide 3, coordinates 98.3×18.0, diameter 32μ, Sparta Sand.
6. D1852, slide 2, coordinates, 83.5×9.3, diameter 32μ, Sparta Sand.

7–9. *Anacolosidites* spp. (p. B15).

7. D1848, slide 2, coordinates 88.4×11.6, diameter 24μ, Reklaw Formation.
8. D3421–B, slide 1, coordinates 87.9×10.6, diameter 20μ, Cook Mountain Formation.
9. D3421–B, slide 3, coordinates 78.3×3.7, diameter 19μ, Cook Mountain Formation.

10–12. *Ilexpollenites* spp. (p. B15).

10. D1852, slide 2, coordinates 87.3×2.9, 30×22μ, Sparta Sand, high focus.
11. Same specimen, low focus.
12. D1852, slide 3, coordinates 105.4×12.6, diameter 25μ, Sparta Sand.

13, 14. *Echiperiporites* spp. (p. B15).

13. D4383–A, slide 1, coordinates 109.7×9.0, diameter 34μ, White Bluff Formation of Wilbert (1953).
14. D4383–B, slide 2, coordinates 110.6×4.2, diameter 32μ, White Bluff Formation of Wilbert (1953).

15–19. *Tricolporopollenites* spp. (fusoid forms) (p. B15).

15. D1858, slide 5, coordinates 111.6×8.0, 32×23μ, Tallahatta Formation.
16. D1858, slide 6, coordinates 91.8×11.2, 28×17μ, Tallahatta Formation.
17. D3227, slide 1, coordinates 110.8×17.6, 27×16μ, Moodys Branch Formation. The specimens represented by figures 17–19 are perhaps most representative of this heterogeneous group.
18. D1848, slide 1, coordinates 113.1×4.8, 26×15μ, Reklaw Formation. Low focus.
19. Same specimen, high focus.

20–22. *Multiporopollenites* spp. (p. B15).

20. D1858, slide 5, coordinates 89.0×5.0, diameter 22μ, Tallahatta Formation.
21. D1858, slide 5, coordinates 97.9×10.6, diameter 32μ, Tallahatta Formation.
22. D1858, slide 5, coordinates 87.2×5.9, diameter 33μ, Tallahatta Formation.

23, 24. *Verrucatosporites* spp. (p. B16).

23. D3699–A, slide 4, coordinates 101.4×16.8, 50×35μ, Yazoo Clay.
24. D3228, slide 1, coordinates 109.2×20.7, 43×31μ, Cockfield Formation.

25–27. *Carya* spp. 29μ–39μ (p. B15).

25. D3697–B, slide 1, coordinates 98.1×14.6, 34×40μ, Yazoo Clay.
26. D3699–A, slide 1, coordinates 85.2×7.3, diameter 38μ, Yazoo Clay. High focus.
27. Same specimen, low focus.

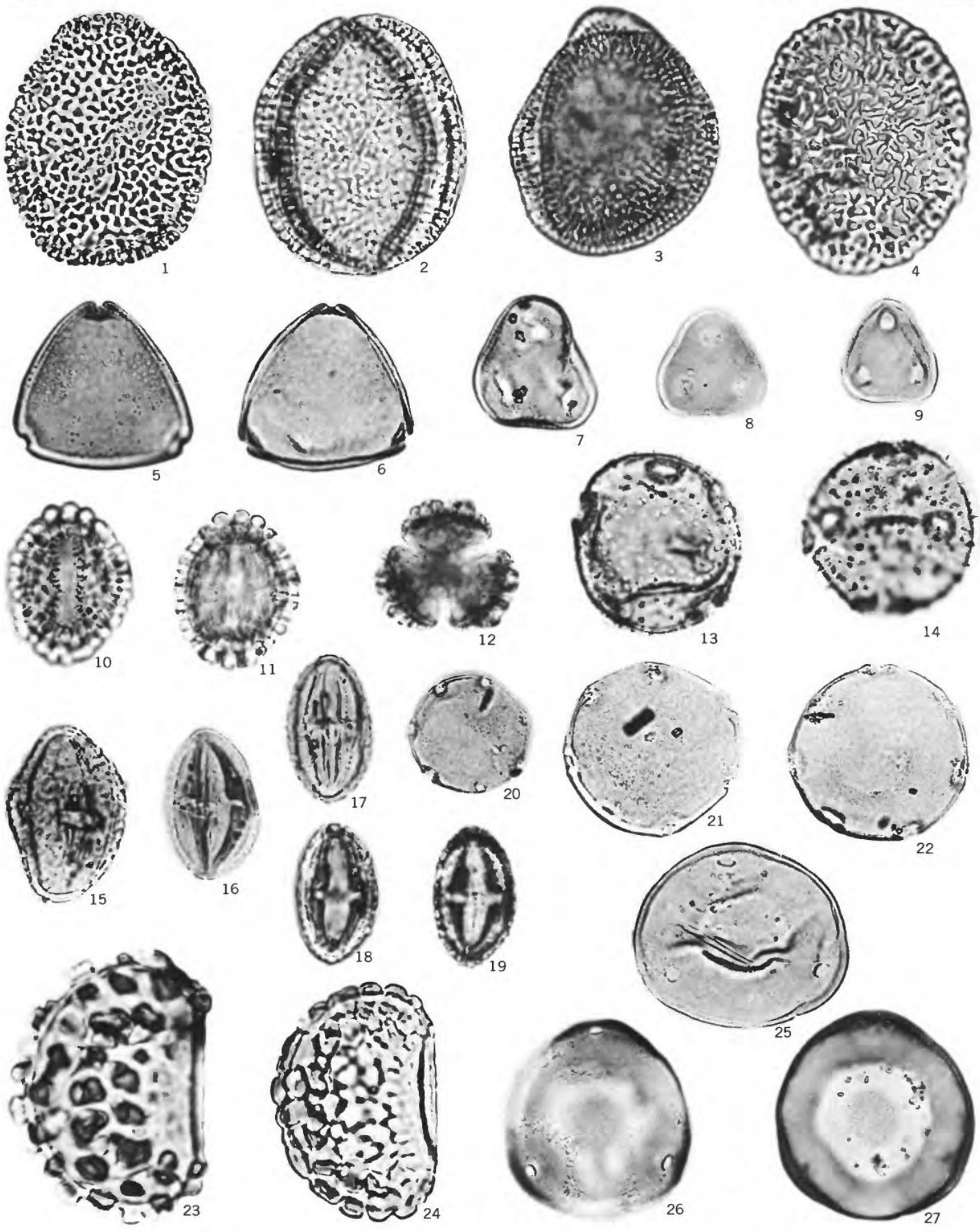

POLLEN AND SPORES FROM CLAIBORNE AND JACKSON GROUPS

PLATE 4

[Magnification × 1,000, figs. 1–35, × 500 figs. 36, 37]

FIGURES 1–3. *Triatriopollenites* sp. of the *T. coryphaeus* type (13μ–18μ) (p. B16)
1. D1856, slide 2, coordinates 78.6×11.6, diameter 14μ, Zilpha Clay.
2. D1858, slide 5, coordinates 91.5×4.8, diameter 17μ, Tallahatta Formation.
3. D1858, slide 6, coordinates 79.6×6.4, diameter 18μ, Tallahatta Formation.

4, 5. *Gothanipollis* spp. (p. B16).
4. D4383–A, slide 1, coordinates 79.3×21.6, diameter 22μ, White Bluff Formation of Wilbert (1953).
5. D1858, slide 3, coordinates 111.1×9.1, diameter 26μ, Tallahatta Formation.

6, 7. *Tricolpopollenites* spp. of the *T. microhenrici* type (p. B16).
6. D1852, slide 1, coordinates 91.4×22.1, 30×16μ, Sparta Sand.
7. D1852, slide 2, coordinates 87.3×8.0, 24×17μ, Sparta Sand.

8. 9. *Porocolpopollenites* spp. (verrucate) (p. B16).
8. D3224, slide 2, coordinates 92.3×13.6, diameter 30μ, Cockfield Formation.
9. D3224, slide 2, coordinates 101.4×6.1, diameter 23μ, Cockfield Formation.

10, 11. *Tricolpopollenites* spp. of the *T. henrici* type (p. B16).
10. D1852, slide 1, coordinates 99.0×19.8, 37×30μ, Sparta Sand. High focus.
11. Same specimen, low focus.

12, 13. *Triatriopollenites* sp. of the *T. coryphaeus* type (20μ–30μ) (p. B16).
12. D1852, slide 2, coordinates 85.5×17.7, diameter 26μ, Sparta Sand.
13. D1852, slide 3, coordinates 81.7×13.3, diameter 27μ, Sparta Sand.

14–17. *Cyrillaceaepollenites* cf. *C. megaexactus* (p. B17).
14. D4407–B, slide 2, coordinates 102.6×6.2, diameter 18μ, Jackson Formation.
15. D4524, slide 1, coordinates 91.6×8.6, diameter 17μ, Cockfield Formation.
16. D4524, slide 1, coordinates 91.5×8.6, 15×14μ, Cockfield Formation.
17. D1856, slide 2, coordinates 82.0×2.6, diameter 13μ, Zilpha Clay.

18, 19. *Tricolporopollenites* n. sp. B (*Parthenocissus* type) (p. B17).
18. D3228, slide 1, coordinates 84.0×17.8, 33×26μ, Cockfield Formation.
19. D3228, slide 1, coordinates 84.2×6.0, 35×24μ, Cockfield Formation.

20, 21. *Cyrillaceaepollenites* of the *Pollenites ventosus* type (p. B17).
20. D3699–A, slide 3, coordinates 82.6×17.1, diameter 17μ, Yazoo Clay.
21. D4383–A, slide 1, coordinates 99.1×5.0, diameter 21μ, White Bluff Formation of Wilbert (1953).

22, 23. *Ephedra* type A of Steeves and Barghoorn (p. B17).
22. D4383–A, slide 1, coordinates 78.0×6.2, 48×22μ, White Bluff Formation of Wilbert (1953).
23. D3699–A, slide 3, coordinates 101.2×10.6, 37×18μ, Yazoo Clay.

24–28. *Tricolporopollenites cingulum* (p. B17).
24. D1858, slide 5, coordinates 111.3×16.3, 21×14μ, Tallahatta Formation.
25. D1858, slide 5, coordinates 111.3×16.3, 21×9μ, Tallahatta Formation.
26. D1858, slide 5, coordinates 114.2×18.5, 17×11μ, Tallahatta Formation.
27. D3227, slide 1, coordinates 105.8×12.4, 18×11μ, Moodys Branch Formation. Low focus.
28. Same specimen, high focus.

29, 30. *Multiporopollenites* sp. of the *Dorstenia* type (p. B17).
29. D3699–A, slide 3, coordinates 81.4×3.4, 21×18μ, Yazoo Clay.
30. D3699–A, slide 3, coordinates 77.7×5.1, 24×23μ, Yazoo Clay.

31–33. *Tricolpopollenites liblarensis* (p. B18).
31. D1854, slide 2, coordinates 112.5×8.3, 17×12μ, Wilcox Formation (formerly Ackerman Formation).
32. D1852, slide 1, coordinates 90.6×19.9, 14×8μ, Sparta Sand.
33. D1856, slide 2, coordinates 80.3×1.9, 20×10μ, Zilpha Clay.

34, 35. *Graminidites* spp. (p. B17).
34. D4407–B, slide 2, coordinates 105.7×10.6, 42×40μ, Jackson Formation.
35. D4383–A, slide 1, coordinates 80.30×6.4, 37×28μ, White Bluff Formation of Wilbert (1953).

36, 37. Peltate leaf hairs of *Engelhardtia*.
36. D4407–B, slide 2, coordinates 86.8×5.5, 100×86μ, Jackson Formation (× 500).
37. D4383–B, slide 3, coordinates 77.3×13.1, 94×86μ, White Bluff Formation of Wilbert (1953) (× 500).

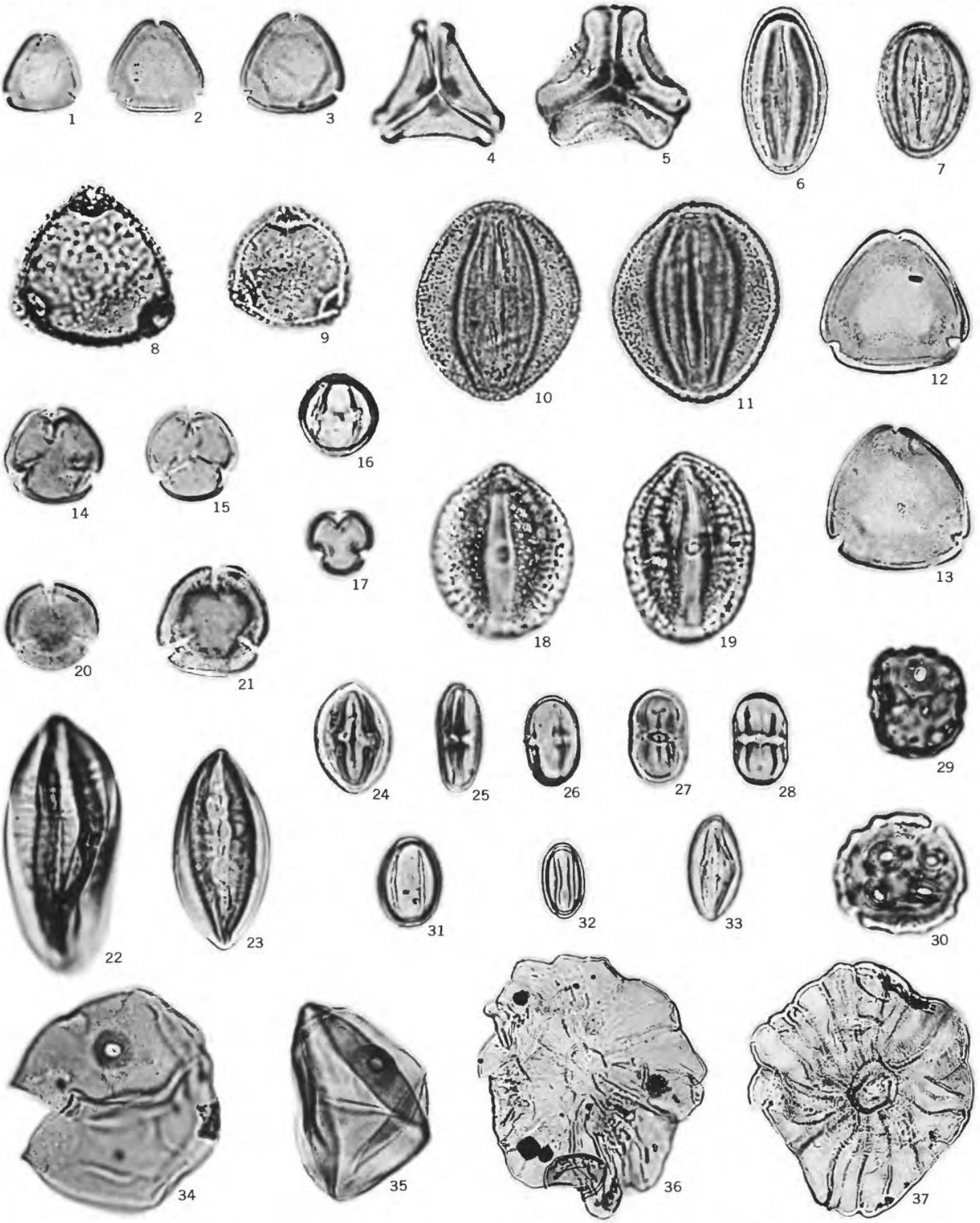

POLLEN AND SPORES FROM CLAIBORNE AND JACKSON GROUPS

U. S. GOVERNMENT PRINTING OFFICE : 1973 O - 490-095


Passages
Grønland
Island
Sverige
Finland
Norge
Hudsonbukta
Labradorsjøen
Danmark
Storbritannia
Irland
Polen
Tyskland
Frankrike
Østerrike
Romania
Italia
Spania
Portugal
Hellas
Tunisia
Middelhavet
Marokko
Algerie
Libya
Vest-Sahara
Mauritania
Mali
Niger
Mexicogolfen
Cuba
Puerto Rico
MB
NU
NL
ON
QC
NB
PE
NS
ME
NH
MA
NY
ND
MN
SD
WI
MI
NE
IA
IL
IN
OH
PA
MD
DE
WV
VA
KY
TN
NC
SC
GA
AL
MS
LA
TX
OK
AR
MO
KS
FL
OCEAN DRILLING
PROGRAM LEG 210
WELLSITE 1276

Plate 1

Figure 1. Adnatosphaeridium vitattum
Figure 2. Adnatosphaeridium vitattum
Figure 3. Adnatosphaeridium vitattum
Figure 4. Adnatosphaeridium vitattum
Figure 5. Adnatosphaeridium sp. Apical view
Figure 6. Adnatosphaeridium sp. Antapical view [same as fig. 5]
Figure 7. Adnatosphaeridium vittatum
Figure 8. Adnatosphaeridium vittatum
Figure 9. Adnatosphaeridium vittatum
Figure 10. Adnatosphaeridium vittatum
Figure 11. Adnatosphaeridium vittatum
Figure 12. Cleistosphaeridium elegatulum
Figure 13. Areoligera gippingensis
Figure 14. Axiodinium sp.
Figure 15. Axiodinium sp.
Figure 16. Cerodinium glabrum
Figure 17. Cleistosphaeridium palmatum [scale: 50um]
Figure 18. Dapsilidinium sp.?
Figure 19. Cleistosphaeridium sp.
Figure 20. Cleistosphaeridium diversispinosum

Plate 1

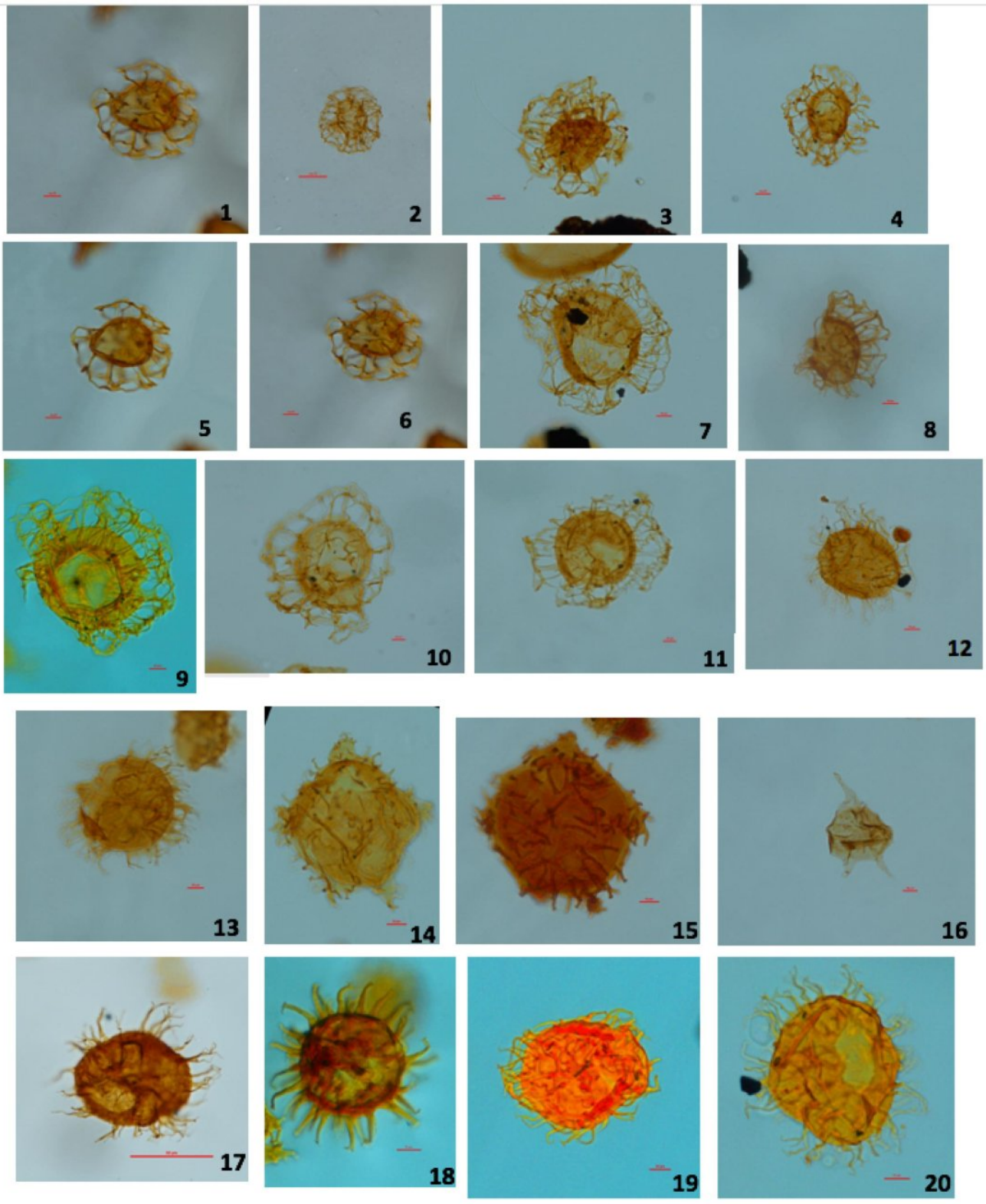

Plate 2

Figure1. Cleistosphaeridium elegatulum
Figure2. Cleistosphaeridium elegatulum
Figure3. Cleistosphaeridium elegatulum
Figure4. Cleistosphaeridium elegatulum
Figure5. Cleistosphaeridium ancryeum
Figure6. Cleistosphaeridium ancryeum
Figure7. Cleistosphaeridium diversispinosum
Figure8. Cleistosphaeridium diversispinosum
Figure9. Cleistosphaeridium diversispinosum
Figure10. Cleistosphaeridium diversispinosum
Figure11. Cordosphaeridium sp.
Figure12. Cordosphaeridium gracile
Figure13. Cordosphaeridium gracile
Figure14. Cordosphaeridium delimurum
Figure15. Cordosphaeridium delimurum
Figure16. Cordosphaeridium delimurum [scale:50um]
Figure17. Cordosphaeridium delimurum
Figure18. Cordosphaeridium cantharellus
Figure19. Cordosphaeridium cantharellus
Figure20. Cordosphaeridium cantharellus

Plate 2

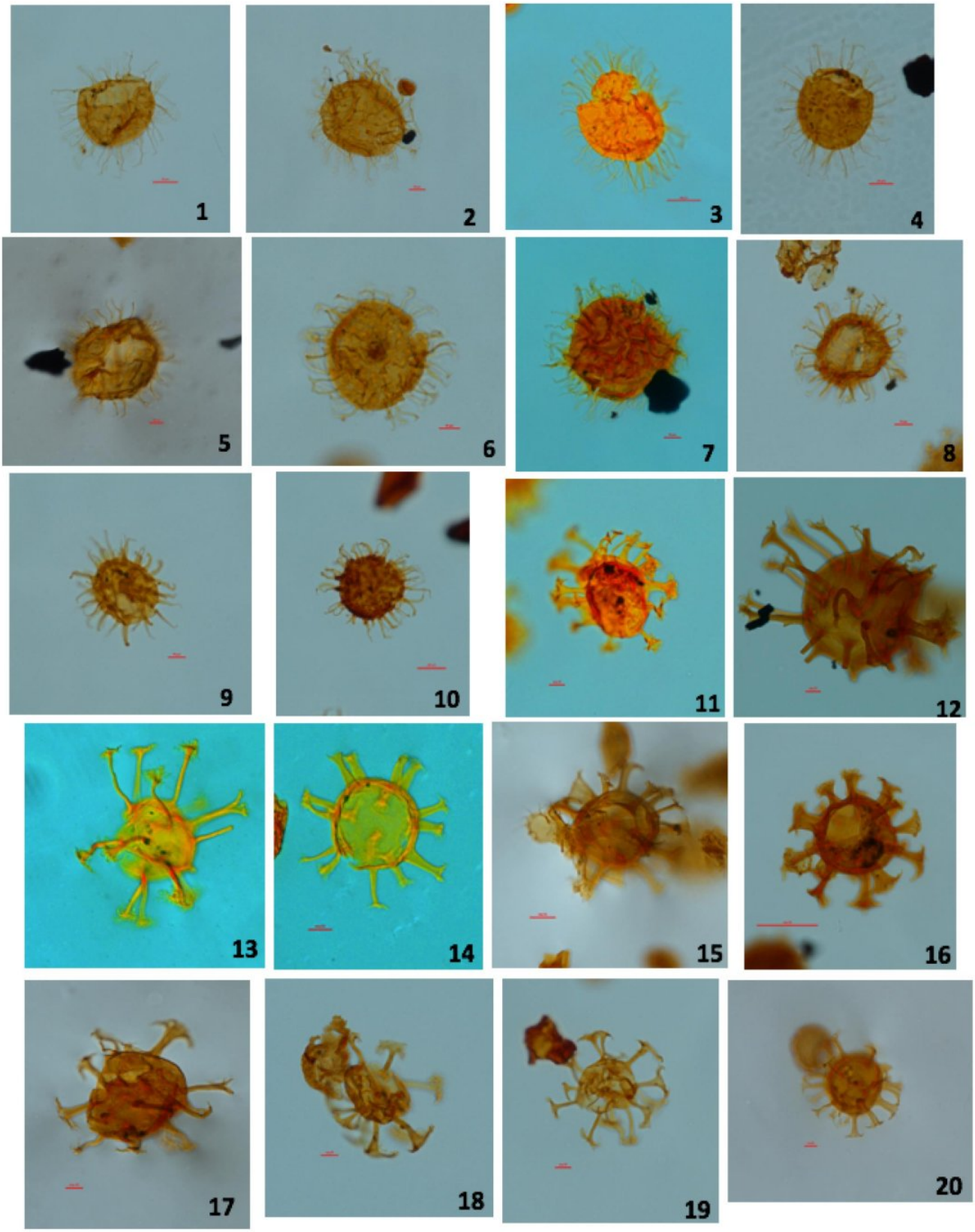

Plate 3

Figure1. Danea sp.
Figure2. Danea sp.
Figure3. Cordosphaeridium delimurum
Figure4. Cordosphaeridium delimurum
Figure5. Cordosphaeridium delimurum
Figure6. Cordosphaeridium delimurum
Figure7. Cordosphaeridium delimurum
Figure8. Cordosphaeridium delimurum
Figure9. Cordosphaeridium delimurum
Figure10. Cordosphaeridium delimurum
Figure11. Dapsilidinium pseudocalligerum
Figure12. Dapsilidinium pseudocalligerum
Figure13. Dapsilidinium pseudocalligerum
Figure14. Deflandrea eocenica
Figure15. Deflandrea eocenica
Figure16. Deflandrea eocenica
Figure17. Deflandrea eocenica
Figure18. Deflandrea phosphoritica
Figure19. Deflandrea sp.
Figure20. Deflandrea sp.

Plate 3

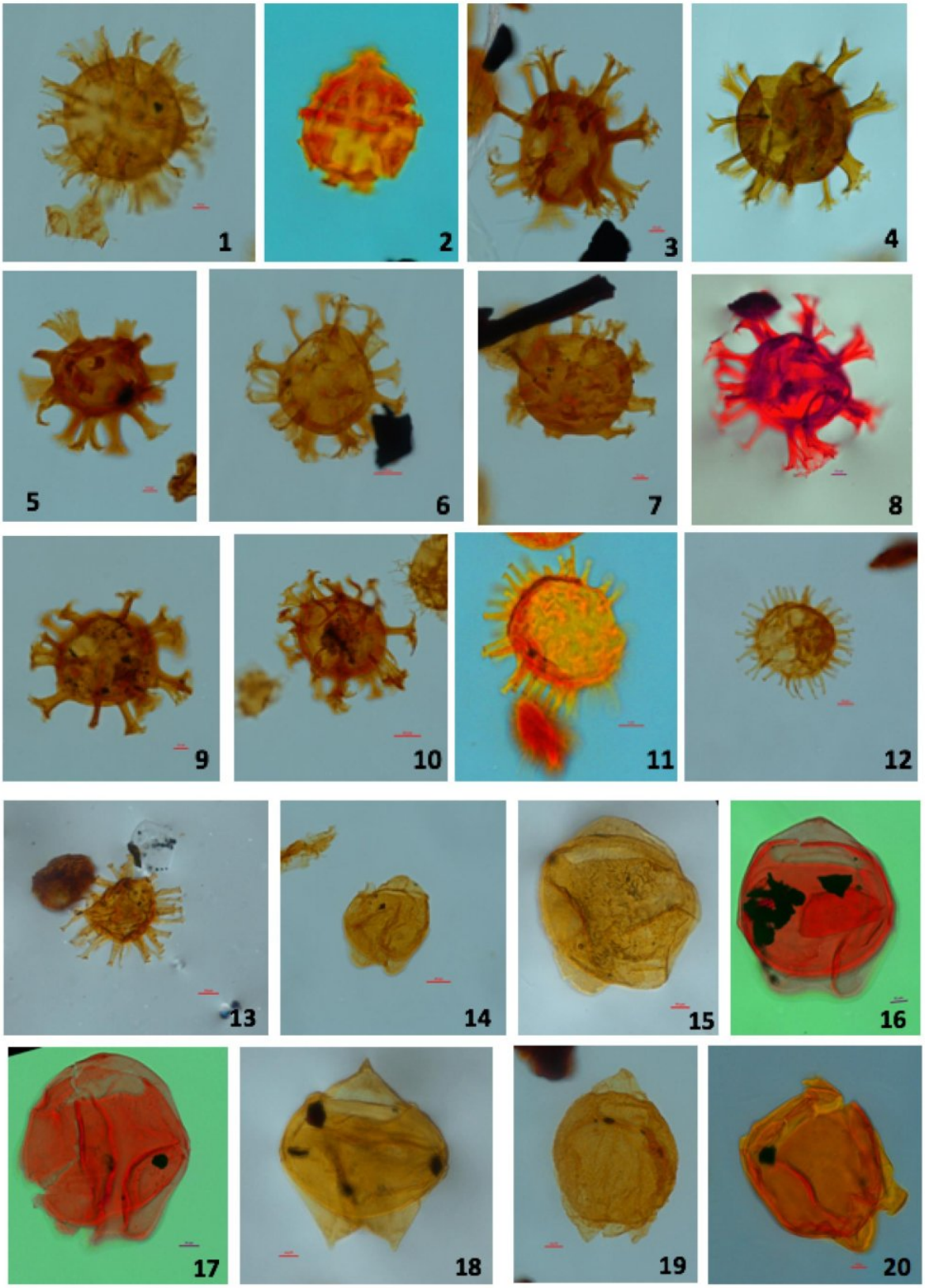

Plate 4

Figure1. Glaphyrocysta divaricata, ventral surface
Figure2. Glaphyrocysta divaricata, ventral view
Figure3. Glaphyrocysta divaricata
Figure4. Glaphyrocysta divaricata
Figure5. Glaphyrocysta divaricata
Figure6. Spiniferites sp.?
Figure7. Glaphyrocysta sp.
Figure8. Glaphyrocysta sp.
Figure9. Glaphyrocysta sp.
Figure10. Glaphyrocysta sp.
Figure11. Hafniasphera delicata
Figure12. Spiniferites sp.?
Figure13. Hystrichostrogylon sp.
Figure14. Impagidinium sp., dorsal view (black arrow: apex)
Figure15. Impagidinium sp., ventral view [same as fig. 14]
Figure16. Impagidinium sp., ventral view
Figure17. Impagidinium sp., dorsal view [same as fig.16]
Figure18. Impagidinium sp. (black arrow: apex)
Figure19. Impagidinium sp. (black arrow: apex)
Figure20. Impagidinium sp. (black arrow: apex)

Plate 4

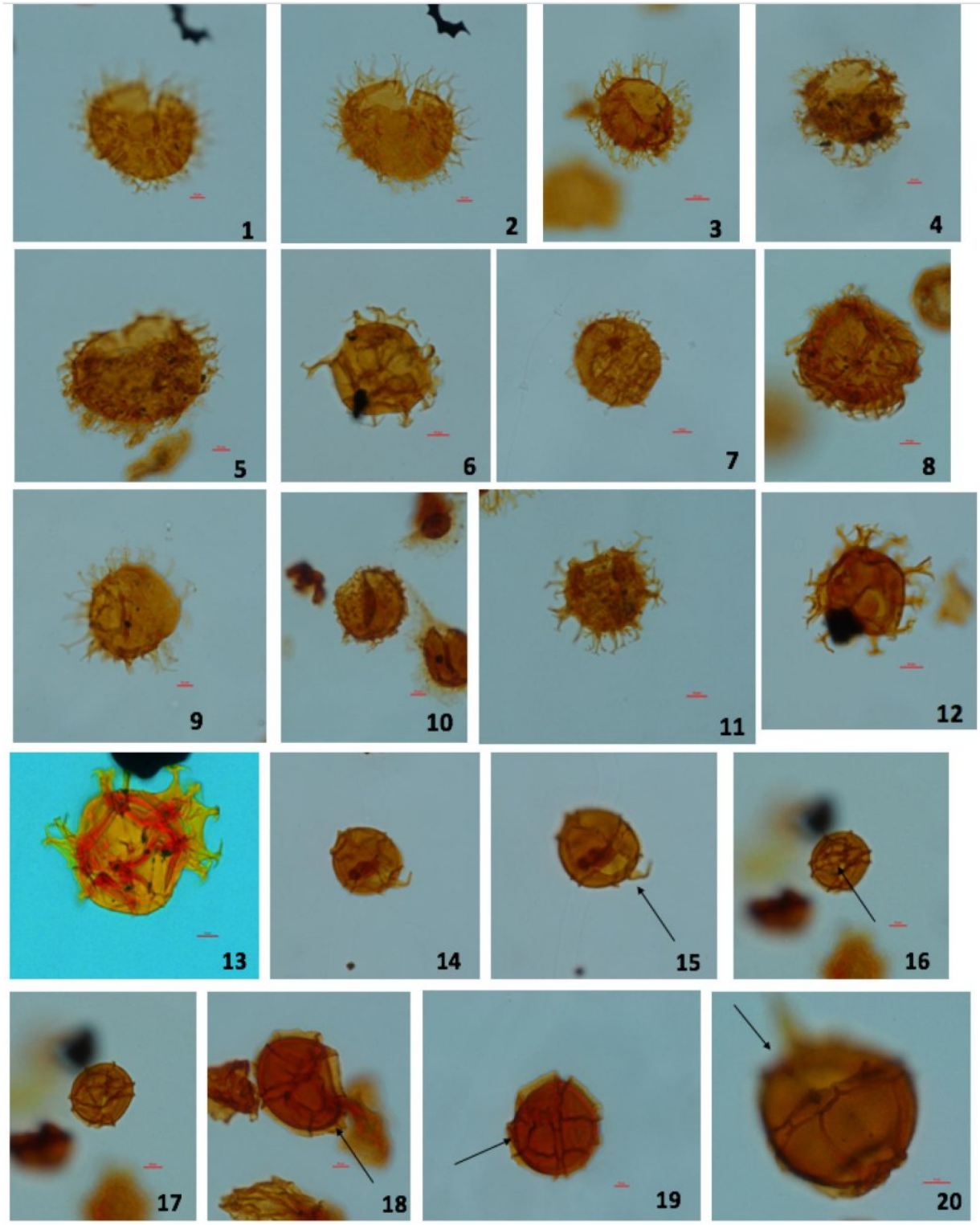

Plate 5

Figure1. Lingulodinium funginum
Figure2. Lingulodinium funginum
Figure3. Dinocyst indet.
Figure4. Lingulodinium funginum
Figure5. Lingulodinium funginum
Figure6. Lingulodinium funginum
Figure7. Lingulodinium funginum
Figure8. Lingulodinium funginum
Figure9. Lingulodinium funginum
Figure10. Lingulodinium funginum
Figure11. Operculodinium sp.?
Figure12. Lingulodinium funginum
Figure13. Dapsilidinium pseuocolligerum
Figure14. Dapsilidinium pseuocolligerum
Figure15. Hafniasphera sp.
Figure16. Operculodinium centrocarpum, archeopyle view [scale 50um]
Figure17. Operculodinium centrocarpum, ventral surface
Figure18. Operculodinium centrocarpum
Figure19. Operculodinium centrocarpum
Figure20. Operculodinium centrocarpum

Plate 5

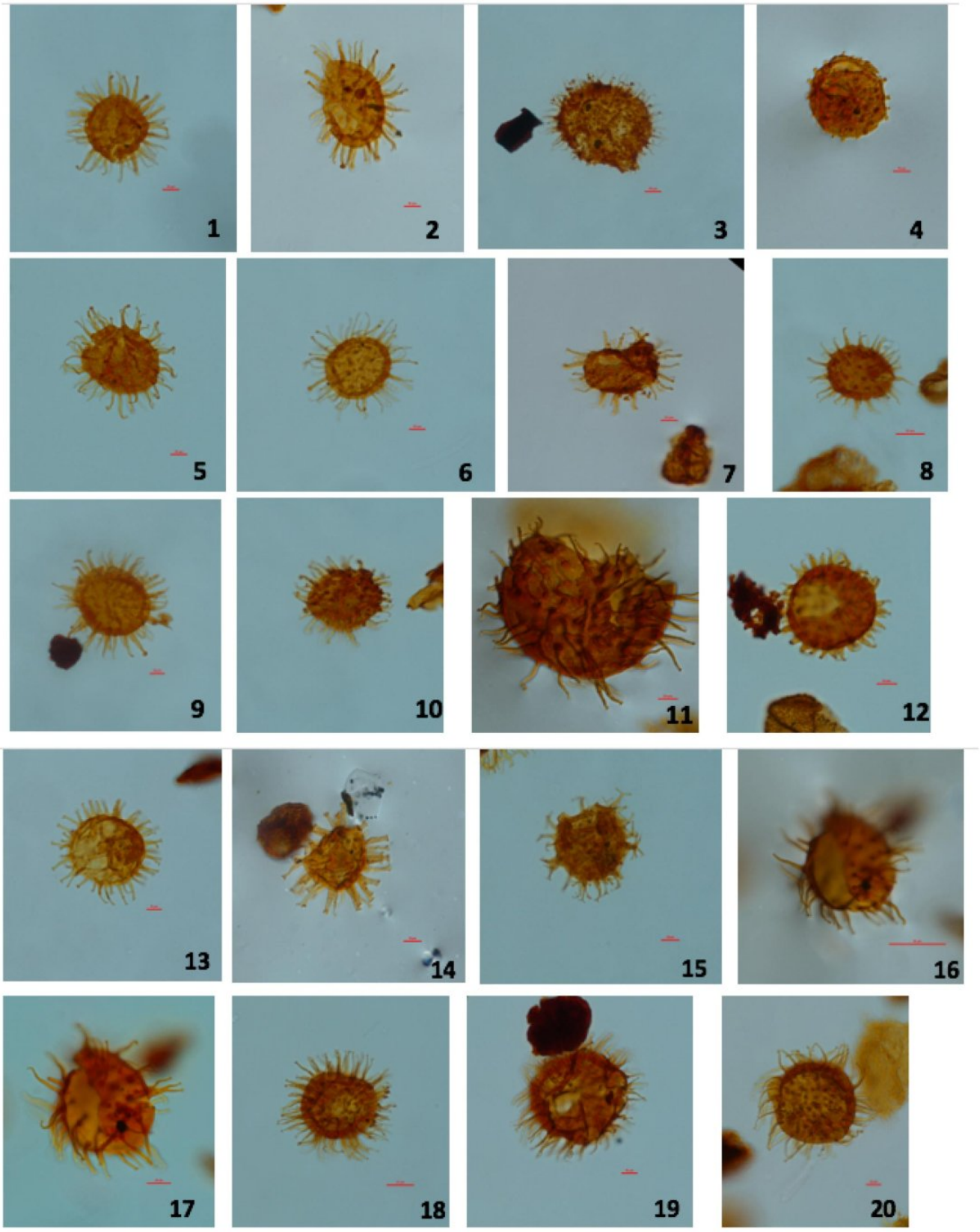

Plate 6

Figure1. Cleistosphaeridium diversispinosum, apical plate
Figure2. Palaeocystodinium bulliforme
Figure3. Palaeoperidinium pyrophorum
Figure4. Palaeoperidinium pyrophorum
Figure5. Palaeoperidinium pyrophorum
Figure6. Palaeoperidinium pyrophorum
Figure7. Lentinia sp.
Figure8. Lentinia sp.
Figure.9. Rhombodinium sp.
Figure10. Rottnestia borussica
Figure11. Wetzeliella caviarticulata, ventral surface
Figure12. Wetzeliella caviarticulata, ventral view [same as fig. 11]
Figure13. Wetzeliella caviarticulata
Figure14. Wetzeliella gochtii
Figure15. Wetzeliella gochtii
Figure16. Spiniferites sp.
Figure17. Spiniferites sp.
Figure18. Spiniferites sp.
Figure19. Spiniferites sp.
Figure20. Spiniferites sp.

Plate 6

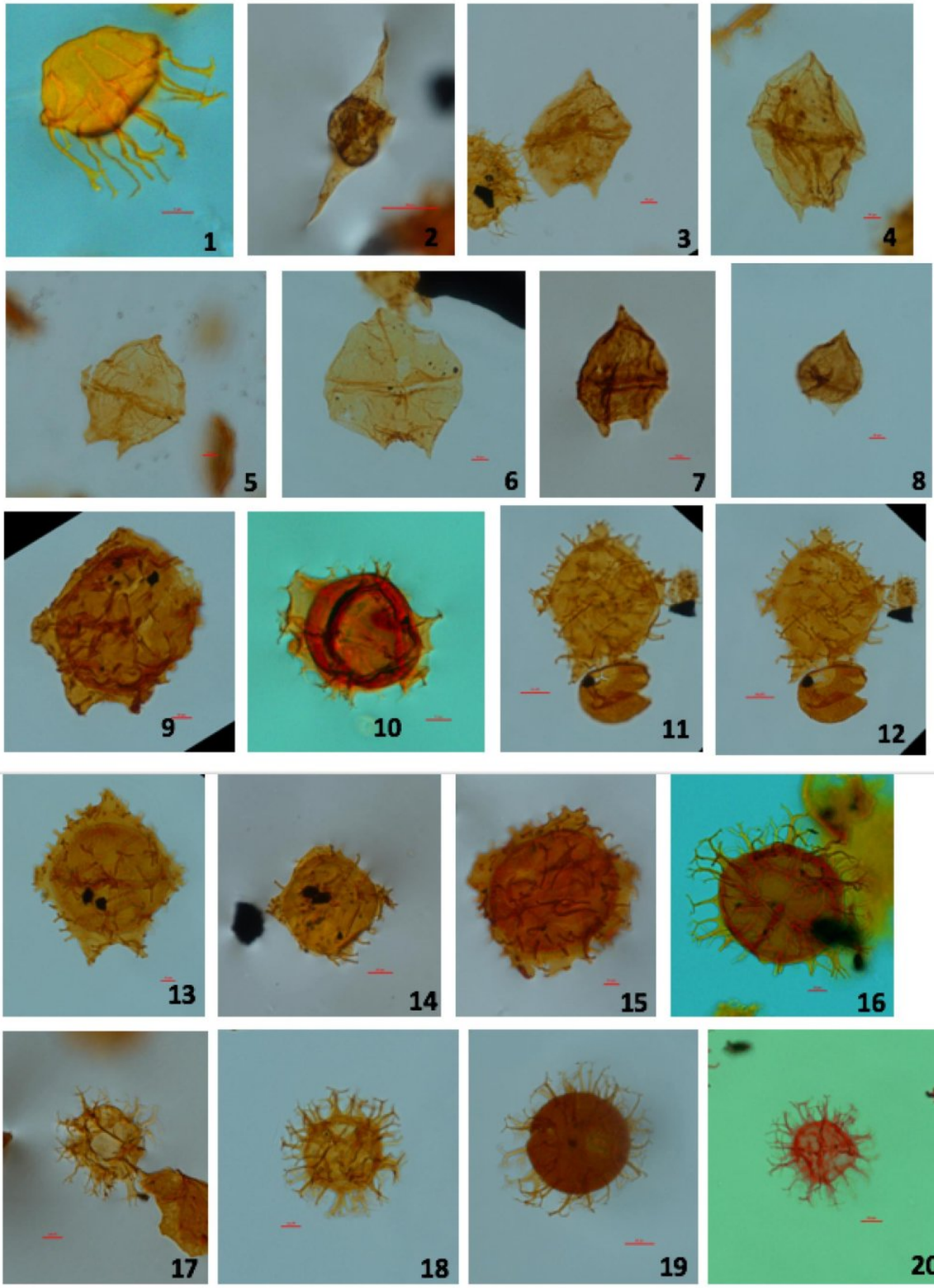

Middle to upper Eocene dysoxic-anoxic Kuma Formation (northeast Peri-Tethys): Biostratigraphy and paleoenvironments

Vladimir N. Beniamovski* Geological Institute of Russian Academy of Sciences, Pyzhevsky 7, 119017, Moscow, Russia

Alexander S. Alekseev Department of Paleontology, Geological Faculty, Moscow State University, 119992, Moscow, Russia

Mariya N. Ovechkina Paleontological Institute of Russian Academy of Sciences, Profsoyuinaya 123, 117868. Moscow, Russia

Hedi Oberhansli* GeoForschung Zentrum Potsdam, Telegrafenberg, D-14473, Potsdam, Germany

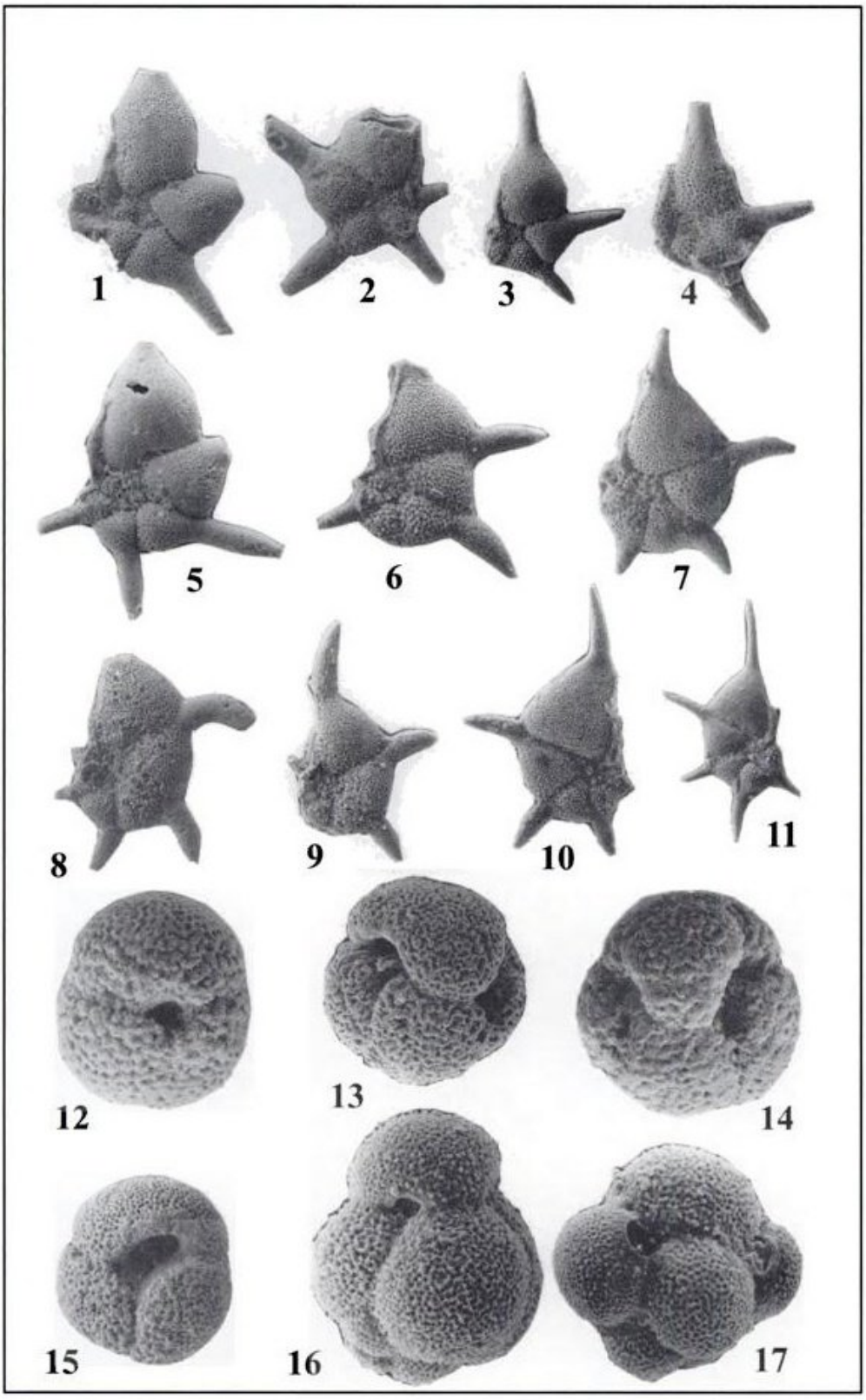

Figure 7. Planktonic foraminifera from the middle Eocene of the Crimea (Bakhchisaray Section), Pre-Caucasus (Keresta Section) and western coast of the Aral sea (Aktumsuk Section). 1–4—*Hantkenina mexicana* Cushman: Bakhchisaray: 1—sample 9 (× 70), 2—sample 34 (× 70), 3—sample 19 (× 70), 4—9 (× 70); 5—*Hantkenina liebusi* Shokhina, sample 19 (× 100); 6—*Hantkenina alabamensis compressa* Parr, sample 43 (× 70); 7—10 *Hantkenina australis* Finlay: 7—Bakhchisaray, sample 43 (× 70), 8—Bakhchisaray, sample 43 (× 70), 9—Bakhchisaray, sample 43 (× 70), 10—Aktumsuk, sample 104 (× 70); 11—*Hantkenina dumblei* Weinzierl and Applin, Bakhchisaray, sample 43 (× 80); 12—*Globigerinatheka micra* (Shutskaya), sample 1 (× 120); 13–14 *Globigerinatheka subconglobata* (Shutskaya) transition to *Globigerinatheka index* (Finlay), 13—Keresta, sample 38 (× 80), 14—Bakhchisaray, sample 19 (× 100), 15—*Globigerinatheka index* (Finlay), Bakhchisaray, sample 38 (× 100), 16—*Catapsydrax unicavus* Bolli, Loeblich and Tappan, Aktumsuk, sample 104(× 130), 17—*Catapsydrax dissimilis* (Cushman and Bermudes), sample 104 (× 100).

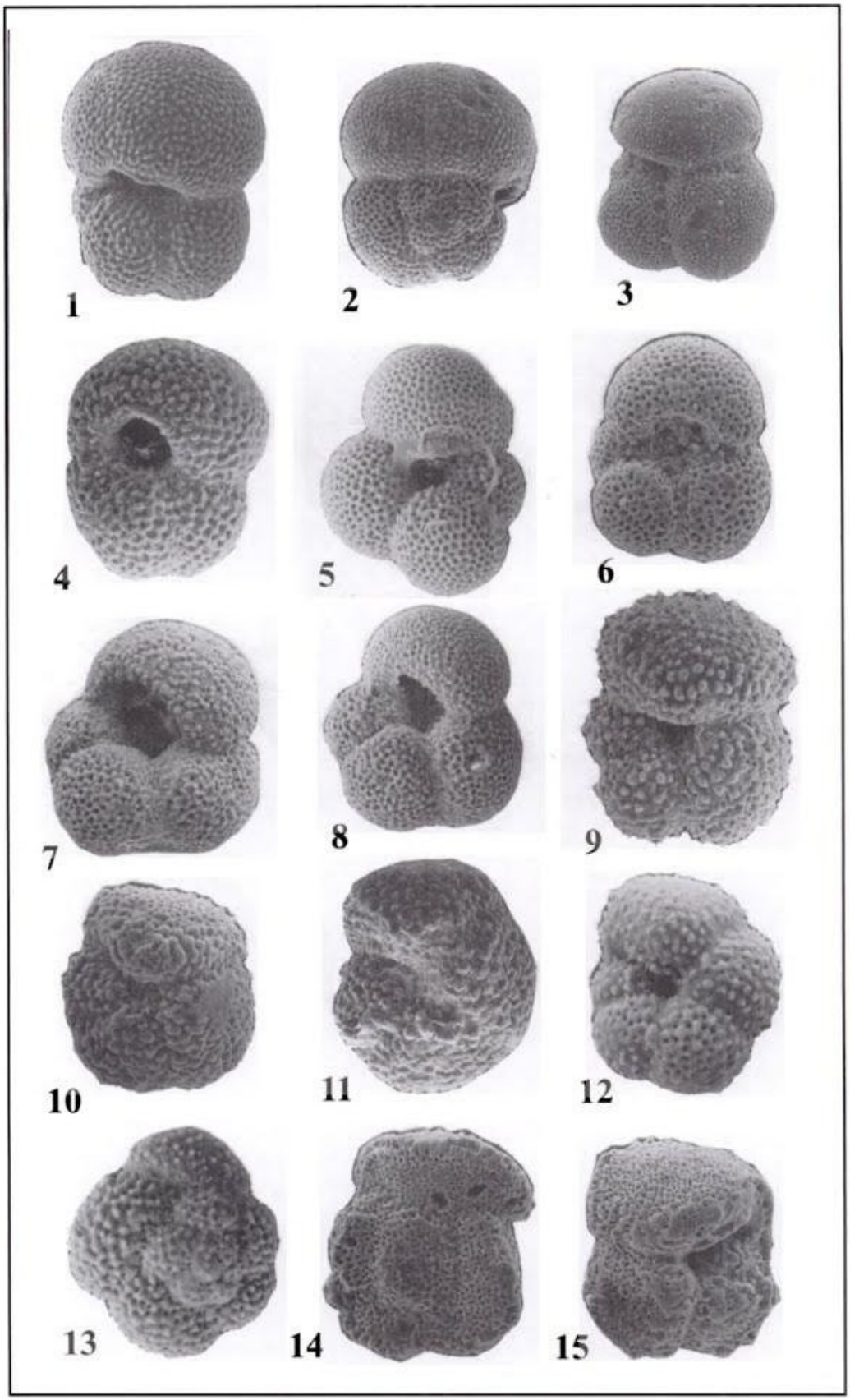

Figure 8. Planktonic foraminifera from the middle Eocene of the Crimea (Bakhchisaray Section) and Pre-Caucasus (Keresta Section). 1, 2—*Turborotalia boweri* (Bolli), Keresta, sample 36 (× 100); 3—*Turborotalia possagnoensis* (Toumarkine and Bolli), Keresta, sample 36 (× 80); 4—*Turborotalia frontosa* (Subbotina), Bakhchisaray, sample 1 (× 150); 5—*Subbotina turcmenica* (Khalilov), Bakhchisaray, sample 48 (× 130); 6—*Subbotina azerbaidjanica* (Khalilov), Keresta, sample 20 (× 120); 7—*Subbotina yeguaensis* (Weinzierl and Applin), Bakhchisaray, sample 48 (× 130); 8—*Subbotina turcmenica* (Khalilov), Keresta, sample 20 (× 120); 9—*Acarinina triplex* Subbotina, Keresta, sample 44 (× 130); 10—*Acarinina bullbrooki* Bolli, Keresta, sample 40 (× 130); 11—*Acarinina rotundimarginata* Subbotina, Bakhchisaray, sample 98/1 (× 130); 12, 13—*Acarinina rugosoaculeata* Subbotina, Bakhchisaray, sample 48 (× 180); 14, 15—*Truncorotaloides topilensis* (Cushman), Keresta, sample 30 (× 100).

The progression of environmental changes during the onset of the Paleocene-Eocene thermal maximum (New Jersey Coastal Plain)

Peter STASSEN Department of Earth and Environmental Sciences, KU Leuven, Celestijnenlaan 200E, B-3001, Leuven, Belgium

Ellen THOMAS Department of Geology and Geophysics, Yale University, Whitney Avenue 210, New Haven, Connecticut 06520-8109, USA

Robert P. SPEIJER Earth and Environmental Sciences, Wesleyan University, Exley Science Center 459, Middletown, Connecticut 06459, USA

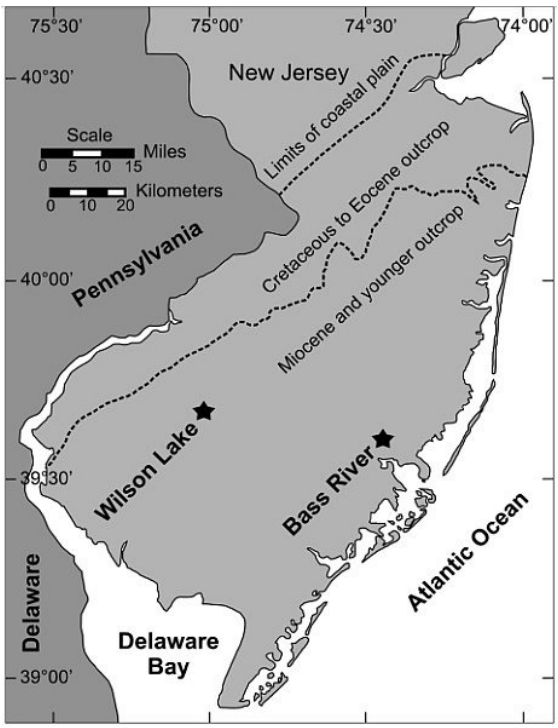

FIGURE 1: Location of the Wilson Lake and Bass River core sites (modified after Miller, 1997).

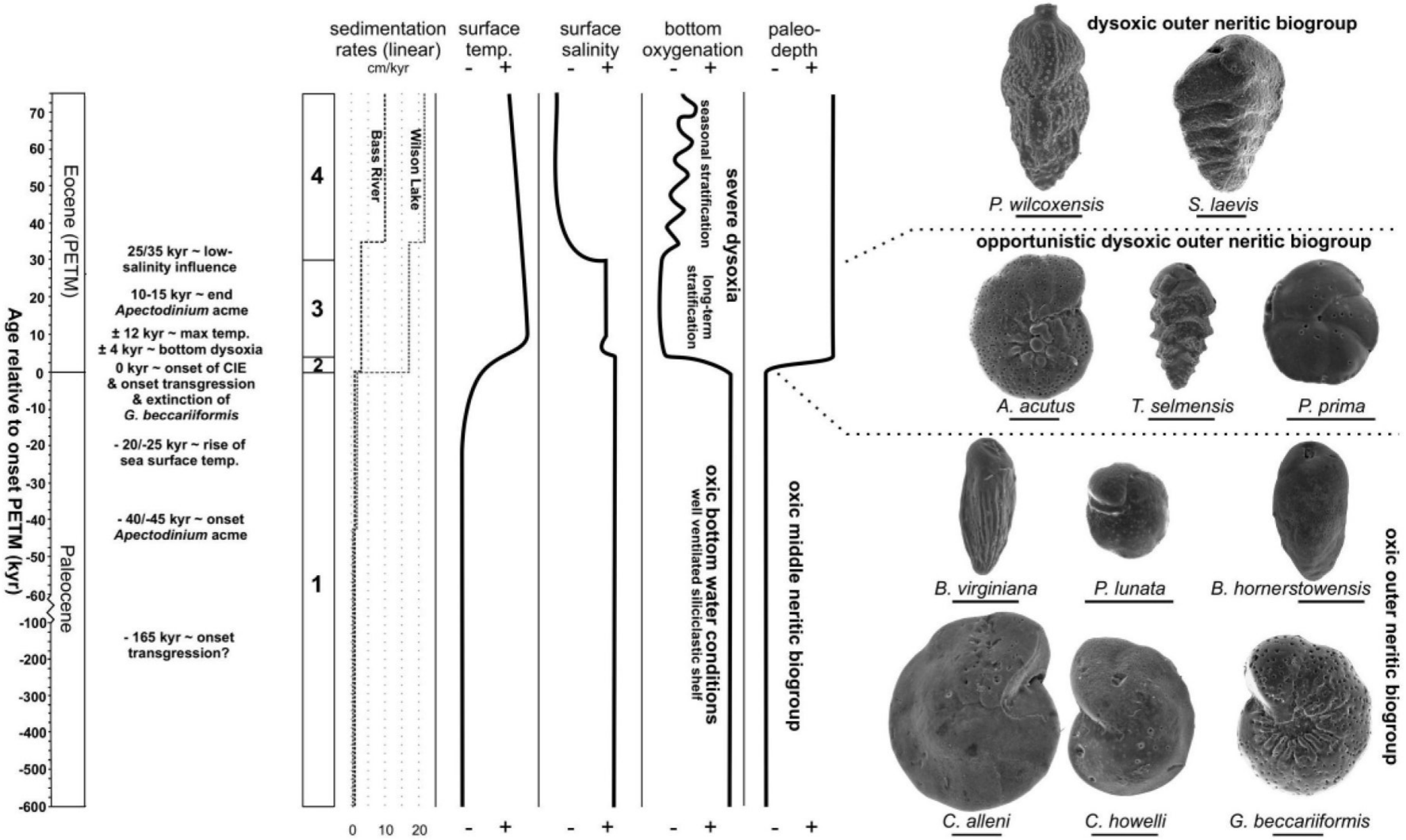
Age relative to onset PETM (kyr)
70
60
50
40
30
20
10
0
-10
-20
-30
-40
-50
-60
-100
-200
-300
-400
-500
-600
Eocene (PETM)
Paleocene
25/35 kyr ~ low-salinity influence
10-15 kyr ~ end Apectodinium acme
± 12 kyr ~ max temp.
± 4 kyr ~ bottom dysoxia
0 kyr ~ onset of CIE & onset transgression & extinction of G. beccariiformis
- 20/-25 kyr ~ rise of sea surface temp.
- 40/-45 kyr ~ onset Apectodinium acme
- 165 kyr ~ onset transgression?
4
3
2
1
sedimentation rates (linear)
cm/kyr
Bass River
Wilson Lake
0
10
20
surface temp.
surface salinity
bottom oxygenation
seasonal stratification
long-term stratification
severe dysoxia
oxic bottom water conditions
well ventilated siliciclastic shelf
paleo-depth
oxic middle neritic biogroup
dysoxic outer neritic biogroup
P. wilcoxensis
S. laevis
opportunistic dysoxic outer neritic biogroup
A. acutus
T. selmensis
P. prima
oxic outer neritic biogroup
B. virginiana
P. lunata
B. hornerstowensis
C. alleni
C. howelli
G. beccariiformis

Jardine, Phil. 2011. The Paleocene-Eocene Thermal Maximum. Palaeontology Online, Volume 1, Article 5, 1-7.

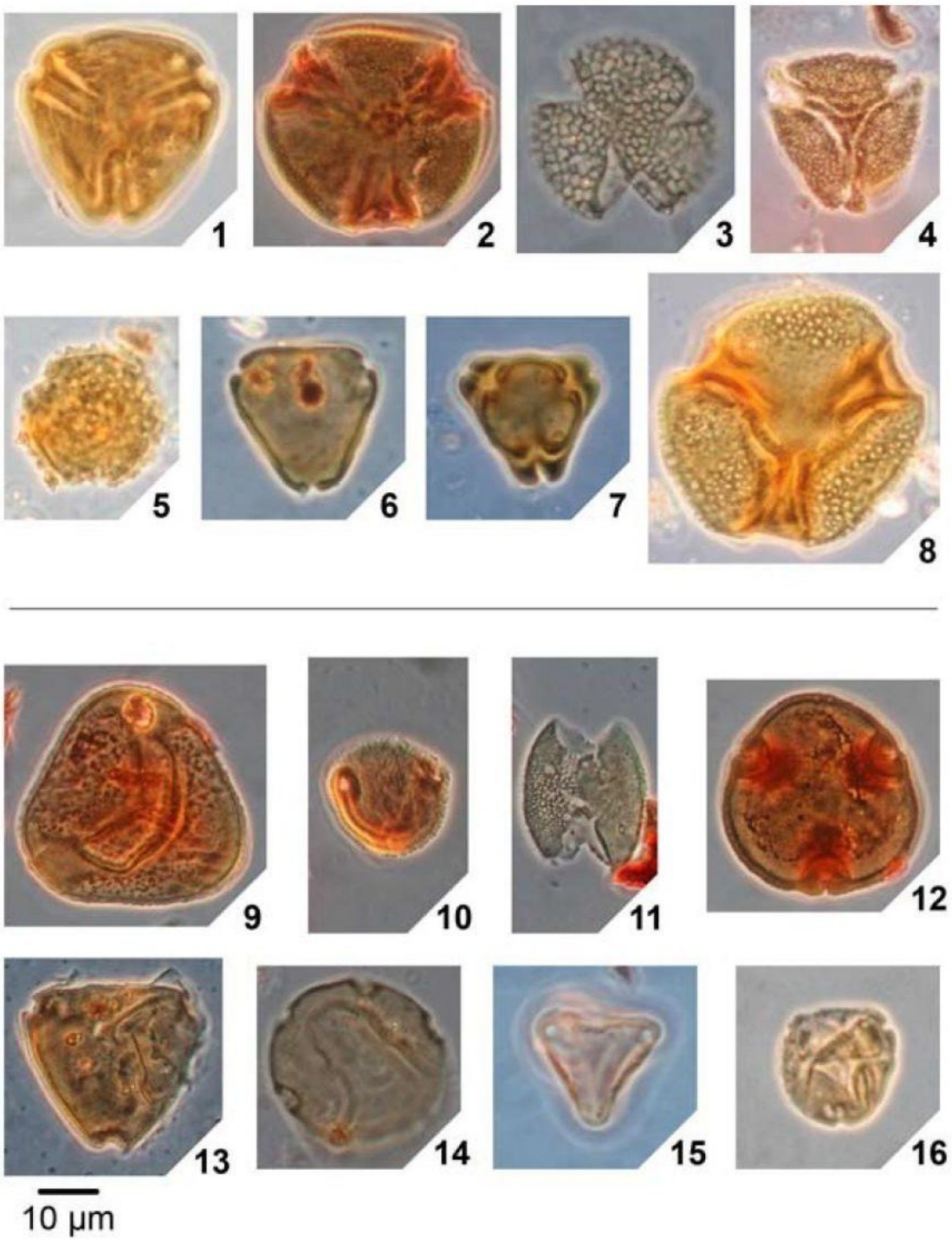

Figure 5 - Pollen and spores from Mississippi and Alabama, United States, representing plant types that either went extinct (1–8) or first appeared (9–16) at the Paleocene–Eocene boundary. 1, Holkopollenites chemardensis; 2, Lanagiopollis cribellata; 3, Retitrescolpites anguloluminosus; 4, Insulapollenites rugulatus; 5, Spinaepollis spinosus; 6, Momipites strictus; 7, Trudopollis plenus; 8, Lanagiopollis lihoka; 9, Granulatisporites luteticus; 10, Brosipollis striata; 11, Dicolpopollis sp.; 12, Intratriporopollenites instructus; 13, Symplocos contracta; 14, Celtis tschudyi; 15, Interpollis microsupplingensis; 16, Platycarya platycaryoides.

Jardine, Phil. 2011. The Paleocene–Eocene Thermal Maximum.
Palaeontology Online, Volume 1, Article 5, 1–7.

Cooling Event in the Boundary of Middle/Late Eocene of Java

Eko Budi Lelono, R&D Center for Oil and Gas Technology “LEMIGAS”, Indonesia

Abstract: The indication of Eocene climatic changes is defined based on the change of abundance and diversity of palynomorphs occurring in the Nanggulan Formation. This is possible because this formation has been found to yield the richest and most diverse palynomorph assemblages of Eocene age in Southeast Asia. Palynological evidence, from the distribution of index taxa and palynological events, indicates that the Nanggulan Formation was deposited during the Middle to Late Eocene as marked by the constant occurrence of Longapertites vaneendenbergi, Proxapertites operculatus, Proxapertites cursus and Cicatricosisporites eocenicus. The Middle Eocene age is characterised by high abundance and diversity of rain forest elements suggesting warm and wet climate which include Palmaepollenites kutchensis, Sapotaceoidaepollenites spp., Retitricolporites equatorialis, Campnosperma sp., Marginipollis concinus and Dicolpopollis malesianus. On the other hand, the Late Eocene age is marked by the appearance of the hinterland element Podocarpidites spp. and the disappearance of the main rain forest elements indicating cool and dry climate. In this case, cooling event is defined by the occurrence hinterland element of Podocarpidites spp. which can be used for recognising Middle/ Late Eocene boundary.

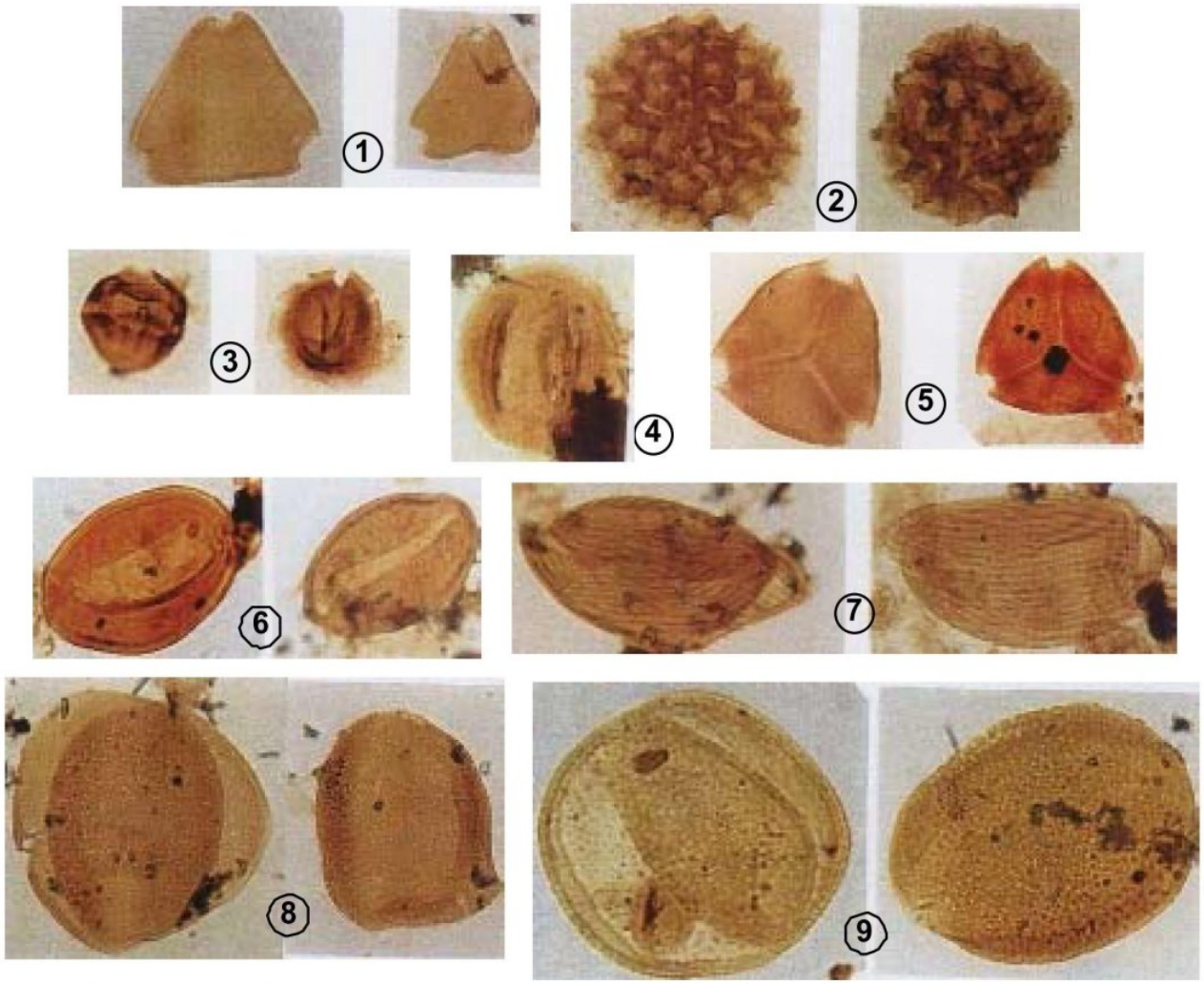

Fig. 4 Key palynomorphs to designate the Eocene age. All taxa are 1000×. (1) aff. Beaupreadites matsuokae; (2) Ruellia type; (3) Polygalacidites clarus; (4) Ixonanthes type; (5) Cupanieidites cf. flaccidiformis; (6) Palmaepolienites kutchensis; (7) Cicatricososporites eocenicus; (8) Proxapertites operculatus; (9) Proxapertites cursus.

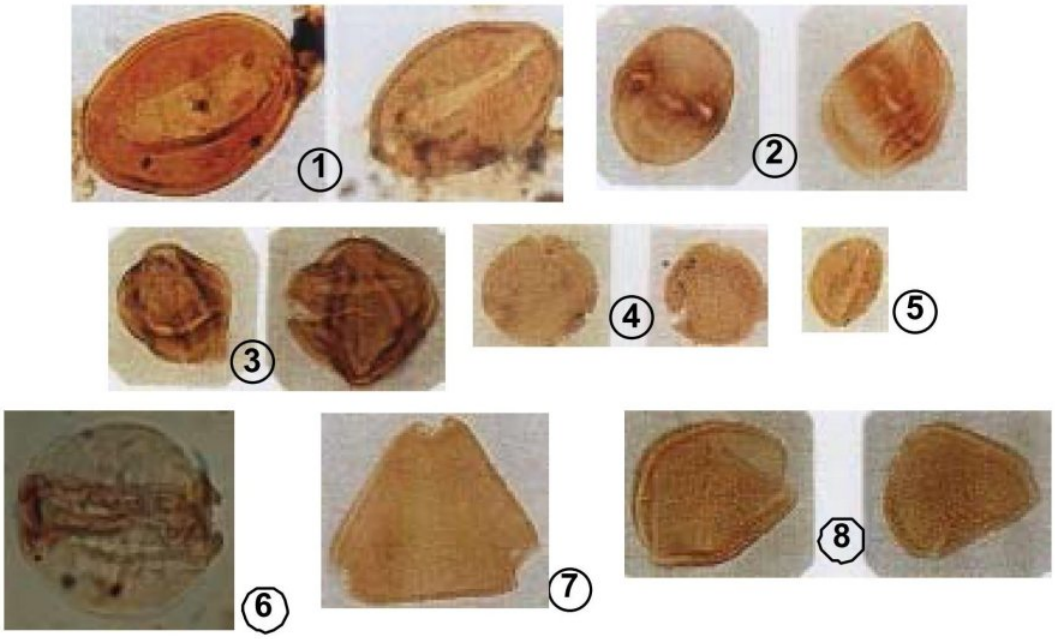

Fig. 5 Some palynomorphs represent lowland/rain forest elements and wet climate indicators. All taxa are 1000×. (1) Palmaepollenites kutchensis; (2) Sapotaceoidaepollenites spp.; (3) Retiricolporites equatorialis; (4) Blumeodendron; (5) Campnosperma; (6) Marginipollis concinus; (7) aff. Beaupreadites matsuokae; (8) Dicolpopollis malesianus.

Fig. 6 The occurrence of cooler climate in Late Eocene as indicated by dramatic decrease of abundance and diversity of palynomorphs.

Fig. 7 Cool/dry climate indicators which commonly occur in the Late Eocene. All taxa are 1000×. (1) Podocarpidites spp.; (2) Restioniidites ounctulosus.

Late Paleocene-early Eocene dinoflagettate cyst records from the Tethys: Further observations on the global distribution of Apectodinium

Erica M. Crouch, Henk Brinkhuis Henk Visscher Laboratory of Palaeobotany and Palynology, Department of Geobiology, Utrecht University, Budapestlaan 4, 3584CD Utrecht, The Netherlands

Thierry Adatte Marie-Pierre Bolle Institut de Geologic, 1 1 Emile Argand, Universite de Neuchatel, 2007 Neuchatel, Switzerland

ABSTRACT To further understand the distribution and abundance of Apectodinium through space and time, dinoflagellate cyst (dinocyst) records from two well-calibrated Paleo- gene sections in the Tethys (Tunisia and Uzbekistan) have been examined. Apecto dinium was present in the southern Tethys (Tunisia) by the late Paleocene (planktonic foraminiferal Subzone P4a), confirming earlier findings that the genus evolved in lower latitudes. Apectodinium abundance was frequent to dominant from the upper Paleocene to lower Eocene in the Tethys. The initial Eocene thermal maximum (IETM) at lower latitudes appears to be characterized by high percentages of Apectodinium, although it may not always have dominated assemblages. Other dinocyst genera with thermophilic preferences may be abundant during the IETM. At mid to high latitudes, Apectodinium has been sporadically recognized during the upper Paleocene. Never theless, the IETM at mid to high latitudes was still characterized by Apectodinium- dominated assemblages. Additional Apectodinium acmes occurred in the lower Eocene, although as yet it is unclear if these are globally isochronous. Intervals of Apectodinium - dominated assemblages are indicative of environmental conditions that were apparently markedly different to “normal background settings” of the late Paleocene-early Eocene. Sea surface temperature (SST) was probably the main con trol in distribution since Apectodinium acmes at mid to high latitudes seem to have oc curred during intervals of highest SSTs, such as the IETM. In addition, the probable heterotrophic Ape ctodinium “blooms” were intricately linked to enhanced runoff and increased delivery of nutrients in surface waters, probably as a result of intensifica tion of the weathering cycle and other possible specific oceanic conditions.

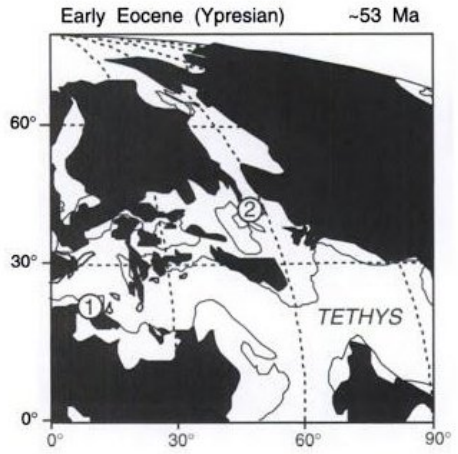

Figure 2. Paleogeographic reconstruction of the Tethys region during the early Eocene (ca. 53 Ma) with location of the Elles section, Tunisia (1) and Aktumsuk section, Uzbekistan (2). Map modified from Smith et al. (1994).

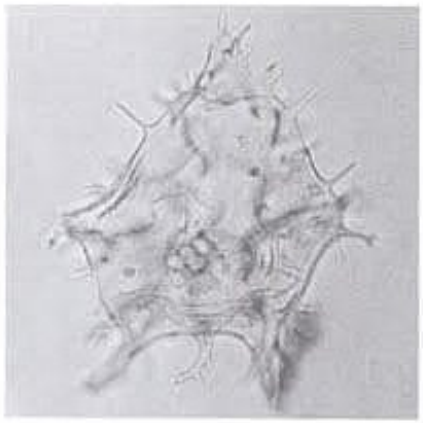
1

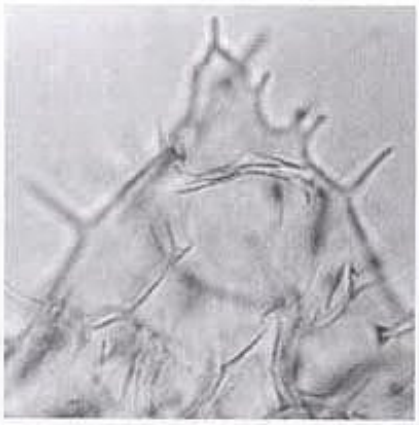
2

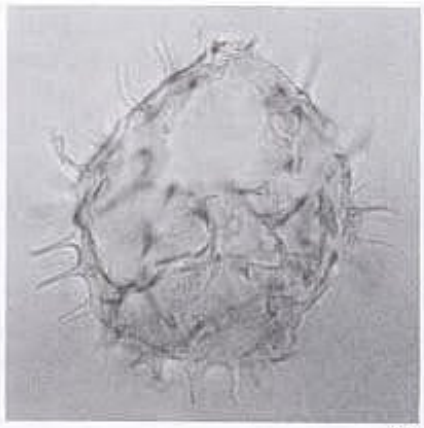
3

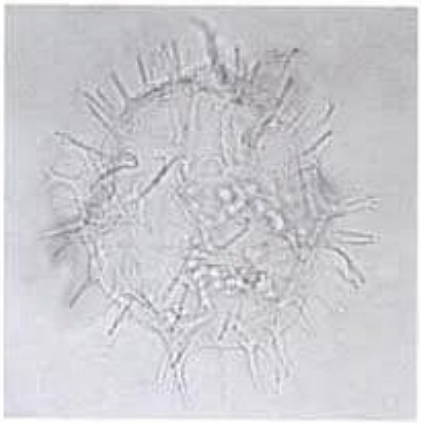
4

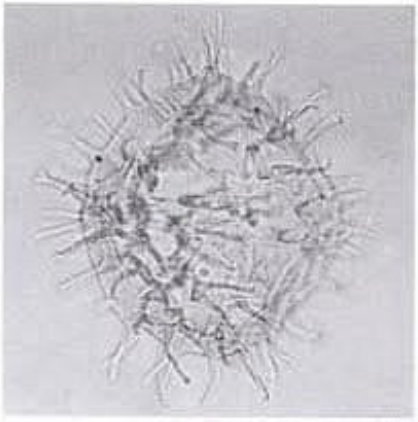
5

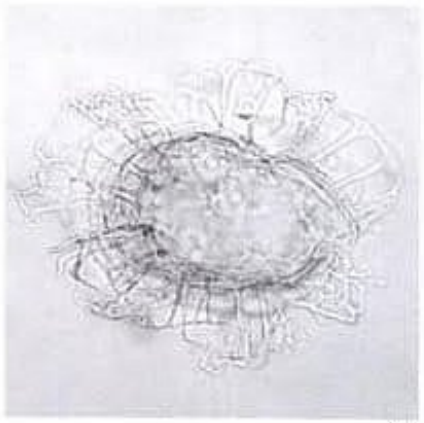
6

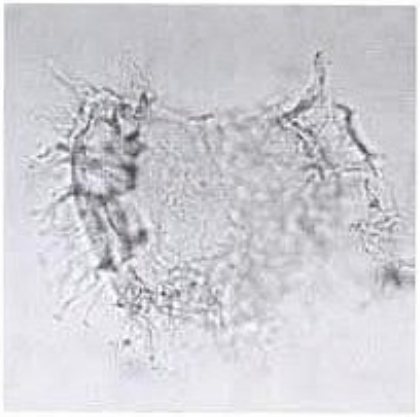
7

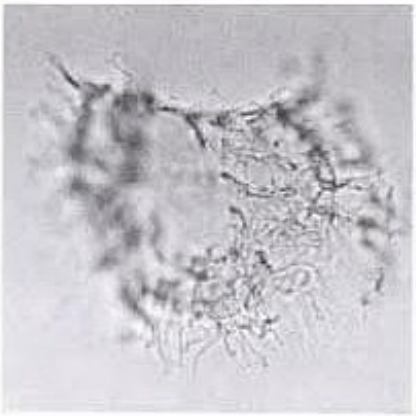
8

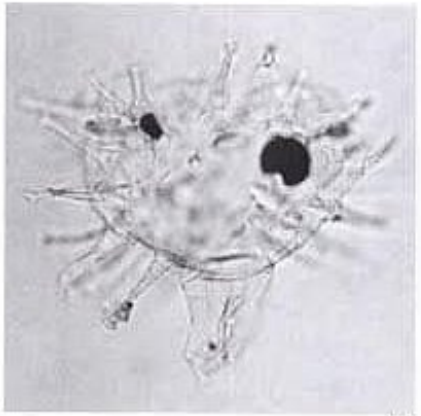
9

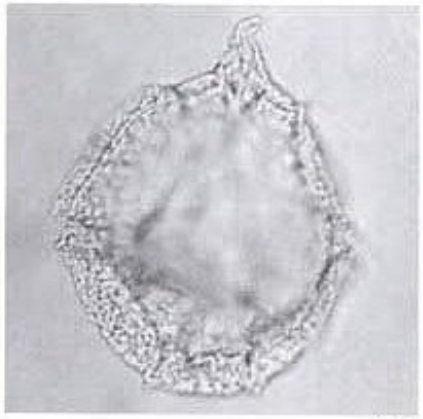
10

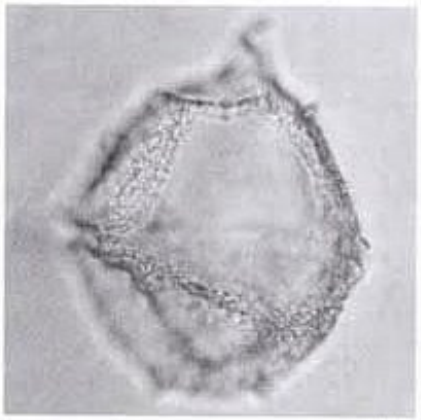
11


12

Plate 1. **1:** *Apectodinium* sp. Sample AM16, Slide 1 (E24/3). Aktumsuk section. Overall dimensions ~87 µm by 103 µm. Archeopyle that involves two plates; 2a and 4″ plates. **2:** *Apectodinium* sp. Sample AM16, Slide 1 (E24/3). Aktumsuk section. Vertical dimension ~60 µm; close up of archeopyle (2a and 4″ plates). **3:** *Apectodinium* sp. Sample EL145 (~35.75 m), Slide 1 (H24/0). Elles section. Overall dimensions ~80 µm by 85 µm. Archeopyle that involves two plates; 2a and 4″ plates. **4:** *Apectodinium* sp. Sample EL136 (~33.43 m), Slide 1 (R22/3). Elles section. Overall dimensions ~79 µm by 85 µm. **5:** *Apectodinium* sp. Sample EL162 (~41.8 m), Slide 1 (E20/0). Elles section. Overall dimensions ~90 µm by 100 µm. **6:** *Adnatosphaeridium multispinosum.* Sample EL59 (~18.4 m), Slide 1 (K20/3). Elles section. Overall dimensions ~78 µm by 98 µm. **7** and **8:** *Areoligera senonensis* group. Sample EL111 (~26.92 m), Slide 1 (U33/3). Elles section. Overall dimensions ~65 µm by 95 µm. **9:** *Diphyes colligerum.* Sample AM17, Slide 1 (P30/0). Aktumsuk section. Overall dimensions ~58 µm by 50 µm. **10** and **11:** *Cribroperidinium* sp. A. Sample AM19, Slide 1 (P35/0). Aktumsuk section. Overall dimensions ~50 µm by 61 µm. **12:** *Deflandrea phosphoritica.* Sample AM17, Slide 1 (R22/0). Aktumsuk section. Overall dimensions ~70 µm by 120 µm.

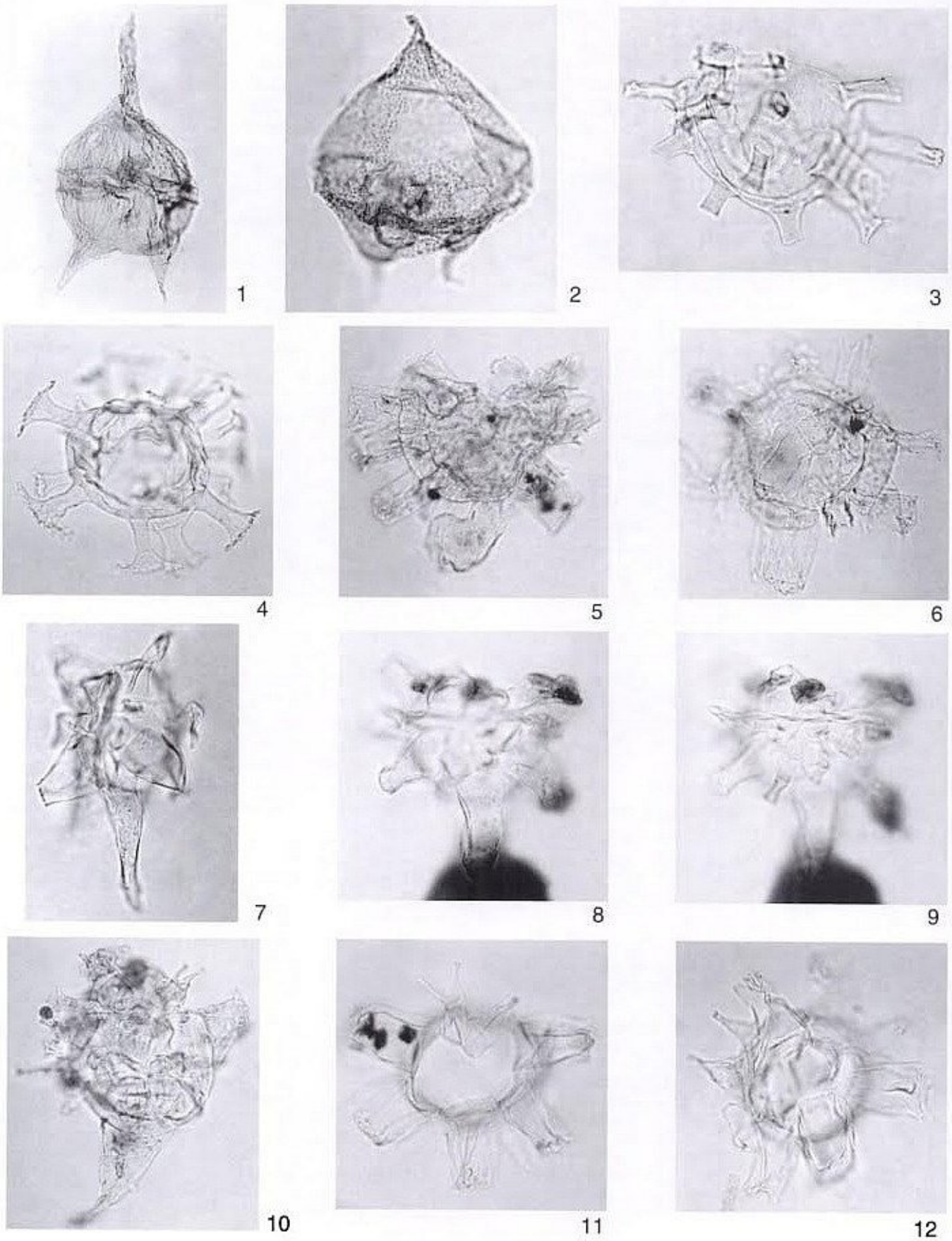

Plate 2. **1:** *Deflandrea denticulaa.* Sample EL76 (~21.8 m), Slide 2 (W28/0). Elles section. Overall dimensions ~52 µm by 104 µm. **2:** *Cerodinium depressum.* Sample EL171 (~42.74 m), Slide 1 (O33/3). Elles section. Overall dimensions ~58 µm by 75 µm. **3:** *Homotryblium pallidum* Sample EL59 (~18.4 m), Slide 1 (P13/1). Elles section. Overall dimensions ~87 µm by 50 µm. **4:** *Hystrichokolpoma* sp. cf. *H. rigaudiae.* Sample EL136 (~33.43 m), Slide 1 (S19/0). Elles section. Overall dimensions ~100 µm by 88 µm. **5:** *Hystrichokolpoma* sp. cf. *H. granulatum.* Sample EL175 (~43.29 m), Slide 1 (P16/0). Elles section. Overall dimensions ~87 µm by 77 µm. **6:** *Hystrichokolpoma* sp. cf. *H. granulatum.* Sample EL152 (~37.38 m), Slide 1 (Q24/0). Elles section. Overall dimensions ~71 µm by 75 µm. **7:** *Hystrichokolpoma* sp. cf. *H. cinctum.* Sample AM20, Slide 1 (G34/0). Aktumsuk section. Overall dimensions ~50 µm by 80 µm. **8** and **9:** *Hystrichokolpoma* sp. cf. *H. cinctum.* Sample AM14, Slide 1a (T24/0). Aktumsuk section. Overall dimensions ~58 µm by 55 µm. **10:** *Hystrichokolpoma rigaudiae.* Sample AM16, Slide 1 (J30/2). Aktumsuk section. Overall dimensions ~75 µm by 92 µm. **11:** *Hystrichokolpoma* sp. cf. *H. salacium.* Sample AM17, Slide 2 (V26/3). Aktumsuk section. Overall dimensions ~73 µm by 65 µm. **12:** *Hystrichokolpoma* sp. cf. *H. salacium.* Sample AM19, Slide 1 (S30/2). Aktumsuk section. Overall dimensions ~60 µm by 60 µm.

1

2

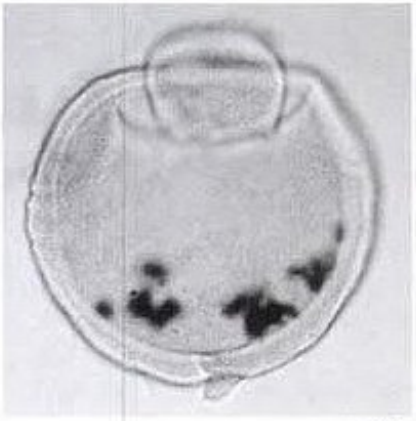

3

4

5

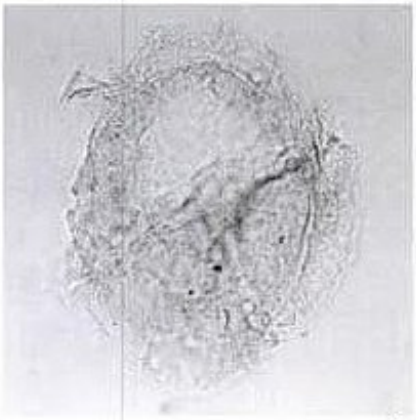

6

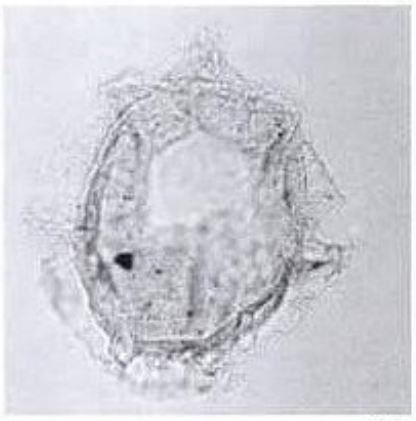

7

8

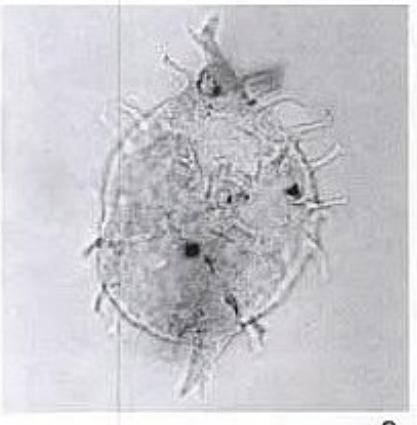

9

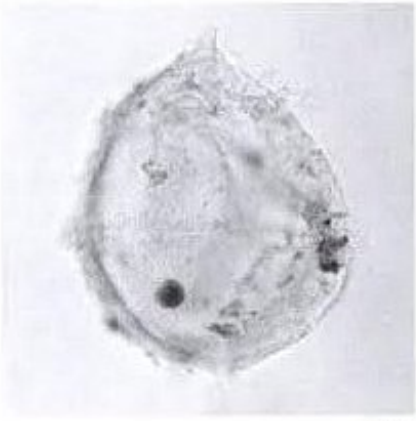

10

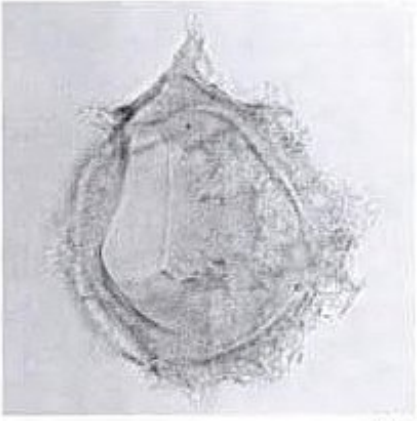

11

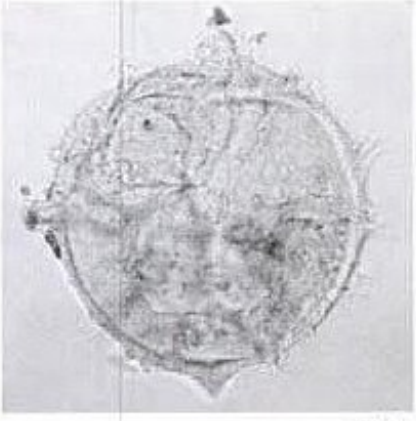

12

Plate 3. **1:** *Kallosphaeridium yorubaense.* Sample EL123 (~30.04 m), Slide 1 (R18/0). Elles section. Overall dimensions ~54 µm by 53 µm. **2:** *Kallosphaeridium yorubaense.* Sample AM19, Slide 1 (U34/1). Aktumsuk section. Overall dimensions ~60 µm by 65 µm. **3.** *Carpatella?* sp. A. Sample AM17, Slide 1 (F23/2). Aktumsuk section. Overall dimensions ~80 µm by 80 µm. **4:** *Kenleyia* complex. Sample EL111 (~26.92 m), Slide 1 (N32/0). Elles section. Overall dimensions ~55 µm by 70 µm. **5:** *Kenleyia* complex. Sample EL166 (~42.21 m), Slide 1 (W19/2). Elles section. Overall dimensions ~75 µm by 93 µm. **6:** *Kenleyia* complex. Sample EL145 (~35.75 m), Slide 1 (X26/0). Elles section. Overall dimensions ~80 µm by 95 µm. **7:** *Kenleyia* complex. Sample EL145 (~35.75 m), Slide 1 (F28/0). Elles section. Overall dimensions ~82 µm by 95 µm. **8:** *Kenleyia* complex. Sample EL123 (~30.04 m), Slide 1 (J16/4). Elles section. Overall dimensions ~65 µm by 85 µm. **9:** *Kenleyia* complex. Sample EL162 (~41.8 m), Slide 1 (R21/0). Elles section. Overall dimensions ~72 µm by 112 µm. **10:** *Kenleyia* complex. Sample AM15, Slide 1 (O28/4). Aktumsuk section. Overall dimensions ~75 µm by 90 µm. **11:** *Kenleyia* complex. Sample AM15, Slide 1 (Q22/3). Aktumsuk section. Overall dimensions ~85 µm by 100 µm. **12:** *Kenleyia* complex. Sample AM16, Slide 1a (T18/0). Aktumsuk section. Overall dimensions ~86 µm by 92 µm.

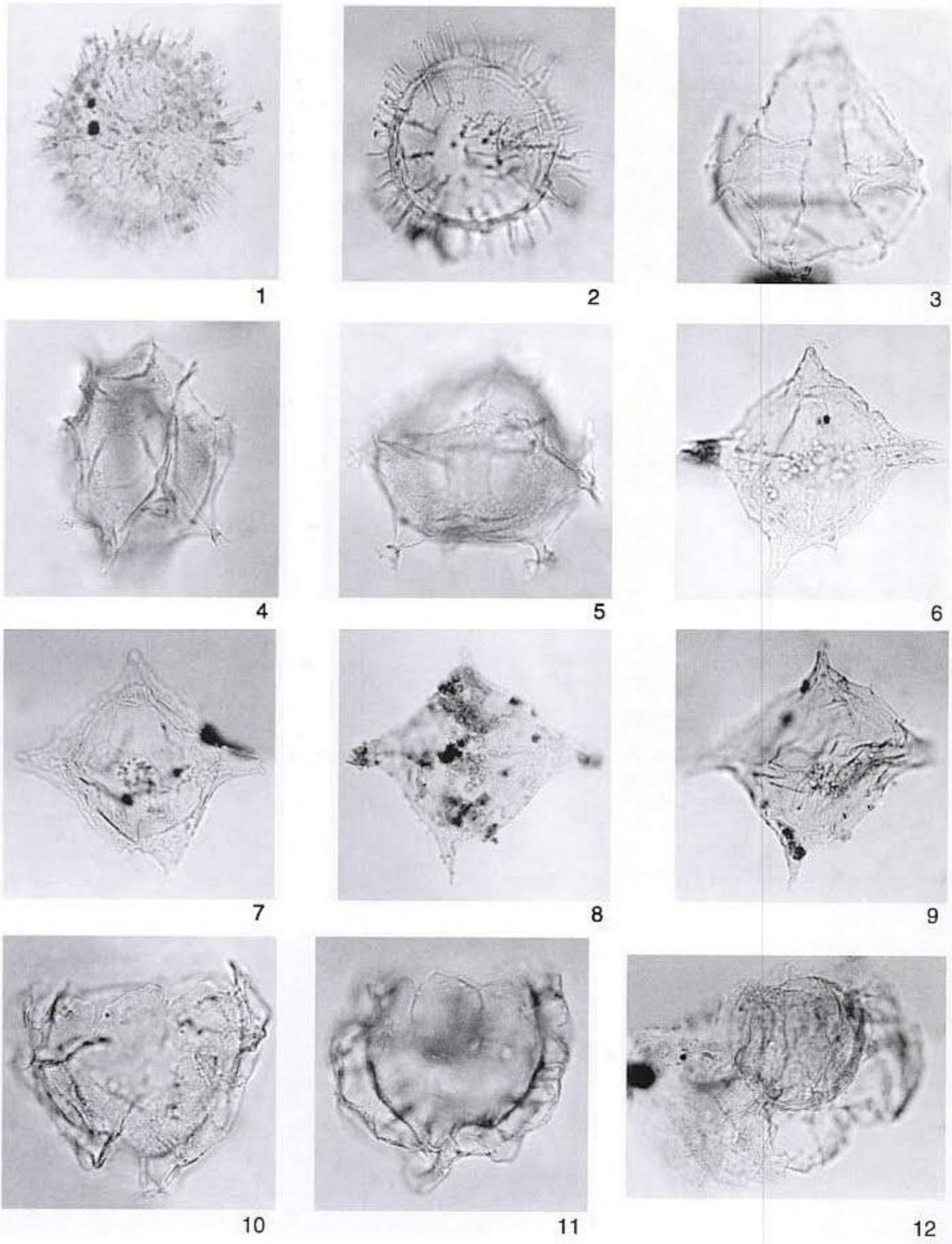

Plate 4. **1:** *Operculodinium severinii.* Sample AM15, Slide 1 (P23/1). Aktumsuk section. Overall dimensions ~80 µm by 85 µm. **2:** *Polysphaeridium* sp. Sample EL59 (~18.4 m), Slide 1 (J24/0). Elles section. Overall dimensions ~70 µm by 72 µm. **3:** *Phthanoperidinium crenulatum.* Sample AM16, Slide 1 (R27/2). Aktumsuk section. Overall dimensions ~54 µm by 63 µm. **4:** *Pentadinium* sp. cf. *P. goniferum.* Sample AM17, Slide 1 (R28/4). Aktumsuk section. Overall dimensions ~65 µm by 83 µm. **5:** *Pentadinium* sp. cf. *P. goniferum.* Sample AM17, Slide 2 (L28/0). Aktumsuk section. Overall dimensions ~100 µm by 90 µm. **6:** *Rhombodinium* sp. Sample AM17, Slide 2 (R37/0). Aktumsuk section. Overall dimensions ~93 µm by 88 µm. **7:** *Rhombodinium* sp. Sample AM18, Slide 1 (W18/2). Aktumsuk section. Overall dimensions ~95 µm by 86 µm. **8:** *Rhombodinium* sp. Sample AM15, Slide 1 (M26/0). Aktumsuk section. Overall dimensions ~98 µm by 92 µm. **9:** *Rhombodinium* sp. Sample AM16, Slide 1 (K26/2). Aktumsuk section. Overall dimensions ~96 µm by 95 µm. **10:** *Senoniasphaera?* sp. Sample AM19, Slide 1 (X20/2). Aktumsuk section. Overall dimensions ~72 µm by 66 µm. **11:** *Senoniasphaera?* sp. Sample AM21, Slide 1 (P20/0). Aktumsuk section. Overall dimensions ~65 µm by 60 µm. **12:** *Thalassiphora velata.* Sample EL111 (~26.92 m), Slide 1 (U34/4). Elles section. Overall dimensions ~125 µm by 100 µm.

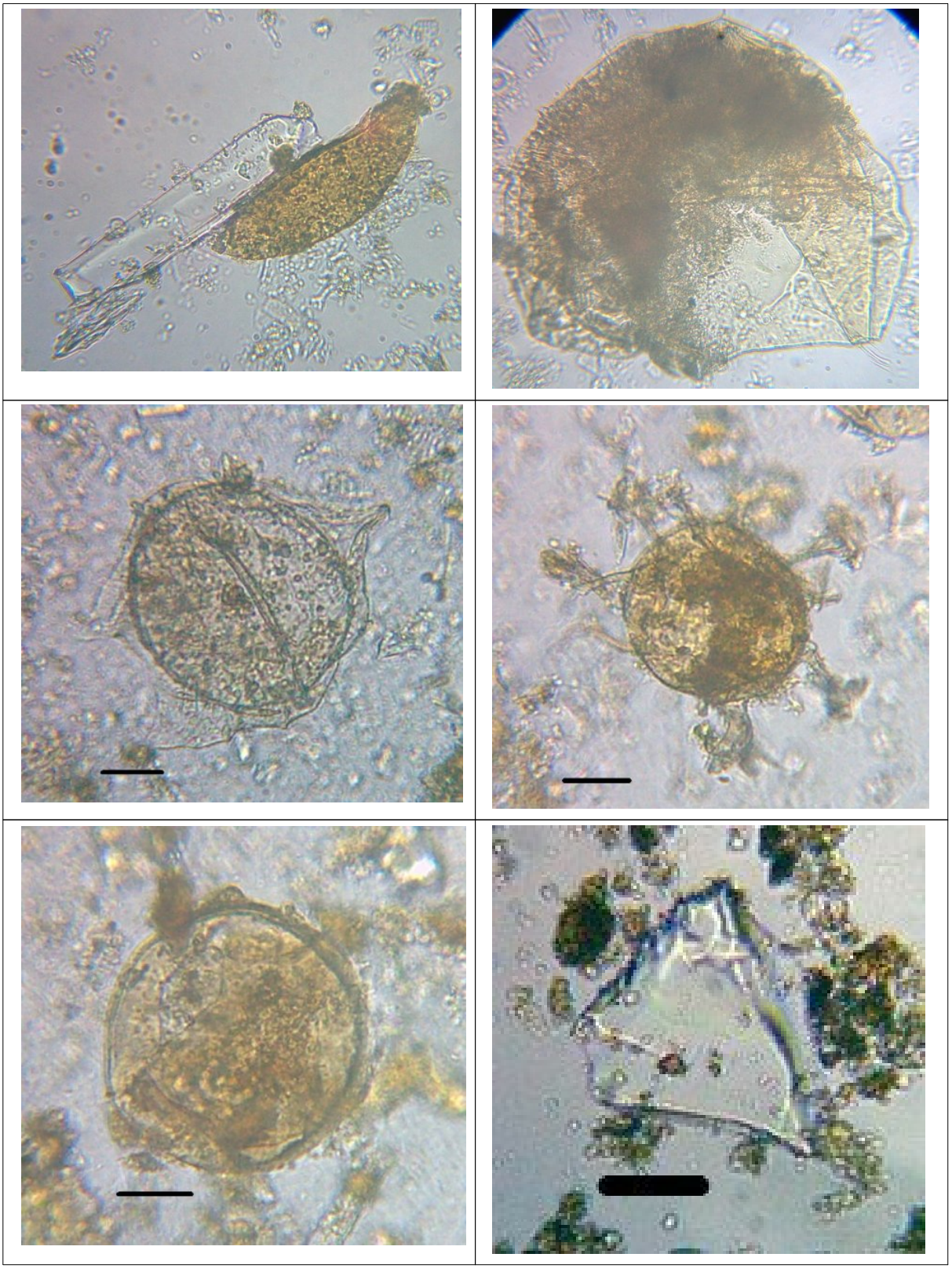

Dinoflaggelater og et korn af vulkansk glas fra lerprøver taget vest for Hanklit, Mors

Diatom turnover in the early Paleogene diatomite of the Sengiley section, Middle Povolzhie, Russia: A response to the Initial Eocene Thermal Maximum?

Tatiana V. Oreshkina, Geological Institute, Russian Academy of Sciences, 7 Pyzhevsky per, Moscow 119017, Russia

Hedi Oberhansli, GeoForschungsZentrum, Projektbereich 3.3, Telegraphenberg, D-14473 Potsdam, Germany

ABSTRACT The lower Paleogene sequence in the Middle Povolzhie (Ulyanovsk-Saratov syncline) of Russia is dominated by a terrigenous-rich siliceous facies with abundant and well-preserved siliceous plankton. Calcareous microfossils are virtually absent. The diatom successions of the Sengiley diatomite are correlated to diatom assemblages of the Fur Formation (Denmark) and the Polosataya Formation (Kazakhstan), and are calibrated to calcareous nannofossil and dinocyst zonations. The Trinacria ventricu- losa Zone, which is found in the lower part of the Sengiley diatomite (Kamyshin For mation), is age equivalent to the upper part of calcareous nannofossil zones NP8 through NP9a. The upper part of the Sengiley diatomite (Kamyshin Formation; Hemiaulus proteus Zone) can be correlated to the uppermost part oftheApectodinwm augustum dinocyst Zone, which corresponds to the NP9b calcareous nannofossil Sub- zone, in which the globally observed negative carbon isotope excursion occurs. A major floral turnover in the upper third of the Sengiley diatomite is character ized by a succession of bioevents, including first appearances at generic and specific levels. Quantitative diatom analyses show pronounced compositional changes: (1) the decline of the meroplanktonic Pyxidicula group, typical of neritic conditions (2) the in crease of the Paralia group, a marker for the proximity of the shoreline, and (3) a rel atively high abundance of pelagic cosmopolitan species. Grain size analyses show an increase in terrigenous input in the upper part of Sengiley diatomite. The floristic and lithologic shifts indicate changes from stable, highly productive neritic conditions dur ing a sea-level lowstand (Phase 1) to the onset of a transgression (Phase 2), which is followed by a highstand (Phase 3). The highstand phase coincides with enhanced ex change between the Tethys and the adjacent epicontinental seas. The diatom bioevents in Phases 2 and 3 in the Sengiley section are most probably coeval to the well- documented biotic changes of the Initial Eocene Thermal Maximum.

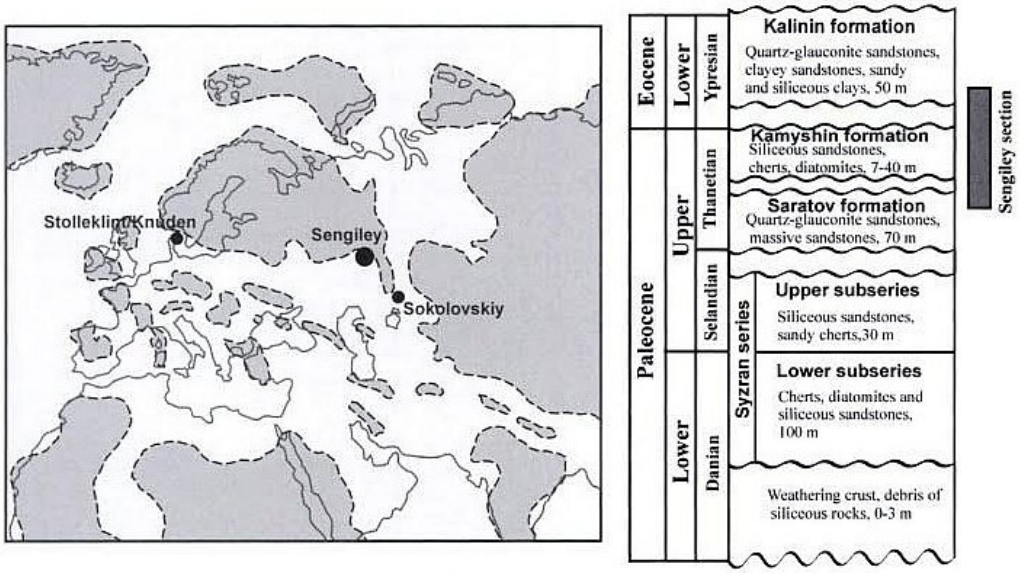

Figure 1. Location of the Sengiley section (Russia), and the correlative sections of the Stolleklint-Knuden (Denmark) and Sokolovskiy (Kazakhstan), shown in the paleogeographic setting of the area in the latest Paleocene. The figure on the right shows the Tertiary succession in the Ulyanovsk-Saratov syncline together with the stratigraphic position of the Sengiley section (shaded area).

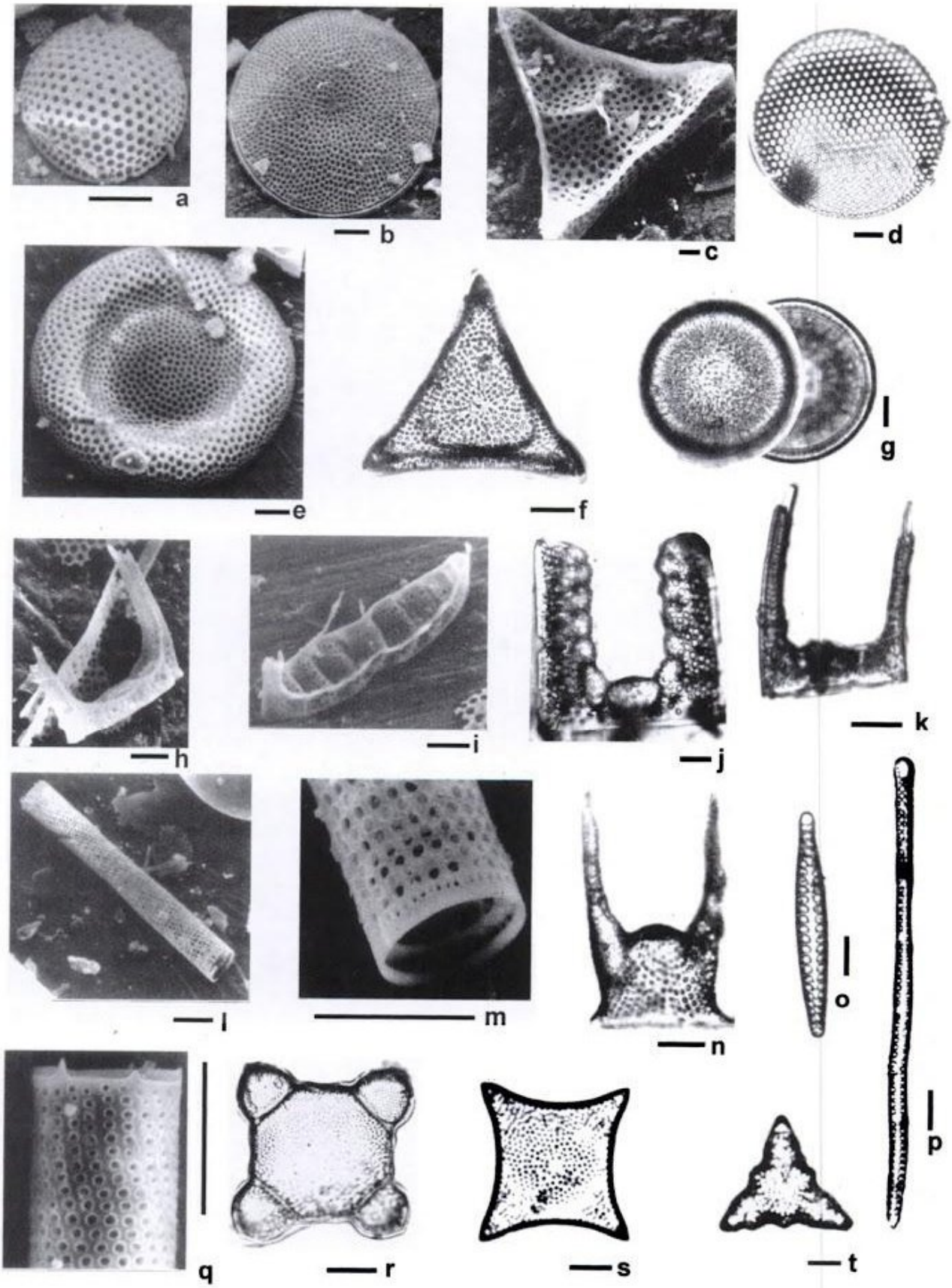

Figure 4. Diatom marker-species of the Sengiley section. a: *Pyxidicula moelleri* (Schmidt) Strelnikova et Nikolaev, sample 58. b: *Moisseevia uralensis* (Jousé) Strelnikova, sample 58. c: *Triceratium heibergii* Grunow sensu Gombos, (1977), sample 58. d: *Thalassiosiropsis wittiana* (Pantocsek) Hasle, sample 100. e: *Craspedodiscus moelleri* sample 58. f: *Trinacria ventriculosa* (Schmidt) Gleser, sample 103. g: *Pseudopodosira anissimovae* (Gleser et Rubina) Strelnikova, sample 100. h: *Hemiaulus inaequilaterus* Gombos, sample 64. i: *Hemiaulus proteus* Heiberg, sample 58. j: *Hemiaulus incurvus* Shibkova, sample 85. k: *Hemiaulus curvatulus* Strelnikova, sample 67. l, m, q: *Gyrocylindrus antiquus* Strelnikova et Nikolaev, sample 62. n: *Hemiaulus incisus* Hajos, sample 58. o: *Grunowiella gemmata* (Grunow) Van Heurck, sample 100. p: *Grunowiella palaeocaenica* Jousé, sample 58. r: *Trinacria exculpta* (Heiberg) Hustedt, sample 67. s: *Trinacria regina* Heiberg, sample 61. t: *Triceratium mirabile* Jousé, sample 98. Scale bar indicates 10 µm.

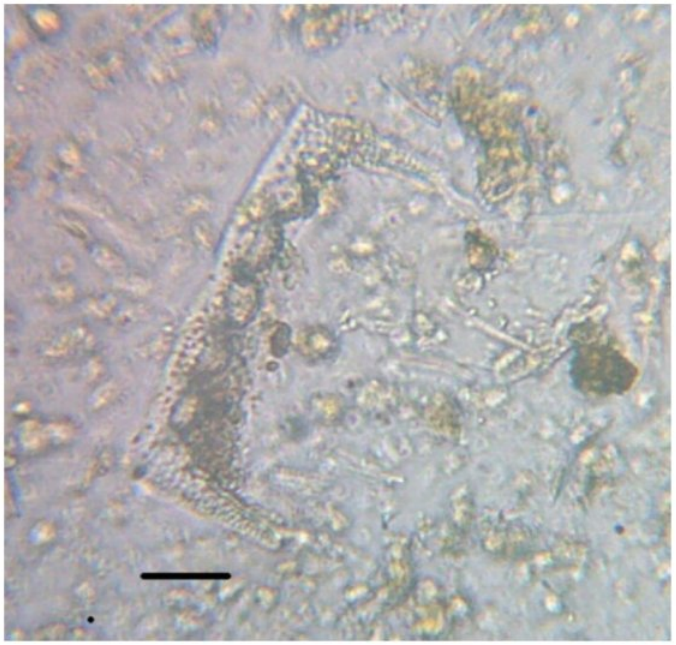

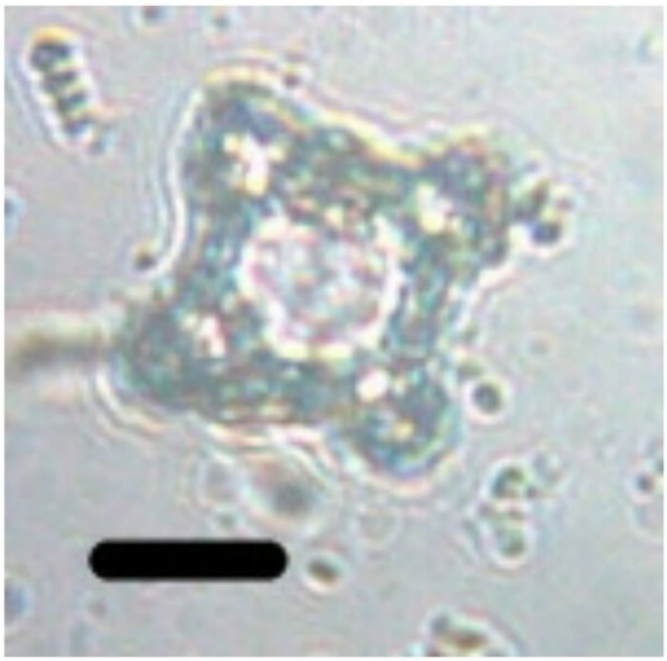

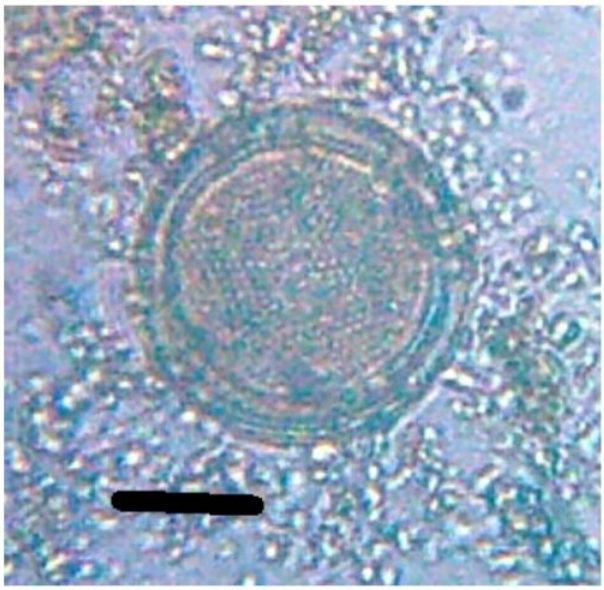

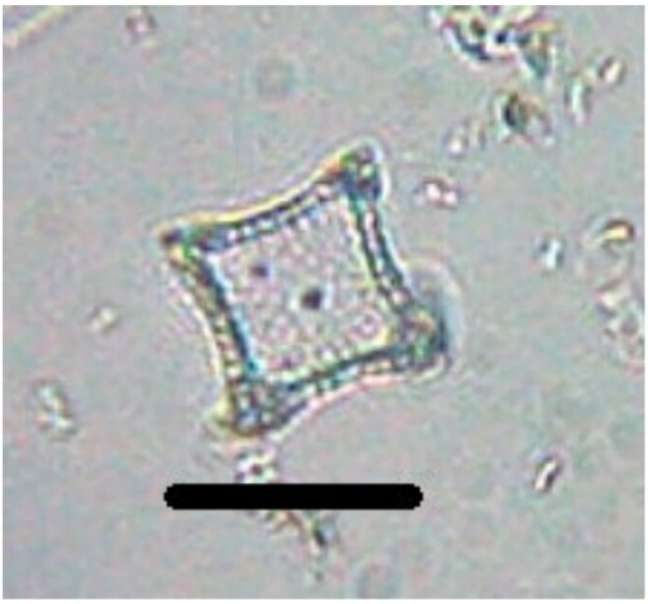

Diatomer fundet vest for Hanklit på Mors.Skala er 0,01 mm

Paleocene biota of the West Siberian plain

Vera M. Podobina, Tomsk State University, 36, Lenin Avenue, Tomsk. 634050 Russia

ABSTRACT In the Paleocene, most of the present West Siberian plain was occupied by a vast epicontinental sea, which reached from the present Arctic and Atlantic oceans in the North to the Aral Basin in the South. Climate and ocean circulation fluctuated and af fected marine and continental biota. Benthic foraminifera that occurred over a large part of the sea throughout the Paleocene were used as representatives of the marine biota, and spores and pollen of terrestrial plants as representatives of the continental biota, in order to study these environmental and biotic changes. Foraminifera and palynomorphs were studied in sedimentary sequences of Danian, Selandian, and Thanetian age. These sequences have regional names, and encompass the upper part of the Gankinskaya Stage, the whole Talitskaya Stage, and the lower part of the Lyulin- vorskaya Stage. In the southwest part of the basin (the Omsk depression), upper Gankinskaya sediments (Maastrichtian to lowermost Danian) contain calcareous benthic fora minifera. Benthic foraminiferal assemblages suggest that sea level fell during the early Paleocene, so that the West Siberian basin shallowed significantly and decreased in size. During the earliest Danian, the basin in the Ust-Tym depression also became shal lower, and “primitive” agglutinated foraminifera were dominant (e.g., Bathysiphon, Glomospira, Ammodiscus). Sea level rose during the Selandian boreal transgression (Talitskaya Stage), and agglutinated foraminifera occurred over large areas. In the Thanetian (represented by the uppermost Talitskaya and the base of the Lyulin- vorskaya Stage) the basin again shallowed, and foraminifera became rare. The analysis of palynomorphs (spores and pollen) in allochthonous assemblages in marine sediments documents that an alluvial plain with lakes and bogs was situated on the southeast coast of the Paleocene West Siberian marine basin. The climate became more arid during the Danian and late Thanetian, with a pronounced phase of drying at the boundary between the Talitskaya and Lyulinvorskaya Stages (early Thanetian).

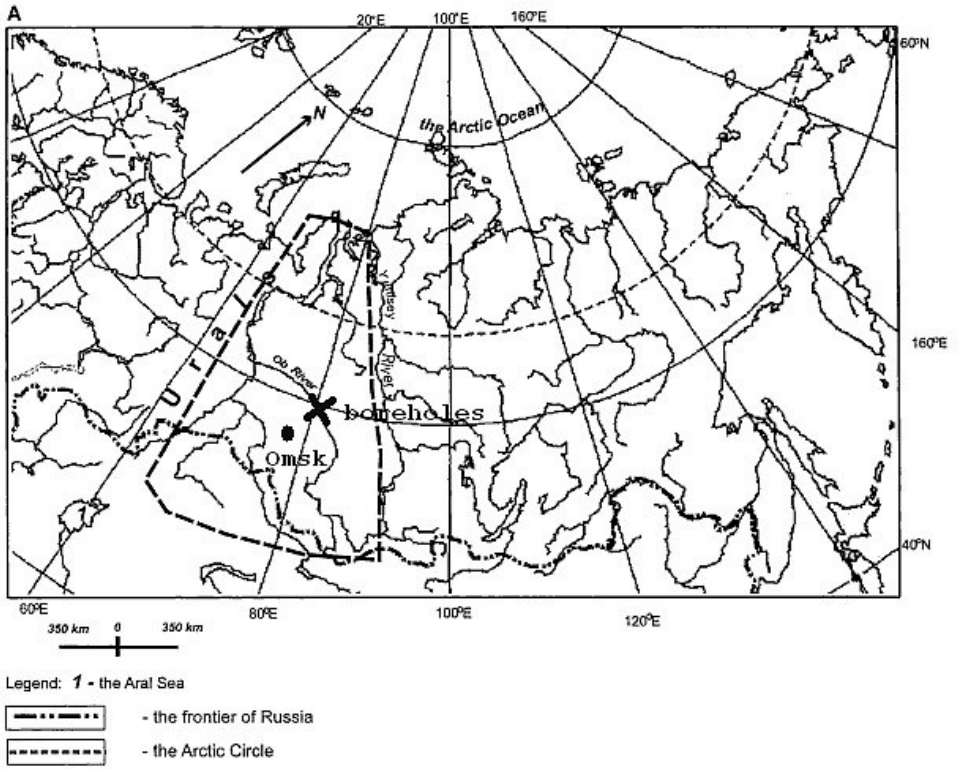

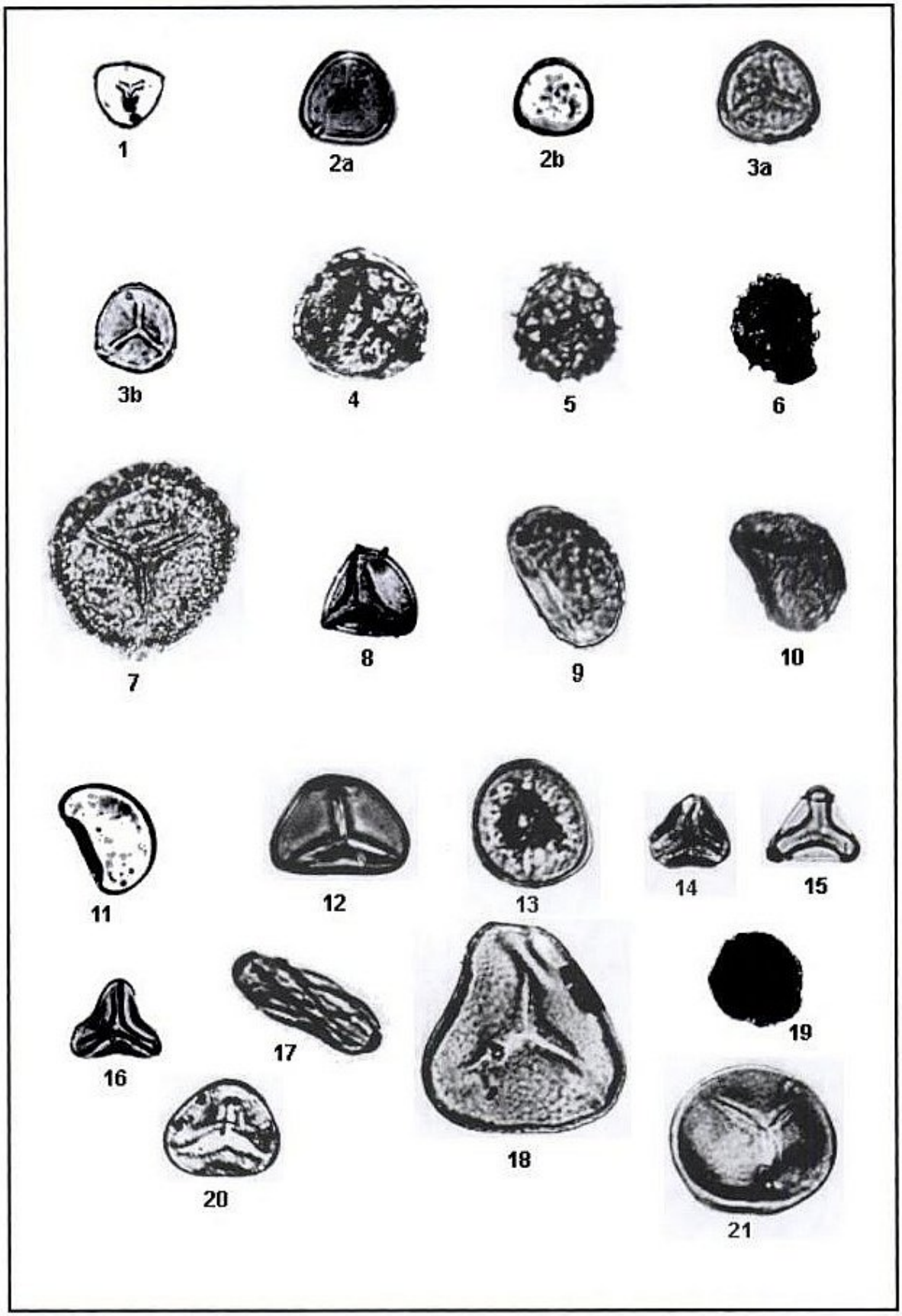

Plate 9. West Siberian Plain; early Paleocene; Sporae (magnification ×600). (All specimens are deposited in the Micropaleontological Laboratory and Paleontological Museum of Tomsk State University.) Figure 1. *Sphagnum australe* (Cook) Drozh; Figure 2a, b. *Sphagnum putillum* Drozh. et Purt. Figure 3a, b. *Sphagnum regium* Drozh. Figures 4–6. *Lycopodium* sp. Figure 7. *Selaginella* sp. Figure 8. *Cyathea* sp. Figures 9–10. Polypodidiaceae. Figures 11–12. *Adiantum* sp. Figure 13. *Cheiropleuria* sp. Figure 14. *Gleichenia umbonata* Bolch. Figure 15. *Gleichenia rara* Chlon. Figure 16. *Gleichenia* sp. Figure 17. *Schizaea dorogensis* (R. Pot.) Chlon. Figure 18. *Lygodium* sp. Figure 19. *Osmunda* sp. Figure 20. *Leiotriletes* Naum. Figure 21. *Stenozonotriletes* Naum.

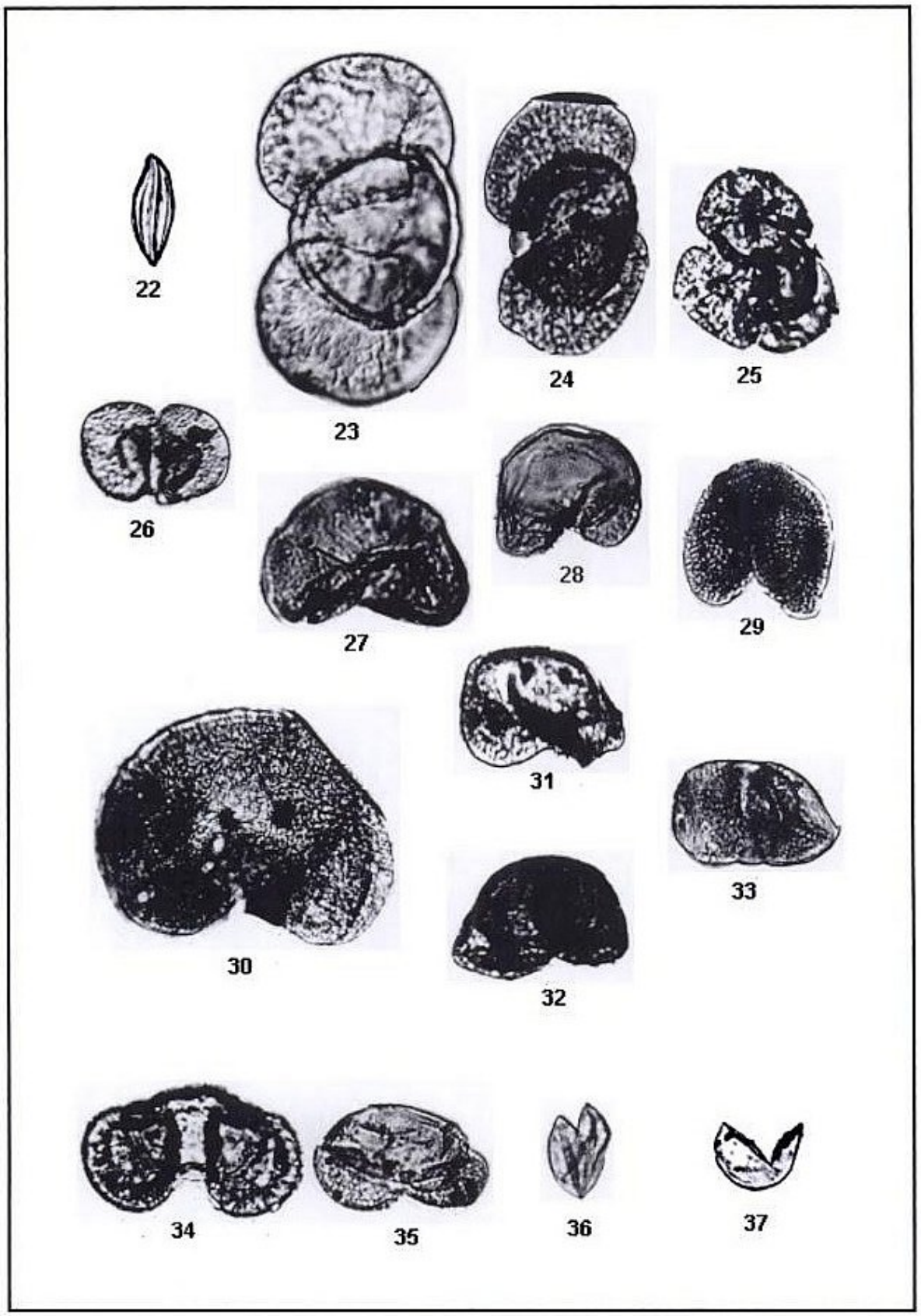

Plate 10. West Siberian Plain; early Paleocene; Gymnospermae Pollen (magnification ×600). (All specimens are deposited in the Micropaleontological Laboratory and Paleontological Museum of Tomsk State University.) Figure 22. *Ginkgo* sp. Figure 23. *Podocarpus unica* Bolch. Figures 24–26. *Podocarpus* sp. Figures 25–27. Pinaceae. Figure 28. *Cedrus parvisaccata* Sauer. Figures 29–32. *Cedrus* sp. Figure 33. *Pinus aequelis* (Naum.) Bolch. Figure 34. *Pinus vulgaris* (Naum.) Bolch. Figure 35. *Pinus* n./p. Dyploxylon. Figure 36. Taxodiaceae. Figure 37. *Taxodium* sp.

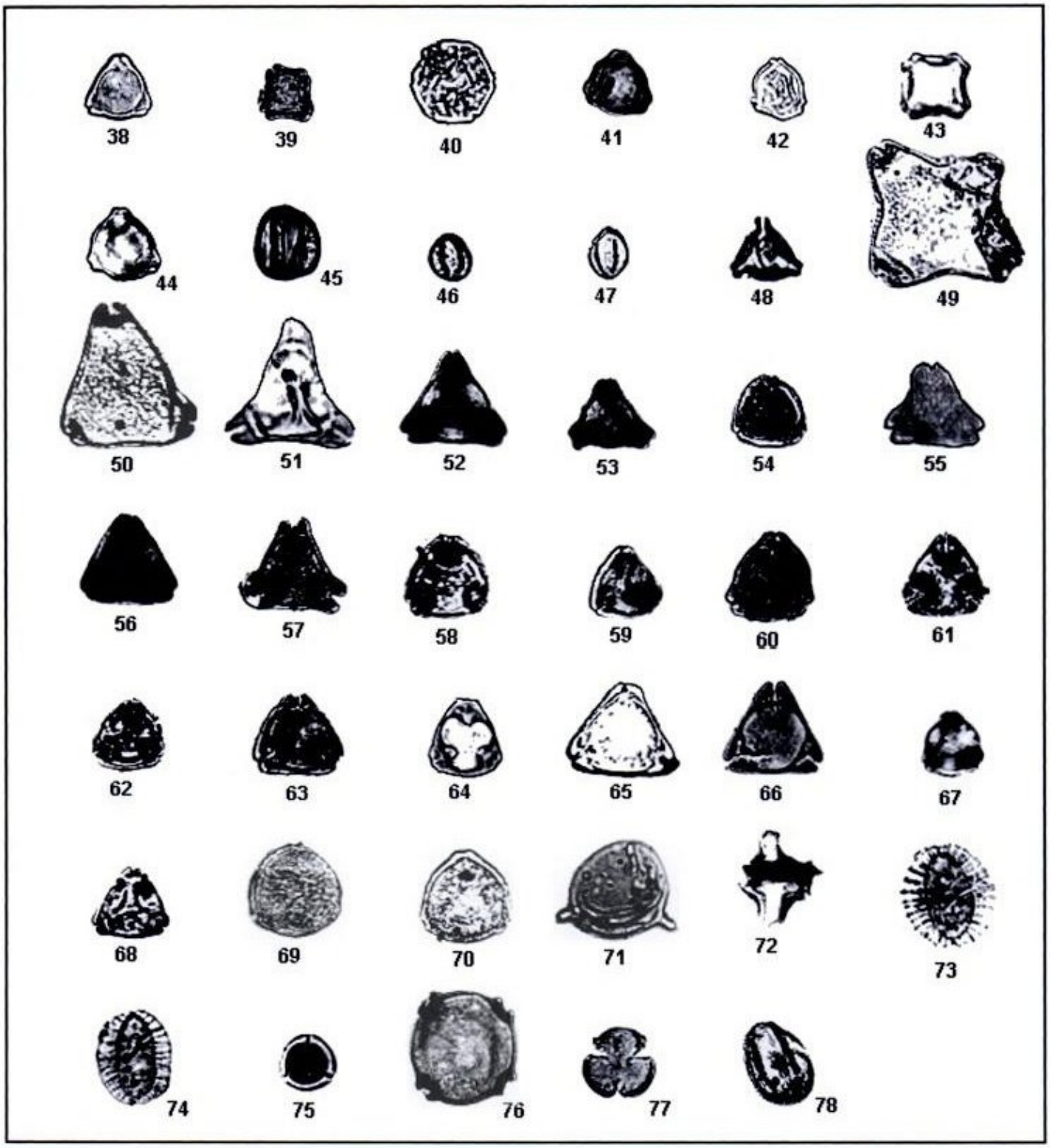

Plate 11. West Siberian Plain; early Paleocene; Angiospermae Pollen (magnification ×600). (All specimens are deposited in the Micropaleontological Laboratory and Paleontological Museum of Tomsk State University.) Figure 38. *Myrica* sp. Figure 39. *Myricacites* sp. Figure 40. *Juglans* sp. Figures 41–42. Betulaceae. Figure 43. *Alnus* sp. Figure 44. *Betula* sp. Figure 45. *Quercus* sp. Figures 46–47. *Quercites sparsus* (Martyn) Samoil. Figure 48. *Santalacites* sp. Figure 49. Proteacea. Figure 50. *Protea* sp. Figure 51. *Nudopollis endangulatus* Pfl. Figures 52–53. *Nudopollis* sp. Figure 54. *Basopollis vestibulatus* Zalkl. Figure 55. *Basopollis* sp. Figure 56. *Oculopollis praedicatus* Weil et Krieg. Figure 57. *Oculopollis torosus* Zakl. Figure 58. *Oculopollis* sp. Figure 59. *Vacuopollis* sp. Figure 60. *Trudopollis conrector* Pfl. Figures 61–64. *Trudopollis* sp. Figures 65–66. *Extratriporopollenites* sp. Figure 67. *Triatriopollenites aroboratus* Pfl. Figure 68. *Triatriopollenites*. Figure 69. *Trioropollenites robustum* Pfl. Figure 70. *Tricolpites* sp. Figure 71. *Triporina globosa* Chlon. Figure 72. *Aquilapolenites* sp. Figures 73–74. *Kryshtofoviana vera* Samoil. Figure 75. *Triporopollenites* sp. Figure 76. *Tetraporopollenites* sp. Figures 77–78. *Tricolpopollenites* sp.

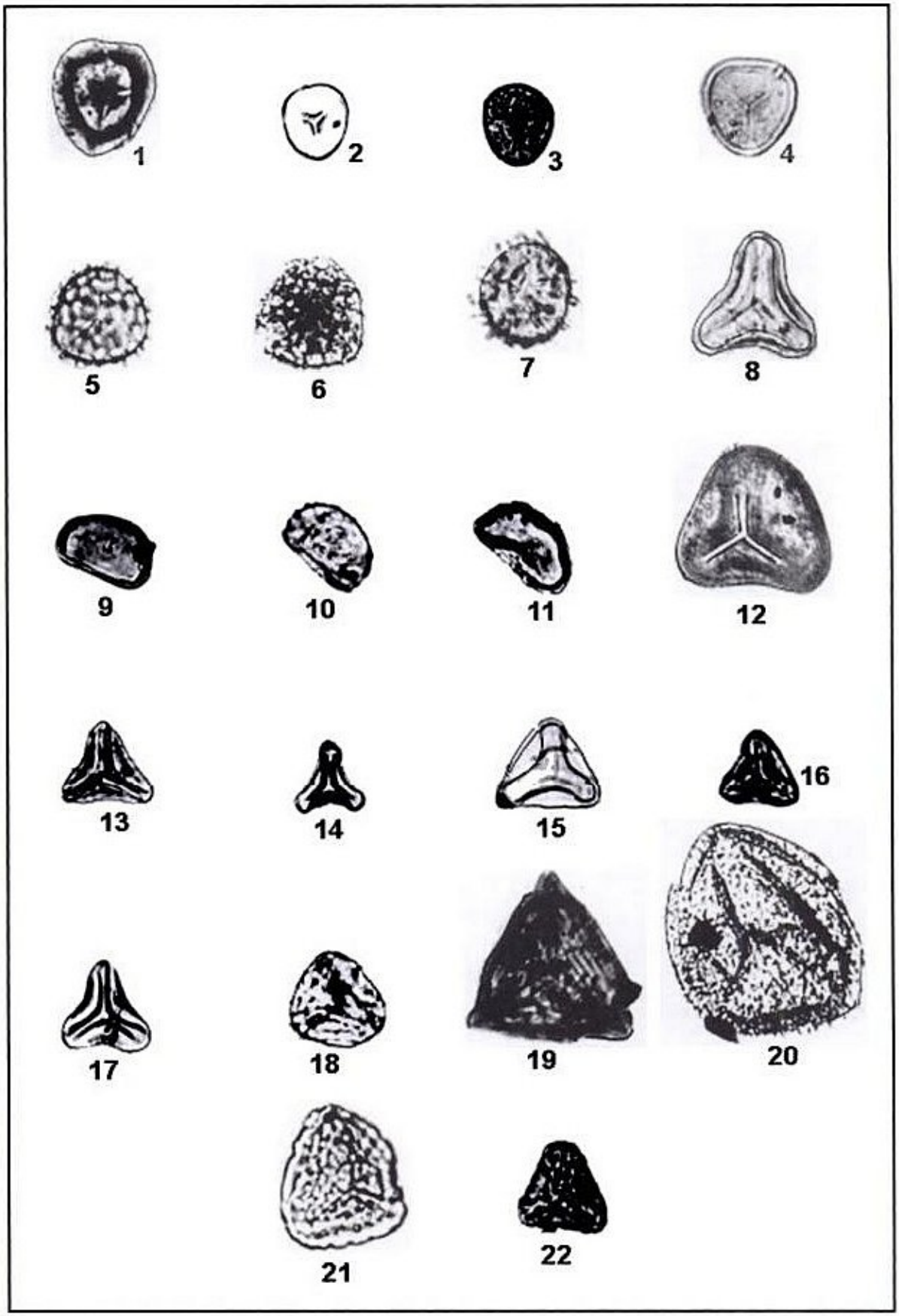

Plate 12. West Siberian Plain; late Paleocene; Sporae (magnification ×600). (All specimens are deposited in the Micropaleontological Laboratory and Paleontological Museum of Tomsk State University.) Figure 1. *Sphagnum australe* (Cook) Drozh. Figure 2. *Sphagnum putillum* Drozh. et Purt. Figure 3. *Sphagnum regium* Drozh. Figure 4. *Sphagnum putillum* Drozh. et Purt. Figures 5–6. *Lycopodium* sp. Figure 7. *Selaginella diuturna* Bolch. Figure 8. *Cyathea* sp. Figures 9–11. Polypodidiaceae. Figure 12. *Matonia* sp. Figure 13. *Gleichenia umbonata* Bolch. Figure 14. *Gleichenia laeta* Bolch. Figure 15. *Gleichenia rara* Chlon. Figures 16–17. *Gleichenia* sp. Figure 18. *Mohria* sp. Figure 19. *Aneimia* sp. Figure 20. *Osmunda* sp. Figures 21–22. *Lophotriletes* Naum (magnification ×600).

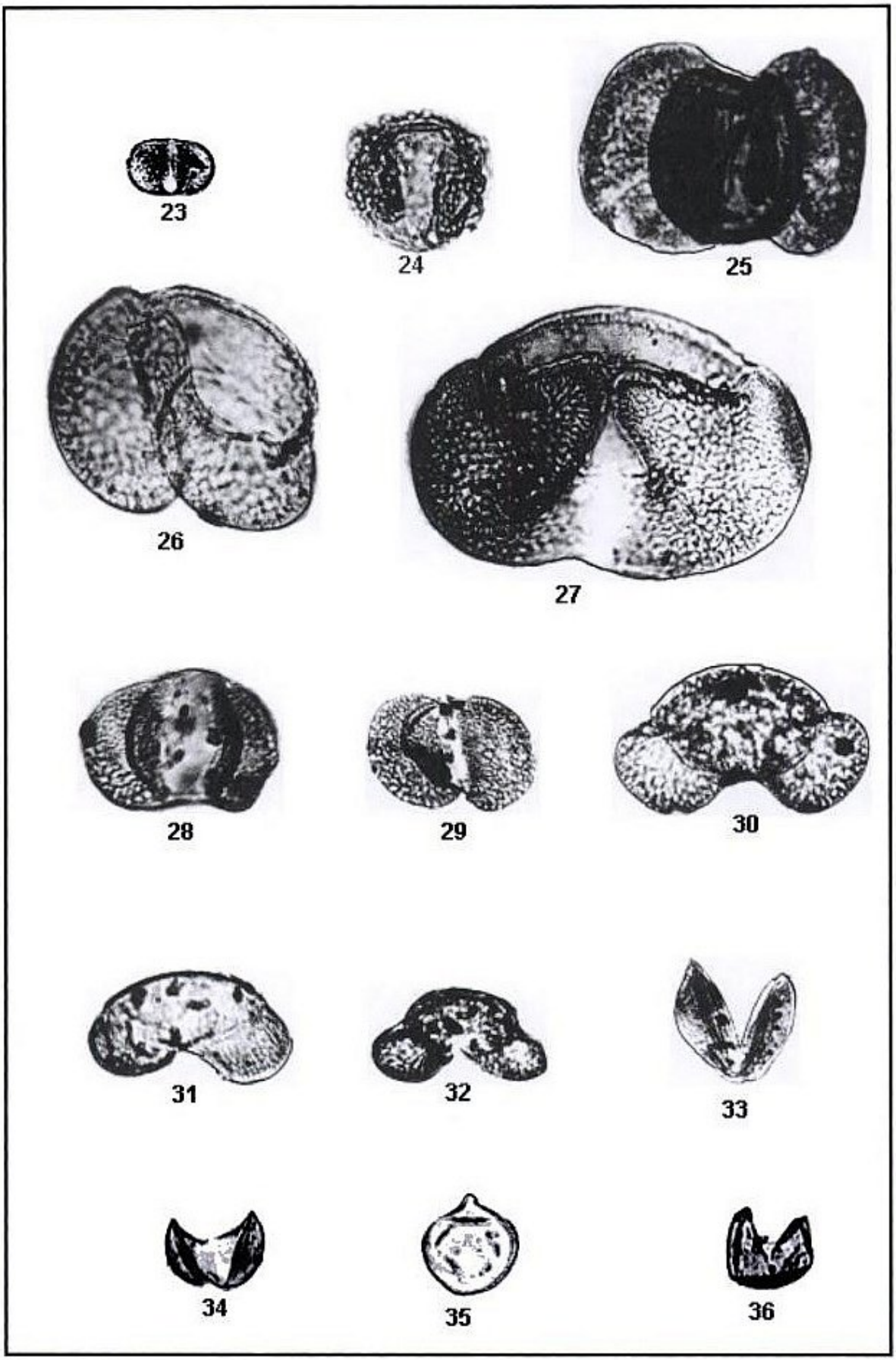

Plate 13. West Siberian Plain; late Paleocene; Gymnospermae Pollen (magnification ×600). (All specimens are deposited in the Micropaleontological Laboratory and Paleontological Museum of Tomsk State University.) Figure 23. *Caytonia* sp. Figure 24. *Dacrydiumites* sp. Figure 25. *Podocarpus* sp. Figure 26. Pinaceae. Figure 27. *Picea* sp. Figures 28–29. *Pinus* n./p. Haploxylon. Figure 30. *Pinus aralica* Bolch. Figures 31–32. *Pinus* n./p. *Diploxylon.* Figures 33–34. Taxodiaceae. Figures 35–36. *Taxodium* sp.

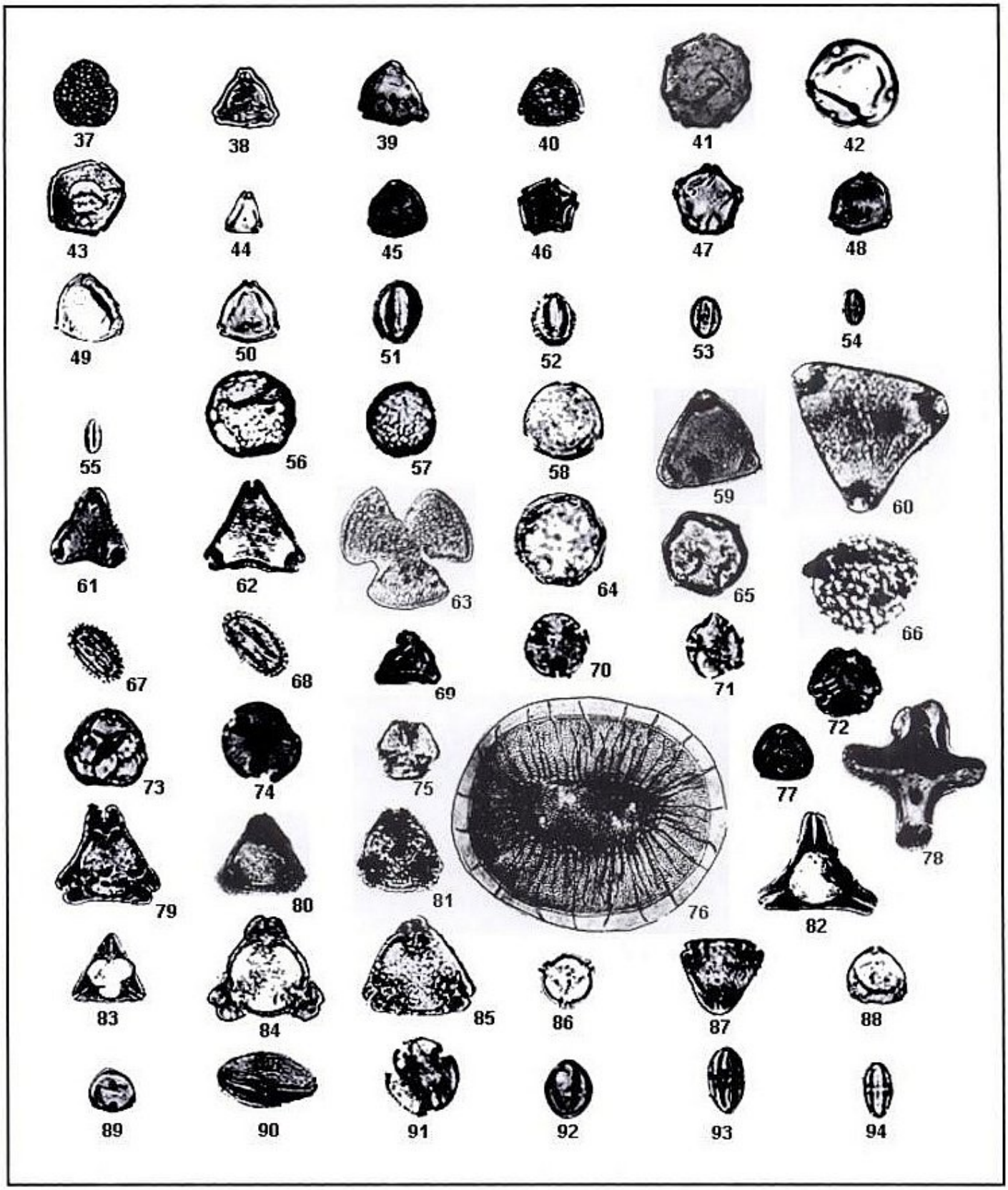

Plate 14. West Siberian Plain; late Paleocene; Angiospermae Pollen (magnification ×600). (All specimens are deposited in the Micropaleontological Laboratory and Paleontological Museum of Tomsk State University.) Figure 37. Solicaceae. Figures 38–40. *Myrica* sp. Figure 41. *Pterocarya* sp. Figure 42. *Carya* sp. Figure 43. *Juglans* sp. Figure 44. *Engelhardtia* sp. Figure 45. Betulaceae. Figures 46–47. *Alnus* sp. Figure 48. *Betula* sp. Figure 49. *Betulites* sp. Figure 50. *Corylus* sp. Figure 51. *Quercus* sp. Figures 52–53. *Quercites sparsus* (Martyn) Samoil. Figures 54–55. *Castanea* sp. Figures 56–57. Ulmaceae. Figure 58. Moraceae. Figures 59–62. Protaceae. Figure 63. Homamelidaceae. Figures 64–65. *Liquidambar* sp. Figure 66. Buxaceae. Figures 67–68. *Ilex* sp. Figure 69. *Santalacites* sp. Figures 70–71. *Tilia* sp. Figure 72. *Nyssa* sp. Figure 73. Ericaceae. Figures 74–75. Euphorbiaceae. Figure 76. *Regina exselsa* Samoil. Figure 77. *Anacolosidites insignis* Samoil. Figure 78. *Aquilapolenites* sp. Figure 79. *Trudopollis conrector* Pfl. Figure 80. *Trudopollis* sp. Figure 81. *Oculopollis* sp. Figures 82–83. *Nudopollis* sp. Figures 84–85. *Basopollis* sp. Figure 86. *Extratriporopollenites pompeckjic* Pfl. Figure 87. *Extratriporopollenites* sp. Figures 88–89. *Triorites* sp. Figures 90–94. *Tricolporopollenites* spp.

Geographic patterns in the floral response to Paleocene-Eocene warming

Guy J. Harrington, Department of Geology, National University of Ireland Cork, Cork, Ireland

ABSTRACT Studies on vegetation change from North America show that floral composition in the early Eocene was very similar to that in the late Paleocene. This interpretation is counterintuitive with expectations that rapid global warming, which marks the Paleocene-Eocene boundary, would have led to intense vegetation turnover. In this review, data on Paleocene-Eocene pollen and spores are taken from published sources from four main regions in North America: (1) The U.S. Gulf Coast (paleolatitude 32 °N) (2) the eastern seaboard of Virginia (paleolatitude 39 °N) (3) the Bighorn and Powder River basins (paleolatitude 47 °N) and (4) the Canadian Arctic (paleolatitude 78 N i. This data set shows that there is no apparent latitudinal pattern to vegetation turnover in the early Eocene, but rather a strong distinction between the continental interior and the coastal areas. No one immigrant taxon characterizes the whole of North America and the coasts have a greater number of Eocene first occurrences than the continental interior. Immigrants can be classified as those that migrated from other continents, of which 40% have European Paleocene records, and those that immigrated from other regions in North America. Intracontinental immigra tion was exclusively from south to north and was restricted to coastal areas. The con sequence of global warming was a complex vegetational response caused by the probable inability of many plants to disperse into North America.

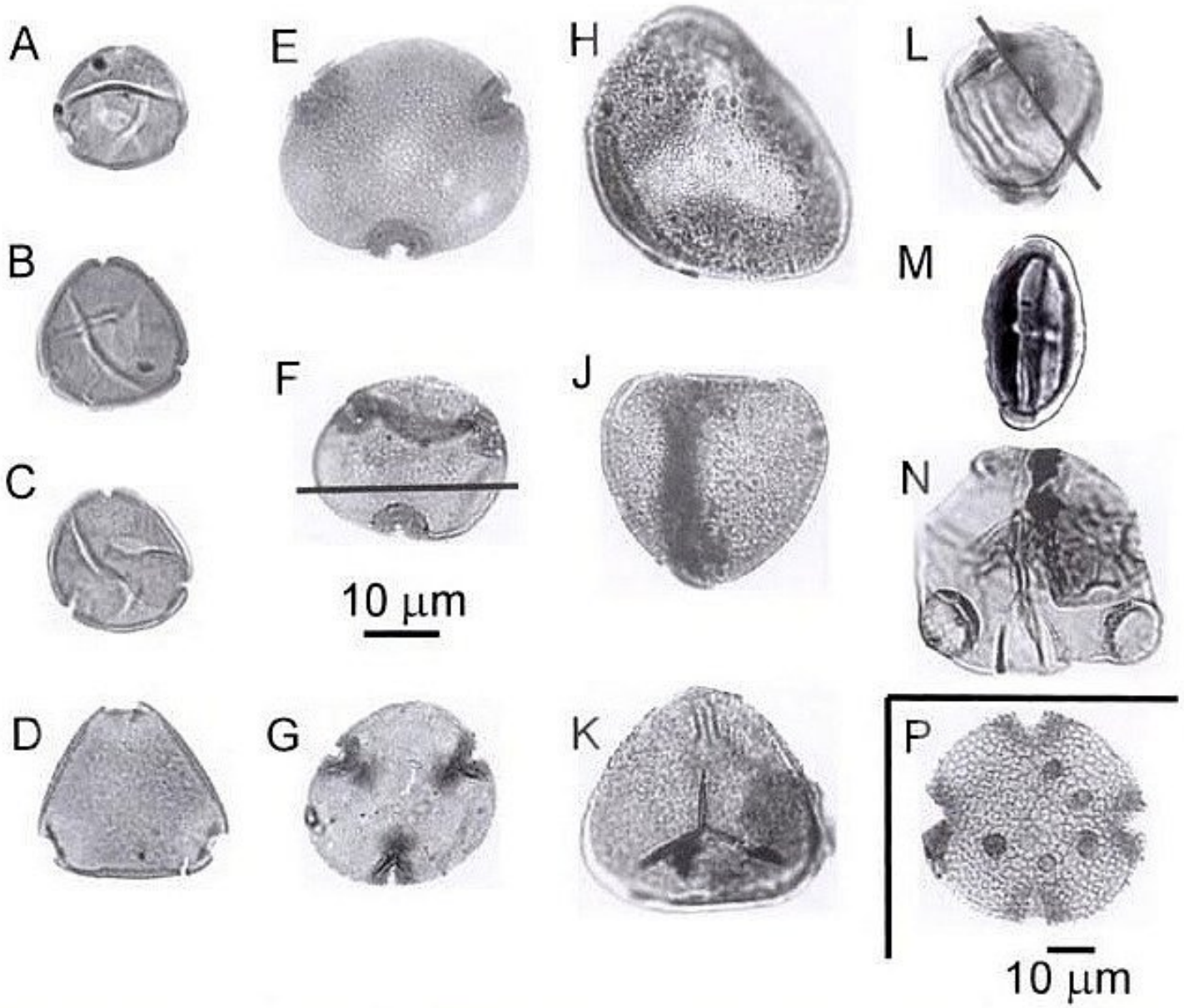

Figure 3. Plate of selected taxa from North America including biostratigraphically significant sporomorphs and those that are currently undescribed. The scale bars represent 10 µm. Notes include the sample number after the species or genus name and the England finder reference taken on Leica microscope LIS 253 housed in the Department of Geology, University College Cork. (A) *Platycarya platycaryoides,* HB15a, O28/center. (B) *Platycarya* sp. similar to *P. anticyclus,* Rh05c b, F34/center. (C) *Platycarya* sp. similar to *P. swasticoidus,* Rh05c a, J35/2. (D) *Symplocos ? contracta,* Wa252.05a, P34/2. (E) *Intratriporopollenites instructus,* PS0004, O34/4, (F) *Intratriporopollenites instructus,* high and low focus, AL620 a, P37/3. (G) *Intratriporopollenites* cf. *instructus,* this specimen is similar to *I. microreticulatus* because the exine is not coarsely reticulated, GH97/1.28a, O21/2. (H) *Punctatisporites* sp. in dorsal view, GH97/1.28c, P27/3. (J) *Punctatisporites* sp. in equatorial view, GH97/1.28a, K40/center. (K) *Granulatisporites* sp., ventral view, Ha35 454.02c, J14/1. (L) *Brosipollis* sp. in high and low focus, Ht/39 265.0a, C22/1. (M) *Nuxpollenites psilatus,* Ht/01a 295.09, B18/1. (N) *Corsinipollenites psilatus,* Ha/05 389.06, C25/4. (P) *Retistephanocolporites* sp., note the different scale bar, RH99–44b, E28/center.




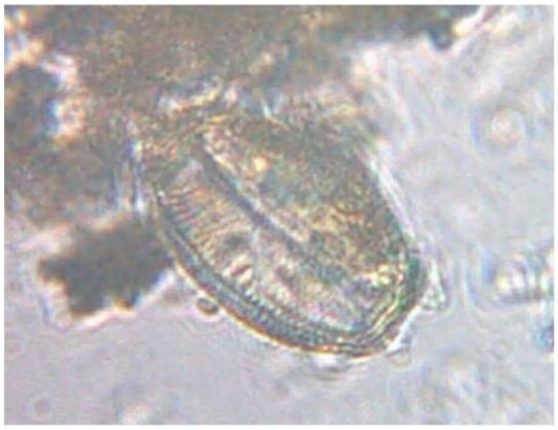

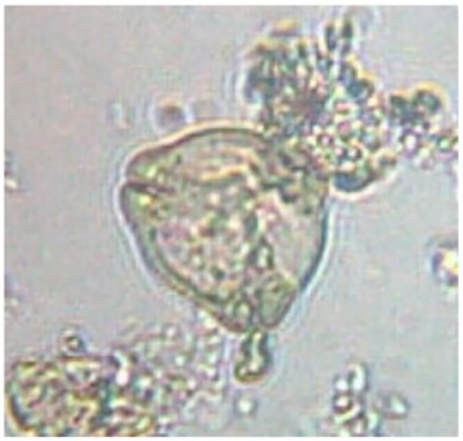

Pollen fra Hanklit

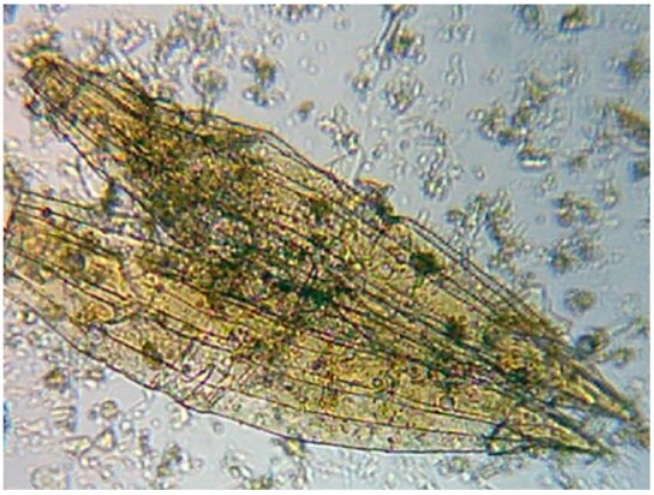

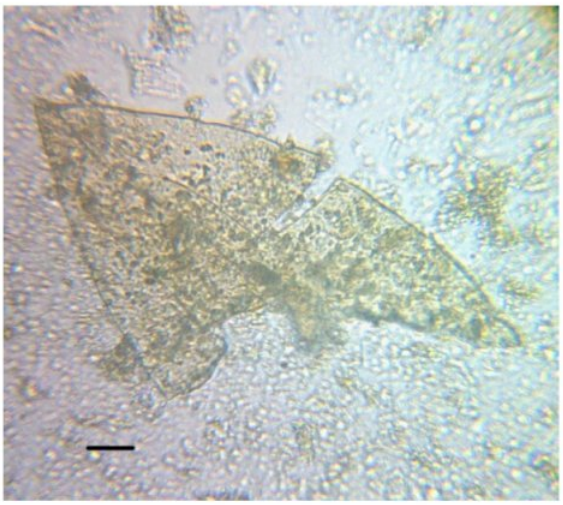

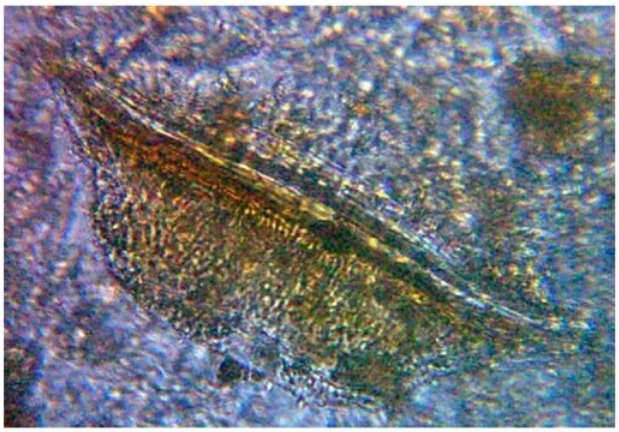

Forskellige objekter fra vest for Hanklit